Contents:

Section 2 Comparative inhibitory effects of different inhibitors on rat Oatp1 (*Slc21a1*)- and Oatp2 (*Slc21a5*)-mediated transport. A search for specific inhibitors of these transporters

Abbreviations

AIC, Akaike's information criteria
AUC, area under the plasma concentration-time curve
BSP, sulfobromophthaleine
CER, cerivastatin
CL_H, hepatic clearance
CL_{int}, hepatic intrinsic clearance
$CL_{int,all}$, overall intrinsic hepatic clearance
CL_{uptake}, uptake clearance
CsA, cyclosporin A
CYP, cytochrome P450
DDI, drug-drug interaction
$E_2$17βG, estradiol 17β-D-glucuronide
f_b, protein unbound fraction
GEM, gemfibrozil
HPLC, high performance liquid chromatography
IC_{50}, inhibitor concentration to produce a 50 % reduction
K_i, inhibition constant
K_m, Michaelis constant
LC/MS/MS, atmospheric pressure ionization liquid chromatography-tandem mass spectrometry
LDL, low density lipoprotein
LUI, liver uptake index
MHW (MHLW), the Ministry of Health and Welfare of Japan (the Ministry of Health, Labour and Welfare of Japan)
NSAIDs, nonsteroidal anti-inflammatory drugs
NTCP, Na+-taurocholate cotransporting polypeptide
OAT, organic anion transporter
OATP, organic anion transporting polypeptide
P_{dif}, nonsaturable transport clearance
$PS_{u,efflux}$, ,membrane permeability clearance of the unbound drugs for the efflux from inside cells
$PS_{u,influx}$, membrane permeability clearance of the unbound drugs for the influx from outside cells
Q_H, hepatic blood flow

SD, Sparague-Dawley

TC, taurocholate

TG, triglyceride

V_{max}, maximum uptake rate

[General Introduction]

In clinical situations, several drugs are often prescribed at the same time for the effective treatment of diseases. However, combination therapies using multiple drugs sometimes cause drug-drug interactions (DDI). Hansten (2002) reported that more than 15,000 papers have been published on DDI in the past 30 years and 2,000 individual interacting combinations have been identified [1]. Some of them result in severe side-effects. For example, in 1993, a serious DDI between 5-FU, an anticancer drug, and sorivudine, an antiherpes drug, was reported. This serious DDI lead to the deaths of 15 Japanese patients [2]. In order not to repeat this tragedy, a number of studies aimed at quantitatively predicting the extent of DDI have been carried out and a method established [3, 4, 5].

After this tragedy, the Ministry of Health and Welfare of Japan (MHW, currently the Ministry of Health, Labour and Welfare of Japan (MHLW)) considered it necessary to prepare guidance for the study of DDI [6]. The MHW organized a “Research Group for the Preparation of Guidance for Drug Interaction Studies” in 1998 and completed the draft of the guidance in 2000 [6]. In 2001, the MHLW sent notification that it should be used as a reference under the name of “Methods for Drug Interaction Studies” [6, 7]. This guidance contains methods for evaluating the DDI occurring by various mechanisms i.e. inhibition of intestinal absorption, plasma protein binding, metabolic enzymes and transporters and induction of metabolic enzymes etc [7]. Although it briefly describes the possibility of transporter-mediated DDI, there were few reports of clinically relevant DDI based on the transporter-mediated uptake process until now [7]. Therefore, this guidance mainly applies to the DDI occurring via metabolic processes (especially cytochrome P450 (CYP)-mediated metabolism). However, some DDI cannot be explained only by CYP-mediated metabolism.

Cerivastatin (CER: Fig. 1) is a potent 3-hydroxy-3-methylglutaryl-coenzyme A

(HMG-CoA) reductase inhibitor (statin) with a high oral availability, allowing this drug to be effective in hypercholesterolemia at low doses [8]. CER is extensively taken up into the liver and subsequently metabolized by 2 different enzymes, CYP2C8 and 3A4 (Fig. 2) [9, 10]. This dual metabolic pathway is a distinctive feature of CER differentiating it from other statins. Due to this distinctive dual metabolic pathway, the frequency of severe DDI was believed to be low [9]. Indeed, the plasma concentration of CER was increased only 120 % compared with the control when concomitantly administered with erythromycin, a potent CYP3A4 inhibitor although its regimen was chosen to ensure the maximum inhibition of CYP3A4 during CER exposure [11]. Other CYP3A4 inhibitors such like itraconazole and mebifrazil have also been reported to have a minimal interaction with CER [12, 13]. However, a DDI between CER and cyclosporin A (CsA: Fig. 3) was reported in 1999 [14] and that between CER and gemfibrozil (GEM: Fig. 4a) was reported in 2001[15, 16]. The area under the plasma concentration-time curve (AUC) of CER was increased 4- and 4~6-fold by the coadministration of CsA [14] and GEM[15, 16], respectively. The high plasma concentration of CER due to DDI may cause severe adverse effects such as myopathy or rhabdomyolysis. Although CsA is a well-known CYP3A4 inhibitor [17], it is less likely that this severe DDI is due to a CYP3A4-mediated reaction as is the case with other CYP3A4 inhibitors, i.e. itraconazole, mebifradil, etc. [12. 13], because of an alternative metabolic pathway by CYP2C8. As CER is mainly metabolized in the liver with little renal elimination [10], this DDI between CER and CsA should be due to a reduction in hepatic clearance (CL_H). Many drugs are taken up into liver by transporters prior to metabolism and, therefore, it is possible that this DDI may be due to the inhibition of transporter-mediated hepatic uptake. Pravastatin, another of the statins, has been reported to be a good substrate of organic anion transporting polypeptide-2 (OATP2: gene symbol *SLC21A6*) [18, 19]. Like pravastatin, CER may be transported into the liver by OATP2, followed by metabolism although the uptake of CER by human hepatocytes has not yet been investigated.

Recent studies of drug transport in the liver have provided detailed information on

drug transporters, including substrate and inhibitor profiles [20]. More recently, a number of transporters have been cloned and their functions are being investigated [21, 22, 23]. In the liver, there are many transporters both on the sinusoidal membrane and bile canalicular membrane, which are responsible for the hepatic uptake from the blood side and excretion via the bile, respectively [21, 22, 23]. As far as the hepatic uptake of organic anions is concerned, there are mainly 2 different families of transporters: OATP and the organic anion transporter (OAT) family (Fig. 5 and 6) [21, 22, 23]. The former is mainly responsible for the uptake of amphipathic substrates while the latter is involved in the uptake of small and hydrophilic organic anions [24]. In humans, OATP2, OATP8 (*SLC21A8*), OATP-B (*SLC21A9*) and OAT2 (*SLC22A7*) are reported to be expressed in the liver (Fig. 5) [18, 19, 25-29]. Also, these families are generally conserved in rats. In rat hepatocytes, Oatp1 (*Slc21a1*), Oatp2 (*Slc21a5*), Oatp4 (*Slc21a10*) and Oat2 (*Slc22a7*) are expressed in the liver (Fig. 6) [30-33]. These transporters are involved in the hepatic uptake of a number of important substrates, including therapeutic drugs [18, 19, 34]. Each transporter has a low substrate specificity and many compounds can be recognized as substrates [35]. Therefore, it is possible that a concomitantly administered drug may function as a competitive inhibitor although there are no reports of clinically relevant DDI occurring during transporter-mediated hepatic uptake, at least up until now [36].

To evaluate the transporter-mediated hepatic uptake, isolated or short-term cultured hepatocytes can be a useful experimental system because they are equipped with all relevant transporters similar to the situation in the intact liver [21, 37]. In the case of humans, cryopreserved human hepatocytes are commercially available and may be a useful tool [38, 39]. However, until now, no validation study has been carried out to show that the transporter activity in cryopreserved human hepatocytes is the same as that in freshly isolated hepatocytes although the CYP-mediated metabolism in both preparations has already been investigated and suggested to be the same [40]. Therefore, initially, I have examined the transporter function in freshly isolated and cryopreserved human hepatocytes

in a comparative fashion (Section 1-1). The transporter expression system is also a good tool for estimation of hepatic uptake. However, the contribution of specific transporters to the total hepatic uptake is unknown and it is required to estimate the total hepatic uptake of substrates from data obtained in the transporter expression system. For the purpose of estimating the contribution of rat Oatp1 and Oatp2 to the total uptake, I have searched for specific inhibitors of these transporters (Section 2).

In Section 1, I have analyzed the mechanism of the DDI between CER and CsA, and CER and GEM while, in Section 2, I have examined the inhibitory effects of different compounds on rat Oatp1 and Oatp2 for the purpose of estimating their contributions.

[Section 1]

Analysis of the mechanism underlying the drug-drug interaction between cerivastatin and cyclosporin A, and that between cerivastatin and gemfibrozil.

1-1

Function of organic anion transporting polypeptide (OATP) family transporters in cryopreserved and freshly isolated human hepatocytes.

Drug disposition in hepatocytes is intiated by the penetration of drugs through the sinusoidal membrane, followed by intracellular metabolism and/or biliary excretion [20]. Therefore, the hepatic uptake process is an important determinant of the hepatic clearance of drugs.

Indeed, assuming a well-stirred model, the CL_H can be described by the following equation:

$$CL_H = \frac{Q_H \cdot f_b \cdot CL_{int,all}}{Q_H + f_b \cdot CL_{int,all}} \quad \ldots(1)$$

where, Q_H is the hepatic blood flow and f_b is the blood unbound fraction. The $CL_{int,all}$ represents the overall intrinsic hepatic clearance which includes membrane permeability, metabolism and biliary excretion, as described by the following equation (2):

$$CL_{int,all} = PS_{u,influx} \times \frac{CL_{int}}{PS_{u,efflux} + CL_{int}} \quad \ldots(2)$$

where, $PS_{u,influx}$ and $PS_{u,efflux}$ represent the membrane permeability clearance of the unbound drug for the influx and efflux process from outside and inside the cells, respectively, and CL_{int} represents the 'exact' intrinsic clearance which includes metabolism and/or biliary excretion of the unbound drug [20]. Therefore, for the estimation of the effect of other compounds i.e. concomitantly administered drugs on net CL_H, it is important to examine the change in $PS_{u,influx}$ i.e. uptake clearance (CL_{uptake}) into hepatocytes obtained by *in vitro* studies. Moreover, for several types of drugs, the hepatic uptake process has been demonstrated to be the rate-limiting step for systemic clearance [41]. For such compounds, the *in vitro* assessment of their uptake across the sinusoidal membrane is important for assessing CL_H in intact liver.

It has also been suggested that many therapeutic drugs are taken up into hepatocytes via drug transporters [18, 19, 34]. For such drugs, freshly isolated hepatocytes represent a useful experimental system for evaluating their uptake. However, the application of this system using human hepatocytes is hampered by their relatively poor availability. Recently, several laboratories have demonstrated that cryopreserved human hepatocytes can be used to evaluate human drug metabolism [40]. However, there have been few published reports on the drug transport properties of cryopreserved human hepatocytes [18]. Therefore, it is important to demonstrate the validity of cryopreserved hepatocytes as a tool for estimating the transport activity of xenobiotics.

In the present study, transport study of estradiol 17β-D-glucuronide ($E_2$17βG: Fig. 7), a representative substrate for OATP2 and OATP8 [26, 27], was carried out to evaluate the usefulness of cryopreserved human hepatocytes for the assessment of CL_H in human. As OATP2 accepts, in particular, a large number of compounds including therapeutic drugs [18, 19, 25], this study will provide information on the usefulness of this experimental system for the assessment of CL_H of many drugs. This study also aims to evaluate this experimental system for the assessment of the extent of transporter-mediated DDI.

<**Results**>

Uptake of $E_2$17βG

The uptake of $E_2$17βG in HH-093 and HH-099 is shown in Fig. 8. For both, the uptake was saturated by excess unlabeled $E_2$17βG in freshly isolated and cryopreserved hepatocytes. The CL_{uptake} of $E_2$17βG was calculated and is shown in Table 1. A reduction in CL_{uptake} of $E_2$17βG following cryopreservation was observed in some lots and the magnitude of this reduction did not depend on the absolute value of the CL_{uptake} in freshly isolated hepatocytes (Table 1).

The mean CL_{uptake} of $E_2$17βG by 5 samples was reduced to 68% after cryopreservation (Table 1).

Kinetic analysis of the uptake

Eadie-Hofstee plots for the uptake of $E_2$17βG in cryopreserved hepatocytes from five donors are shown in Fig. 9. Both saturable and nonsaturable components were found (Fig. 9). The obtained Michaelis constants (K_m) were 3-18 μM (Table 2). The mean values for the kinetic parameters obtained from multiple lots of hepatocytes revealed a saturable component for $E_2$17βG uptake, which was estimated by the maximum transport rate (V_{max}) divided by K_m, as 66 % of the total uptake (V_{max}/K_m + non-saturable transport (P_{dif})) (Table 2).

<Discussion>

The results of these studies suggest that active transport is retained in cryopreserved human hepatocytes. Of the five human hepatocyte preparations, the CL_{uptake} in cryopreserved hepatocytes, expressed as a percentage of the activity of the hepatocytes before cryopreservation, ranged from 38% to 195% for $E_2$17βG uptake (Table 1). The change in CL_{uptake}, before and after cryopreservation, exhibited an inter-lot variability although the exact mechanism for this remains to be clarified (Table 1). Both saturable and nonsaturable components were observed in the uptake of these compounds (Fig. 9). The K_m for the saturable portion of the $E_2$17βG uptake (3-18 μM: Table 2) was close to that reported in human OATP-C/OATP2 (8 μM) [26] and OATP8 (5 μM) transfected cells [27].

Large inter-lot variations in the transport activity observed (Table 1) may be due to intrinsic inter-individual differences, in part, by the genetic polymorphism of transporters such as OATP-C/OATP2 [42, 43] or due to an artifact produced during the isolation and/or cryopreservation of hepatocytes. However, it also should be noted that such variations were observed in freshly isolated hepatocytes (Table 1). In addition, drug disposition profiles in humans are generally thought to be more variable than those in animals [44]. Therefore, I cannot conclude that the variations observed in this study were solely due to an artifact. However, I cannot find a factor clearly responsible for the inter-lot difference in the CL_{uptake} of $E_2$17βG as far as sex, tobacco usage and alcohol usage (Table 3) are concerned, due to the limited amount of liver samples available.

The kinetic analyses of $E_2$17βG uptake in cryopreserved human hepatocytes have shown that inter-lot differences were observed both in V_{max} /K_m and P_{dif} (Table 2). The range in the V_{max} /K_m values may be due to interindividual differences in the expression level and/or function of transporters although it may be caused by other factors such as the cell integrity being affected during the cell isolation and/or cryopreservation process. It may be also due to inter-lot differences in the driving force for transporters (i.e. the

intracellular glutathione content [45, 46]) although this was not confirmed in the present study. Considering that multiple transporters accept $E_2$17βG as a substrate [26, 27], a large variation in the K_m of $E_2$17βG emphasizes the necessity for further studies to clarify the variability in the contribution of each transporter to the uptake of this substrate in each hepatocyte preparation.

The results obtained in the present studies are consistent with the known species-differences in active transport. Sandker et al. (1994) have reported that the uptake of TC and ouabain in freshly-isolated human hepatocytes was much lower than that in rat hepatocytes [47]. In the report by Kouzuki et al. (1999), the V_{max}/K_m for the uptake of $E_2$17βG in primary cultured rat hepatocytes was 101 μL/min/mg protein, which was much larger than that in cryopreserved human hepatocytes (3.94 μL/min/10^6 cells) [48]. In their report, the K_m for $E_2$17βG in primary cultured rat hepatocytes was 12.9 μM [48], which is higher than that in humans (8.4 μM) (Table 2), whereas the V_{max} in rats was 1300 pmol/min/mg protein [45], which was much higher than that observed in this study in human hepatocytes (33.1 pmol/min/10^6 cells) (Table 2), suggesting that the difference in $E_2$17βG uptake between rats and humans was mainly due to the difference in V_{max} values.

In conclusion, cryopreserved human hepatocytes retain, at least in part, their transporter function for $E_2$17βG i.e. OATP transporter function. Cryopreserved human hepatocytes appear to be a useful tool for examining the mechanism of hepatic uptake of drugs. As isolated hepatocytes are equipped with numbers of enzymes and coenzymes involved in drug metabolism under conditions close to those in the intact liver together with transporters, they can be used as a tool for a more precise estimation of *in vivo* drug metabolism [38, 39]. Recently, to avoid drug-drug interactions (DDI), many *in vitro* assays using microsomes and/or expression systems of metabolizing enzymes have been performed. For this purpose, isolated hepatocytes are a better tool because this experimental system is close to the intact liver and also enables the prediction of transporter-mediated DDI.

1-2

The mechanism of the clinically relevant drug-drug interaction between cerivastatin and cyclosporin A.

Patients who develop hypercholesterolemia after tissue transplantation are sometimes treated with combination therapy with statins and CsA [49]. CsA is an inhibitor of CYP3A4 and, therefore, this immunosuppressant is likely to cause a DDI with simvastatin, lovastatin and atorvastatin, which are all substrates of CYP3A4 [50]. This DDI may also cause an increase in the plasma concentration of statins and result in myopathy and/or fatal rhabdomyolysis. Since CER can undergo metabolism via two pathways, the frequency of DDI was believed to be low. However, Mück et al. (1999) have reported that the plasma concentrations of CER are increased in kidney transplant patients following CsA treatment [14]. They found that the AUC of CER was increased 4-fold by the coadministration of CsA compared with the control [14]. The plasma concentrations of CER were not affected by coadministration of erythromycin [11], a potent mechanism-based inhibitor of CYP3A4 [51], suggesting that it is unlikely that the DDI between CER and CsA is due to CYP3A4-mediated metabolism [9]. Moreover, the AUC of pravastatin, which is not a substrate of CYP3A4, is also increased approximately 21-fold by CsA [52]. Until now, the mechanism of this DDI between CsA and these statins has remained unknown.

Statins are taken up into the liver before undergoing metabolism. The hepatic uptake of some statins has already been studied. For example, in rats, the hepatic uptake of CER [53] and pravastatin [54] has been investigated and their saturable transport systems have been studied. Pravastatin also exhibits saturable uptake in human hepatocytes [18]. However, the uptake of CER by human hepatocytes has not yet been investigated.

In the present study, I examined the uptake of CER into cryopreserved human hepatocytes and OATP2-expressing cells to analyze its hepatic uptake. I also examined the effect of CsA on the hepatic uptake of CER together with its metabolism in order to

clarify the mechanism of the DDI.

<Results>

Uptake into human hepatocytes

Eadie-Hofstee plots of the uptake of [^{14}C]-CER into human hepatocytes prepared from 3 donors are shown in Fig. 10. Both saturable and non-saturable components were observed in all of 3 lots (Fig. 10). The obtained kinetic parameters were 3 - 18 μM, 360 - 5200 pmol/min/10^6 viable cells and 42-70 μL/min/10^6 viable cells for K_m, V_{max} and P_{dif} (Table 4). The saturable component estimated by V_{max}/K_m ranged from 70 to 80 % of the total uptake (V_{max}/K_m+P_{dif}) (Table 4). In lots HH-088 and -117, the inhibitory effect of CsA was examined (Fig. 11). In both lots, a concentration-dependent inhibitory effect was observed (Fig. 11) and the inhibitor concentration to produce a 50 % reduction (IC_{50}) for HH-088 and -117 was 0.280 ± 0.215 and 0.685 ± 0.286 μM (mean ± computer calculated S.E.), respectively.

Uptake study in OATP2-expressing MDCKII cells

The time-courses of uptake of [^{14}C]-CER into human OATP2-expressing MDCKII cells and vector-transfected cells are shown in Fig. 12. The uptake of [^{14}C]-CER into OATP2-expressing cells was 2.6-times higher at 9 min. than that into vector-transfected cells (Fig. 12). In OATP2-expressing cells, the uptake of [^{14}C]-CER observed in the presence of excess unlabeled CER (30 μM) was reduced to the same level as that in vector-transfected cells (Fig. 12). Fig. 13 shows the Eadie-Hofstee plot of the uptake of [^{14}C]-CER in OATP2-expressing and control MDCK cells. The K_m, V_{max} and P_{dif} values for its uptake in OATP2-expressing MDCK cells were 4.28 ± 0.98 μM, 4.30 ± 0.98 pmol/min/mg protein and 0.863 ± 0.038 μL/min/mg protein, respectively. OATP2-mediated uptake of [^{14}C]-CER was also inhibited by CsA in a concentration-dependent manner (Fig. 14). The IC_{50} value for the OATP2-mediated uptake of [^{14}C]-CER was 0.238 ± 0.129 μM (mean ± computer calculated S.E.) (Fig. 14).

Metabolic stability of [^{14}C]-CER

The metabolic stability of [^{14}C]-CER in human microsomes was examined. In Fig. 15, a time-profile of the metabolic stability of [^{14}C]-CER in pooled human microsomes is shown. As a linear metabolic rate in human microsomes was observed for up to 45 min (Fig. 15), the inhibitory effects of CsA, 10 μM quercetin (a CYP2C8 inhibitor [55]) and 0.2 μM ketoconazole (a CYP3A4 inhibitor [56]) on the metabolism of [^{14}C]-CER were followed for 45 min. In Fig. 16a, the metabolic rates of [^{14}C]-CER when incubated in human microsomes in the absence or presence of inhibitors are shown. CsA did not alter the metabolic rate of [^{14}C]-CER up to a concentration of 3 μM and reduced it to at most 71 % of the control value at 10-30 μM while 10 μM quercetin and 0.2 μM ketoconazole reduced it to 63 % and 72 % of the control value, respectively (Fig. 16a). The effect of CsA on testosterone 6β-hydroxylation, which is mediated by CYP3A4, was also followed for 2 min (Fig. 16b). The metabolic rate of testosterone 6β-hydroxylation measured in the absence of inhibitors was 1560 pmol/min/mg protein and it was reduced to 30 and 5.9 % of the control value in the presence of 3 and 30 μM CsA, respectively (Fig. 16b). It was also reduced to 6.5 % of the control value by 0.2 μM ketoconazole and 52 % by 10 μM quercetin (Fig. 16b).

<Discussion>

In vitro uptake studies in isolated hepatocytes revealed saturable transport of [^{14}C]-CER in human hepatocytes (Fig. 10), suggesting the involvement of transporters in the uptake process. In this study, uptake of CER into human hepatocytes was found to be saturable, with a saturable, i.e. transporter-mediated, portion accounting for 70–80 % of the total hepatic uptake. In clinical situations, the maximum plasma concentration (C_{max}) of CER is approximately 4 nM (after a single oral dose of 0.2 mg) [14], which is much lower than the K_m values (2.6–18 μM) obtained in the present study (Fig. 10 and Table 4), suggesting that the hepatic uptake of CER is largely mediated by transporters over the therapeutic range.

The present study revealed a concentration-dependent inhibition of transporter-mediated [^{14}C]-CER uptake by CsA in human hepatocytes with IC_{50} values of 0.28 – 0.69 μM (Fig. 11). The obtained data may, at least partly, explain the clinically observed DDI [14]. Mück et al. (1999) reported that the C_{max} and the AUC of CER in kidney transplant patients given CsA was increased 4- and 3-fold, respectively, when the C_{max} of CsA was approximately 1 μM [14]. In the present study, the saturable component of the uptake of [^{14}C]-CER was mostly inhibited in the presence of 1 μM CsA (Fig. 11). However, considering that approximately 90 % of the CsA in blood is bound to plasma proteins which consist of mainly lipoproteins [57], the clinically relevant unbound concentration of CsA is estimated to be 0.1 μM, which may not be enough to inhibit hepatic uptake of CER. This discrepancy may be explained by a number of factors. Firstly, in the case of oral administration, the plasma concentration of CsA in the circulating blood and portal vein are different and, therefore, the concentration exposed to the liver may be much higher than that observed in the circulating blood [3, 4, 58, 59]. Ito et al. (1998 and 2002) have suggested that the maximum inhibitor concentration at the inlet to the liver can be described by the following equation [3, 4, 58]:

$$I_{in,max} = I_{a,max} + I_{pv,max} = I_{a,max} + \frac{F_a \cdot Dose \cdot k_a}{Q_H} \quad ...(3)$$

where, $I_{in,max}$, $I_{a,max}$ and $I_{pv,max}$ are the maximum inhibitor concentration at the inlet to the liver, in the circulating blood and portal vein, k_a is the absorption rate constant, F_a is the fraction absorbed from the gut to the portal vein, and Q_H is the hepatic blood flow. Using the unbound fraction in the blood (f_u), the maximum unbound inhibitor concentration at the inlet to the liver ($I_{in,max,u}$) can be described by the following equation:

$$I_{in,max,u} = f_u \cdot I_{in,max} \quad \cdots(4)$$

From this equation, the maximum unbound concentration of CsA at the inlet to the liver was calculated to be 0.66 μM, which was enough to lead to a DDI when 225 mg CsA was orally administered. Secondly, the increase in the plasma concentration of CER reported by Mück et al. (1999) could be partly due to the change in the intrinsic hepatic clearance associated with renal failure and/or kidney transplantation[14].

In the present study, CER was shown to be a substrate of human OATP2 (Fig. 12), like pravastatin [18, 19]. The K_m values for the uptake of CER in human hepatocytes were 2.6 – 18 μM while that in OATP2-expressing cells was 4.3 μM (Fig. 13). OATP2-mediated uptake of [^{14}C]-CER was also inhibited by CsA (Fig. 14) and the obtained IC_{50} value (0.24 μM) was within the same range as the values obtained in the inhibition study using human hepatocytes (0.28–0.69 μM) (Fig. 11). These results suggest that the inhibition by CsA on the uptake of CER in human hepatocytes is partly due to OATP2-mediated transport. Since OATP2 accepts a wide variety of compounds as substrates [19, 25], these substrates in addition to CER may possibly exhibit DDI. Indeed, a DDI between pravastatin, a substrate of OATP2, and CsA has been reported, which could also be due to OATP2-mediated uptake in the liver [52]. To avoid this kind of DDI, the characterization of transporters, which are responsible for the drug uptake, and their contributions to total hepatic uptake are very important [21, 22, 48, 60]. The increase in the plasma concentration of drugs associated with a transporter-mediated DDI may be quantitatively predicted from *in vitro* studies that

determine the extent of inhibition of transport in hepatocytes and/or in transporter-expressing cells [61].

We also examined the effect of CsA on the metabolism of [^{14}C]-CER in human microsomes (Fig. 16a). CsA did not markedly reduce the metabolic rate of [^{14}C]-CER up to a concentration of 3 μM and 10-30 μM CsA reduced it only to 70 % of the control value (Fig. 16a). On the other hand, 30 μM CsA markedly reduced testosterone 6β-hydroxylation, which was mediated by CYP3A4, to 30 % of the control value (Fig. 16b). To explain these different effects of CsA on the metabolism of CER and testosterone, we examined the effect of ketoconazole, a potent CYP3A4 inhibitor [56]. As the K_i values of ketoconazole for the inhibition of CYP2C8 and 3A4 functions are 2.5 μM and 0.03 μM, respectively [56, 62], 0.2 μM ketoconazole should be enough to inhibit most of the CYP3A4-mediated metabolism of [^{14}C]-CER and have only a slight effect on that mediated by CYP2C8. Indeed, we have confirmed that 0.2 μM reduced the CYP3A4-mediated metabolism of testosterone to 7 % of the control value. However, 0.2 μM ketoconazole reduced the metabolism of [^{14}C]-CER only to 72 % of the control (Fig. 16a). This study supports the hypothesis that CYP3A4 plays a limited role in the metabolism of CER as previously reported by Mück (2000) [10] and CYP3A4 inhibitors such as ketoconazole and CsA reduce the metabolism of CER to only a limited extent. From the present study, the contribution of CYP3A4 to the total metabolism of CER is estimated to be approximately 38 % (Fig. 15a). We also examined the effect of quercetin, a CYP2C8 inhibitor [55]. As the K_i value of quercetin for the inhibition of CYP2C8-mediated metabolism is 1.3 μM [63], 10 μM quercetin should be enough to inhibit most of the CYP2C8-mediated metabolism of [^{14}C]-CER although it also reduces the CYP3A4-mediated metabolism of testosterone to 50 % of the control value (Fig. 16b). In the presence of 10 μM quercetin, the metabolism of [^{14}C]-CER was reduced to 63 % of the control value (Fig. 16a). This result suggests that CYP2C8 also partly contributes to the metabolism of CER (Fig. 16b). The present study suggests that, at low concentrations (< 3 μM), CsA does not inhibit the metabolism of

CER (Fig. 16a) while it does inhibit its transporter-mediated hepatic uptake at a much lower concentration (< 1 μM) (Fig. 11). This confirms that it is less likely that the DDI between CER and CsA is due to the metabolism of CER.

In conclusion, we should pay more attention to DDI which may originate from the inhibition of transporter-mediated hepatic uptake, since it may occur with a large number of drug combinations, when their elimination (metabolism and/or biliary excretion) takes place following transporter-mediated hepatic uptake.

1-3

***In vitro* to *in vivo* correlation of the effect of cyclosporin A on the disposition of cerivastatin in rats**

I have shown that the clinically relevant DDI between CER and CsA reported by Mück et al. (1999) [14] was, at least in part, due to inhibition of transporter-mediated hepatic. However, the IC_{50} of CsA for the uptake of CER into human hepatocytes (0.2 - 0.7 μM) was higher than the therapeutic unbound concentration of CsA and, therefore, it is hard to fully explain the clinically relevant DDI quantitatively. This may be due to a difference in the CsA concentration between the circulating blood and that at the inlet to the liver [3, 4, 58, 59]. The drug concentration at the inlet to the liver is suggested to be higher than that in the circulating blood when it is orally administered, because of the contribution from the absorbed drug coming from the intestine via the portal vein into the liver [3, 4, 58, 59]. Indeed, the extent of the DDI based on the inhibition of the metabolism in the liver was accurately predicted by using the maximum unbound concentration of inhibitors at the inlet to the liver i.e. that in the circulating blood plus that in the portal vein [58, 64, 65].

CER has been reported to be taken up by primary cultures of rat hepatocytes as well as by human hepatocytes [53]. In human hepatocytes, OATP2 is, at least partly, responsible for CER uptake. In rat hepatocytes, the Oatp family of transporters are also conserved and Oatp1, 2 and 4 are localized in the liver [30-32]. Although the specific transporters responsible for CER uptake in rat hepatocytes remain to be identified, its inhibition of rat Oatp1 and Oatp2 takes place in a concentration-dependent manner, suggesting that these Oatp family transporters may also be responsible for the uptake in rats (data obtained in my own study; Section 2). Moreover, as CsA also inhibits the function of rat Oatp1 and 2 (data obtained in my own study; Section 2), it is possible that the coadministration of CsA resulted in a transporter-mediated DDI in rats similar to that in humans [21, 22].

In the present study, we have examined the inhibitory effect of CsA on the *in vivo* plasma

concentration and hepatic uptake of CER as well as the *in vitro* uptake of CER in isolated rat hepatocytes. The data obtained in the *in vivo* study were compared with those obtained in the *in vitro* study.

<Results>

***In vivo* study**

The steady-state plasma concentrations of CER and the blood concentrations of CsA in rats 5 hours after intravenous infusion are shown in Table 5. The plasma concentration of CER significantly increased in parallel with the blood concentration of CsA (1.40- and 1.44-fold for 1.2 and 3.0 μM CsA: Table 5). The total body clearance (CL_{tot}) of CER was significantly reduced from 1.53 to 1.14 and 1.07 [L/hr/kg] at steady-state blood concentrations of 1.2 and 3.0 μM CsA, respectively.

Uptake into isolated rat hepatocytes

The Eadie-Hofstee plot of the uptake of [^{14}C]-CER into isolated rat hepatocytes is shown in Fig. 17a. Kinetic analyses revealed that the K_m, V_{max} and P_{dif} for the uptake of [^{14}C]-CER into isolated rat hepatocytes were 9.24 ± 2.28 μM, 1520 ± 340 pmol/min/10^6 viable cells, 35.1 ± 4.2 μL/min/10^6 viable cells (mean ± computer calculated S.D.), respectively (Fig. 17a). The saturable component of the hepatic uptake, estimated by V_{max}/K_m, accounted for 82.5 % (Fig. 17a). Uptake studies were also conducted in the presence of 90 % rat plasma to investigate the effect of plasma protein binding (Fig. 17b). The CL_{uptake} of [^{14}C]-CER was reduced in the presence of plasma (Fig. 17b). The kinetic parameters were 16.0 ± 2.4 μM, 480 ± 53 pmol/min/10^6 viable cells and 2.37 ± 0.22 μL/min/10^6 viable cells (mean ± computer calculated S.D.) for K_m, V_{max} and P_{dif}, respectively (Fig. 17b). The saturable component accounted for 92.6 % of the uptake (Fig. 17b).

Inhibition of the uptake of [^{14}C]-CER into isolated rat hepatocytes by CsA.

The uptake of [^{14}C]-CER was examined in the presence of CsA (Fig. 18). Both in the absence and presence of rat plasma, CsA inhibited the uptake of CER into isolated rat hepatocytes in a concentration-dependent manner (Fig. 18). The IC_{50} values were 0.196

± 0.028 and 2.33 ± 0.33 μM (mean ± computer calculated S.D.) in the absence and presence of rat plasma, respectively (Fig. 18).

To determine the inhibition type, the initial uptake rate of [^{14}C]-CER in rat hepatocytes in the absence and presence of CsA was fitted to the following equations (5) and (6) for competitive and noncompetitive inhibition, respectively, and the type of inhibition was determined by the Akaike's Information Criteria (AIC) [65] (Fig. 19).

$$v_0 = \frac{V_{max} \cdot S}{K_m \cdot (1 + I/K_i) + S} + P_{dif} \cdot S \qquad \ldots(5)$$

$$v_0 = \frac{V_{max}/(1 + I/K_i) \cdot S}{K_m + S} + P_{dif} \cdot S \qquad \ldots(6)$$

where, v_0 is the initial uptake rate (pmol/min/10^6 cells), S is the substrate concentration (μM), K_m is the Michaelis constant (μM), V_{max} is the maximal uptake rate (pmol/min/10^6 cells), P_{dif} is the nonsaturable uptake clearance (μL/min/10^6 cells) and K_i is the inhibition constant. In the presence of 0.1 and 0.3 μM CsA, the apparent kinetic parameters (K_m and V_{max}) were changed (Fig. 19). The AIC values obtained by fitting based on eqs. (5) and (6) were –8.83 and 2.10, respectively. Thus, competitive inhibition was observed in the presence of CsA (Fig. 19), with a K_i value of 0.310 ± 0.100 μM (mean ± computer calculated S.D.).

Uptake of [^{14}C]CER into rat Oatp1-expressing cells.

The Eadie-Hofstee plot of the rat Oatp1-mediated uptake of [^{14}C]CER is shown in Fig. 20. The K_m and V_{max} values for the rat Oatp1-mediated uptake of CER were 6.43 ± 1.16 μM and 167 ± 21 pmol/min/mg protein (mean ± computer calculated S.D.), respectively. Rat Oatp1-mediated uptake was also inhibited by CsA (Table 6).

Liver uptake index (LUI) study

The hepatic uptake of CER *in vivo* was also examined by an LUI study in rats (Fig.

21). The %LUI value was reduced following coadministration of CsA in a concentration-dependent manner up to 4 μM (Fig. 21). The reduction in %LUI was 66.9, 54.0 and 49.7 % of the control for 2.0, 2.7 and 4.0 μM of CsA, respectively (Fig. 21).

Metabolism of CER

The metabolism of [^{14}C]-CER in rat microsomes was examined. After a 2 hour-incubation, approximately 74% of [^{14}C]-CER remained unchanged in the absence of inhibitors (metabolic rate was 5.05 ± 0.32 pmol/min/mg protein (mean ± S.E.)) (Fig. 22a). The metabolism of [^{14}C]-CER was not inhibited by CsA up to a concentration of 30 μM while it was significantly inhibited by 0.2 μM ketoconazole (to 24.8 % of the control) (Fig. 22a). The metabolism of testosterone in rat liver microsomes was also examined and the metabolic rate of 6β- and 16α-hydroxylation was 996 ± 22 and 1520 ± 10 pmol/min/mg protein (mean ± S.E.), respectively, in the absence of inhibitors (Fig. 22b). Both 6β- and 16α-hydroxylation were significantly inhibited by 0.3 μM or more CsA (Fig. 22b). Also, 0.2 μM ketoconazole significantly inhibited both reactions (Fig. 22b).

<Discussion>

The present *in vivo* study showed that a DDI between CER and CsA could be reproduced in rats in a dose-dependent manner (Table 5). However, the increase in the steady-state plasma concentration of CER was only 1.4-fold even in the presence of 3 μM CsA (Table 5) while, in humans, the AUC and maximum plasma concentration (C_{max}) increased 3.8- and 5.0-fold, respectively when the C_{max} of CsA was approximately 1 μM [14]. This difference in the severity of the DDI between rats and humans may be partly due to the dosage regimen and experimental system, i.e. in rats, CsA, the inhibitor, was given intravenously and the biliary excreted CsA was eliminated via cannulation while, in humans, it was given orally and biliary excreted, with the CsA being transported to the portal vein via enterohepatic circulation [3, 4, 58]. However, other mechanisms governing DDI and/or renal failure or kidney transplantation may have affected the plasma concentration of CER in the clinical case reported by Mück et al. [14].

In vitro uptake studies in isolated hepatocytes revealed saturable transport of CER in rat hepatocytes both in the absence and presence of rat plasma (Fig. 17). Saturable transport of CER in primary cultured rat hepatocytes has already been reported by Hirayama et al. (2000) [53] although the CL_{uptake} (44.4 μL/min/mg protein calculated by V_{max}/K_m) was lower than that in the present study (165 μL/min/10^6 cells calculated by V_{max}/K_m). This may be due to differences in the experimental system (i.e. isolated and primary cultured hepatocytes) as the transporter function can be affected by the primary culture [37]. In the present study, the transporter-mediated portion was found to account for more than 80 and 90 % of the total hepatic uptake of CER in the absence and presence of plasma, respectively, at concentrations of CER lower than the K_m (Fig. 17). The large saturable portion of the uptake of [^{14}C]-CER in hepatocytes was similar to that in humans (70 - 80 %), suggesting that transporters play an important role in the hepatic uptake and disposition of CER both in rats and humans.

The inhibition study by CsA showed concentration-dependent and competitive

inhibition of the transporter-mediated CER uptake in rat hepatocytes (Fig. 18 and 19). The Oatp1-mediated uptake of CER was also inhibited by CsA (Table 6). The IC_{50} and K_i values (0.2 – 0.3 μM) obtained in the present study were within the same range as that obtained in human hepatocytes (0.2 - 0.7 μM). In the presence of 90 % rat plasma, the IC_{50} value increased approximately 12-fold (Fig. 18), which can be explained by the plasma protein binding of CsA, assuming that only unbound CsA inhibits the uptake of CER. In fact, approximately 90 % of CsA is bound to plasma proteins, mainly lipoprotein, in rats [57]. The LUI study confirmed that the hepatic uptake measured *in vivo* was also affected by CsA (Fig. 21). When the blood concentration of CsA was 4 μM, the hepatic uptake of CER was reduced to 50 % of the control value (Fig. 21), which was similar to the *in vitro* value observed using isolated hepatocytes (Fig. 18b).

I have also examined the effect of CsA on the metabolism of CER in rat liver microsomes. The metabolic rate of CER in rat liver microsomes was slower than that in human liver microsomes. As this metabolism of [^{14}C]-CER was not significantly inhibited by CsA up to a concentration of 30 μM, microsomal metabolism was not the mechanism for the DDI in rats examined in the present study.

The results obtained in *in vitro* studies should be discussed in relation to those *in vivo*. Without administration of CsA, the CL_{tot} was estimated to be 1.53 L/hr/kg (Table 5). In the case of CER, the urinary excretion is negligible [67] and, therefore, the CL_{tot} is close to the hepatic clearance (CL_H). Assuming a well-stirred model, the CL_H can be described by equation (1) and (2) [20, 68]. When the CL_{tot} is 1.53 L/hr/kg, the $f_b \cdot CL_{int,all}$ can be calculated to be 3.12 L/hr/kg assuming the hepatic blood flow rate is 3 L/hr/kg. As shown in Eq. (2), the $CL_{int,all}$ will be reduced to 50 % of the control when the $PS_{u,influx}$ falls to 50 % of the control (Fig. 18). In the presence of 1 and 3 μM CsA, the $PS_{u,influx}$ falls to 68 and 47 % of the control, respectively, (Fig. 17) and, therefore, the $f_u \cdot CL_{int,all}$ is reduced to 2.12 and 1.48 L/hr/kg (i.e. 68 and 47 % of the control), which gives a predicted CL_H value of 1.24 and 0.99 L/hr/kg, respectively, from the equations (1) and (2) in the *in vitro* inhibition study. This

predicted CL_H is comparable with the CL_H observed in the present *in vivo* study (1.14 and 1.07 L/hr/kg, respectively) (Table 4), suggesting that the DDI between CER and CsA in rats can be quantitatively explained only by inhibition of the transporter-mediated uptake of CER.

In conclusion, the DDI between CER and CsA has also been reproduced in rats. This increased plasma concentration of CER when coadministered with CsA to rats can be quantitatively explained only by inhibition of transporter-mediated uptake.

1-4

The mechanism of the drug-drug interaction between cerivastatin and gemfibrozil in humans.

HMG-CoA reductase inhibitors (statins) and fibrates are now well-established treatments for hyperlipidaemia and help prevent cardiovascular diseases [69]. Statins are used to reduce the level of low density lipoprotein (LDL) while fibrates are used to treat hypertriglyceridaemia or as second-line agents in patients intolerant to statins [69, 70]. The combination therapy of statins and fibrates is widely used in clinical practice. However, there are reports of rhabdomyolysis by this combination therapy, mainly involving GEM with lovastatin and CER [71-73]. This may be partly due to DDI caused by events at a pharmacokinetic level although an event at a pharmacodynamic level, i.e. a strong direct effect on myocytes by combination therapy, may be also involved [16, 74, 75]. Indeed, concomitant use of GEM markedly increased the AUC of simvastatin acid, lovastatin acid and CER and produced a small increase in the concentrations of pravastatin and pitavastatin [16, 74, 76-78]. Staffa et al. (2002) reported that 31 patients taking CER had died due to rhabdomyolysis and 12 of them were concomitantly taking GEM [79]. Due to this severe side-effect, CER was voluntarily withdrawn from the market in August 2001.

Reports have appeared describing the mechanism of the pharmacokinetic interaction between CER and GEM [80-82]. In humans, CER is subject to a dual metabolic pathway mediated by CYP2C8 and 3A4 [13]. Wen et al., (2001) and Wang et al. (2002) reported that GEM inhibits multiple isoforms of CYPs including 2C8 but has no inhibitory effects on 3A4 [80, 81]. Therefore, the inhibition of CYP2C8-mediated metabolism may be one mechanism responsible for this clinically relevant DDI. In addition, Prueksaritanont et al. (2002) have suggested that UGT-mediated glucuronidation of stains is an important metabolic pathway because statins are spontaneously converted to the corresponding lactones following UGT-mediated glucuronidation [84]. They have also reported that GEM inhibits this

UGT-mediated glucuronidation of CER as well as CYP-mediated oxidation [82, 83]. The K_i and IC_{50} values in their reports were as high as the total plasma concentration of GEM in the therapeutic range [80-82]. However, taking the high protein binding into consideration, the unbound concentration of GEM is much less than the reported K_i or IC_{50} values, and other mechanism should be considered [16, 80-83, 85-88].

We have already shown that CER is actively taken up into the liver via transporter(s) including OATP2, and this transporter-mediated uptake process was inhibited by CsA in clinical situations (Section 1-2). However, until now, there have been no reports of interaction between GEM and transporters. Gemfibrozil 1-O-β-glucuronide (GEM-1-O-glu), a metabolite of GEM, is taken up and accumulates in isolated perfused rat liver [89-91]. This uptake is inhibited by coadministration of dibromosulfophthalein and clofibric acid while acetoaminophen and its glucuronide produced no inhibition [90, 91]. These results suggest an involvement of transporter(s) in the hepatic uptake of GEM-1-O-glu and, therefore, GEM-1-O-glu might possibly have some effects on the transporter-mediated uptake of CER.

GEM is metabolized to M1-4 by CYPs with M3 being the major metabolites [86]. GEM also undergoes glucuronidation, mainly to gemfibrozil 1-O-β-glucuronide (GEM-1-O-glu) [86]. The plasma concentrations of these metabolites are reported to be relatively high [86, 87]. Therefore, I examined the effects of these metabolites on CYP2C8- and CYP3A4-mediated metabolism of CER, as well as GEM. GEM and its metabolites may inhibit transporter-mediated uptake of CER in the liver, similar to CsA. Therefore, I also examined the effects of GEM and its metabolites on the OATP2-mediated uptake of CER.

<Results>

Inhibitory effects of GEM and its metabolites on OATP2-mediated uptake of [^{14}C]CER.

The effects of GEM, M3 and its glucuronide on the OATP2-mediated uptake of [^{14}C]CER were examined (Figure 23). GEM and both metabolites examined in the present study inhibited OATP2-mediated uptake of [^{14}C]CER in a concentration-dependent manner, without any effects on the uptake in vector-transfected cells (Figure 23). The IC_{50} values of GEM, M3 and its glucuronide for the OATP2-mediated uptake of [^{14}C]CER were 72.4 $\pm$ 28.4, 323 $\pm$ 108 and 24.3 $\pm$ 19.8 μM, respectively (mean $\pm$ S.D.).

Inhibitory effects of GEM and its metabolites on the *in vitro* metabolism of [^{14}C]CER in CYP2C8 and 3A4 expression systems.

The *in vitro* metabolism of [^{14}C]CER was examined in CYP2C8 and 3A4 expression systems. [^{14}C]CER was metabolized at the rate of 7.29 $\pm$ 0.29 and 3.93 $\pm$ 0.21 nmol/h/nmol CYP in CYP2C8 and 3A4 expression systems, respectively, in the absence of inhibitors (Figure 24). 2 different metabolites (M1 and M23) were detected in CYP2C8 expression system while only 1 metabolite (M1) was detected in CYP3A4 expression system. The extents of rate for the M1 and M23 formations in CYP2C8 expression system were 3.79 $\pm$ 0.14 and 2.35 $\pm$ 0.12 nmol/h/nmol CYP, respectively (Figure 25). We examined the effects of GEM and its metabolites, M3 and glucuronide, on the metabolism of [^{14}C]CER in CYP2C8 and 3A4 expression systems (Figures 24 and 25). GEM and its glucuronide preferentially inhibited CYP2C8-mediated metabolism of [^{14}C]CER and produced a slight inhibition on CYP3A4-mediated metabolism, while M3 had no effect (Figure 24). The IC_{50} values of GEM and its glucuronide for the CYP2C8-mediated metabolism were 28.8 $\pm$ 4.8 and 4.25 $\pm$ 1.39 μM (mean $\pm$ S.D.), respectively, and the corresponding values for the CYP3A4-mediated metabolism were 361 $\pm$ 88 and 235 $\pm$ 51 μM (mean $\pm$ S.D.), respectively (Figure 24). The IC_{50} values of GEM and GEM-1-O-glu for the CYP2C8-mediated M1 formation were 37.2 $\pm$ 5.5 and 5.45 $\pm$ 1.34 μM (mean $\pm$ S.D.),

respectively, and those for the CYP2C8-mediated M23 formation were 48.0 ± 10.8 and 5.26 ± 2.73 μM (mean ± S.D.), respectively (Figure 25). The corresponding values for the CYP3A4-mediated M1 formation were 398 ± 94 and 260 ± 54 μM (mean ± S.D.), respectively (Figure 25). Table 7 summarizes IC_{50} values obtained in the present study.

Estimation of the contributions of CYP2C8 and 3A4 to the metabolism of [^{14}C]CER in pooled HLM.

To estimate the contributions of CYP2C8 and 3A4, we examined the effect of a specific inhibitory antibody (Ab) for CYP2C8 and ketoconazole, a potent inhibitor of CYP3A4, on the metabolism of [^{14}C]CER in the pooled HLM (Figure 26). The inhibitory Ab for CYP2C8 inhibited the microsomal metabolism of [^{14}C]CER in a concentration-dependent manner at low concentrations and maximum inhibition was reached at 5 μL/100 μg microsomes (Figure 26a). At maximum inhibition, the microsomal metabolism of [^{14}C]CER decreased to 38.9 ± 2.7 % (mean ± S.E.) of the control (Figure 26a) and, therefore, the contribution of CYP2C8 was estimated to be 61 %. In the presence of inhibitory Ab for CYP2C8, M23 formation was completely inhibited while M1 formation fell only to 61.2 ± 2.9 % (mean ± S.E.) of the control (Figures 26b and 26c). Ketoconazole also reduced the microsomal metabolism of [^{14}C]CER in a concentration-dependent manner (Figure 26d). However, the inhibition studies using CYP2C8 and 3A4 expression systems showed that it inhibited not only CYP3A4-mediated metabolism but also that mediated by CYP2C8 (Figure 26d). At 0.1 μM, most of the CYP3A4-mediated metabolism of [^{14}C]CER was inhibited with only a minimal effect on that mediated by CYP2C8 (Figure 26d) and, therefore, 0.1 μM ketoconazole was used to estimate the contribution of CYP3A4. 0.1 μM ketoconazole reduced the metabolism of [^{14}C]CER to 63.4 ± 7.2 % (mean ± S.E.) of the control (Figure 26d), suggesting that the contribution of CYP3A4 was, at most, 37 %. 0.1 μM ketoconazole reduced the M1 formation to 62.6 ± 5.6 % (mean ± S.E.) of the control and slightly decreased M23

formation to 77.6 ± 11.3 % (mean ± S.E.) of the control (Figures 26e and 26f). Table 8 summarizes the results.

Inhibitory effects of GEM and its metabolites on the *in vitro* metabolism of [^{14}C]CER in pooled HLM.

We examined the inhibitory effects of GEM and GEM-1-O-glu on the metabolism of [^{14}C]CER in pooled HLM (Figure 27). GEM and GEM-1-O-glu inhibited the metabolism of [^{14}C]CER in pooled HLM in a concentration-dependent manner (Figure 27) while M3 had no effects (data not shown). Figure 27 also shows simulation curves for the inhibitory effects of GEM and GEM-1-O-glu in pooled HLM using IC_{50} values for CYP2C8- and 3A4-mediated metabolism obtained in the inhibition study in CYP expression systems (Table 7) and the contributions of CYP2C8 and 3A4 (Table 8).

Human serum protein binding of GEM and its metabolites.

We examined the protein binding of GEM and its metabolites in 50 mM phosphate buffered human serum (pH7.4). The unbound fractions (f_u) of GEM, M3 and GEM-1-O-glu were 0.648 ± 0.037, 1.23 ± 0.00, 11.5 ± 2.3 % (mean ± S.E.), respectively.

<**Discussion>**

It has already been reported that GEM is an inhibitor for CYP- and UGT-mediated metabolism of CER [80, 82, 83]. In the present study, GEM inhibited the OATP2-mediated uptake of CER as well as its metabolism (Figure 23). The IC_{50} value of GEM for OATP2-mediated uptake of [^{14}C]CER (72 μM) was similar or lower comparing with the reported IC_{50} values for metabolism [80, 82, 83]. It was also found that a metabolite of GEM, GEM-1-O-glu, was a potent inhibitor of OATP2-mediated hepatic uptake of CER with a lower IC_{50} value (24 μM) than that of GEM itself (Figure 23). This finding was matched with the fact that many glucuronides are recognized by OATP family transporters as substrates and/or inhibitors with a high affinity [26, 27, 92].

I also examined the inhibitory effect of GEM and its metabolites on the CYP2C8- and 3A4-mediated metabolism of [^{14}C]CER in the present study. This observation should be discussed in relation to the previous reports [80, 82]. Wang et al. (2002) reported that GEM inhibited CYP2C8-mediated metabolism of CER into M1 and M23 with IC_{50} values of 78 and 68 μM, respectively [80]. The corresponding values in the present analysis were 37 and 48 μM, respectively (Figure 25) and are comparable with the values reported by Wang et al. (2002) [80]. Prueksaritanont et al. (2002) reported the IC_{50} values of GEM for M1 and M23 formations in HLM to be 220 and 87 μM, respectively [82], and Wang et al. (2002) reported the corresponding values to be >250 and 95 μM, respectively [80]. As shown in Figure 27, I also observed a concentration-dependent reduction of M1 and M23 formations in HLM. The apparent IC_{50} values of GEM for M1 and M23 syntheses in HLM was calculated to be 237 and 27 μM, respectively (Figure 27), and are also similar to those from previous reports [80, 82].

In the present study, it was clarified that GEM and GEM-1-O-glu inhibited both OATP2-mediated hepatic uptake and metabolism. The overall hepatic intrinsic clearance ($CL_{int,all}$) can be described by the equation (2) [20, 68]. In the case of GEM and GEM-1-O-glu, they may affect $PS_{u,influx}$ and CL_{int} of CER. $CL_{int,all}$ is directly affected by $PS_{u,influx}$, i.e.

hepatic uptake, and it can be also affected by CL_{int}, i.e. metabolism. Hence, the coadministration of GEM may lead to a DDI due to the inhibition of hepatic uptake and metabolism of CER. The possibility of clinically relevant DDI should be discussed taking the therapeutic concentration of inhibitor drugs into consideration. Concomitantly administered drugs, which are inhibitors of drug metabolism and transporter-mediated hepatic uptake, will reduce the $PS_{u,influx}$ and CL_{int} in equation (2) to $1/(1+\frac{I}{IC_{50}})$ of the control [61]. In this case, the maximum reduction in $CL_{int,all}$ is described by the following equation [61]:

$$\frac{1}{1+I/IC_{50\_OATP2}} \times \frac{1}{1+I/IC_{50\_metabolism}} = \frac{1}{1+I/IC_{50\_OATP2}} \times \left(\frac{R_{CYP2C8}}{1+I/IC_{50\_CYP2C8}} + \frac{R_{CYP3A4}}{1+I/IC_{50\_CYP3A4}} \right) \quad \ldots(7)$$

where $IC_{50\_metabolism}$ is the apparent IC_{50} value for the total metabolism of [^{14}C]CER in HLM, R_{CYP2C8} and R_{CYP3A4} represent the contributions of CYP2C8 and 3A4 to the metabolism of CER (Table 8). This equation suggests that the ratio of the therapeutic concentration of inhibitors to the IC_{50} values determine the degree of DDI in clinical situations. Table 9 summarizes the total and unbound plasma concentrations of GEM and its metabolites. In the report by Backman et al. (2002), the mean maximum concentration of GEM after repeated oral administration of 600 mg twice a day was 150 μM [16]. Okerhelm et al. (1976) measured the plasma concentrations of free GEM, its glucuronide conjugates and other metabolites after a single oral administration of 600 mg [^{3}H]GEM in normal human subjects receiving 600 mg unlabeled GEM twice daily for 6 days [87]. In their report, the maximum concentration of glucuronide conjugates, mainly GEM-1-O-glu, was approximately 20 μM while that of total GEM (GEM + glucuronide conjugate) was approximately 100 μM. In the report by Hengy and Kölle (1985), 10 - 15 % of GEM in plasma was present as glucuronide conjugates [88]. Although the inhibitory effect of M3 on the hepatic uptake and the metabolism of CER examined in the present study is minimal, its plasma concentration seems to be high. After a single oral administration of 450 mg

GEM, the plasma concentration of M3 was high as far as metabolites were concerned [86] and the plasma concentration of total metabolites reached 50 μM in the report by Okerhelm et al. (1976) [87]. The total concentrations of GEM and GEM-1-O-glu were similar or higher than the IC_{50} values for the metabolism and the hepatic uptake of CER in the present study (Table 9). However, taking the high plasma protein binding into consideration, the unbound concentrations of GEM, M3 and GEM-1-O-glu were at most 0.97, 0.62 and 2.3 μM, respectively, i.e. less than the IC_{50} values obtained in the present study (Table 9). The unbound concentrations of GEM and GEM-1-O-glu give only a small reduction in the overall hepatic clearance of CER with $1+\frac{I}{IC_{50\_metabolism}}$ values of 1.0 and 1.4, respectively (Table 9), suggesting that this is unlikely to cause the reported serious DDI between CER and GEM. However, it is possible that GEM or its metabolites inhibit the metabolism of CER in the liver if they are actively transported to the liver and accumulate there. Indeed, Sallustio et al. (1996) have reported that GEM-1-O-glu is actively taken up by perfused rat liver and the liver/perfusate concentration ratio is 35 – 42 [89]. Assuming that it also accumulates also in the human liver, its unbound concentration there would be higher than the IC_{50} value for the microsomal metabolism, which gives a $1+\frac{I}{IC_{50\_metabolism}}$ value of 3.4 - 3.6 (Table 9).

In the present study, GEM and GEM-1-O-glu preferentially inhibited CYP2C8-mediated metabolism of CER (Figures 24 and 25). These results support the findings by Backman et al. (2002) [16]. They reported that the AUC of M23 was markedly reduced to 17 % of the control while that of the open acid form of CER, the lactone form of CER and M1 were 4.4, 3.5 and 3.5 times higher than the control. M23 formation is specifically mediated by CYP2C8, and not by 3A4 in the present study. Therefore, the inhibition on CYP2C8 satisfactorily explains this DDI. In the report by Backman et al. (2002), all the ratios of AUC for each of the metabolites to the open acid form of CER fell,

following coadministration of GEM, to 82, 8.8 and 80 % of the control for M1, M23 and the lactone form of CER, respectively [16]. The reduction in the AUC of M1 and the lactone form may be partly due to inhibition on the hepatic uptake of CER, which might alter its elimination in the liver (Table 9).

Other statins, including simvastatin, lovastatin, pravastatin and pitavastatin, are also affected by the coadministration of GEM [74, 76-78]. GEM increases the AUC of the open acid form of these statins [16, 74, 76-78]. However, it does not affect the AUC of the lactone form of simvastatin and lovastatin, and reduces that of pitavastatin [74, 76, 78]. On the other hand, GEM has no effects at all on the plasma concentration of fluvastatin [93]. The limited effect of GEM only on the plasma concentrations of the open acid forms of simvastatin and lovastatin can be explained by inhibition of lactone formation followed by UGT-mediated glucuronidation [82]. The reduced AUC of the lactone form of pitavastatin may also be explained by the same mechanism [94]. On the other hand, the increase in the AUC of the open acid forms of pravastatin and pitavastatin may be partly explained by inhibition of their OATP2-mediated uptake, as these statins are substrates of OATP2 [18, 19, 95]. Indeed, cyclosporin A, an inhibitor of OATP2, markedly increases the AUC of pravastatin and pitavastatin as well as CER [52, 96]. However, GEM increases the AUC of pravastatin and pitavastatin only by 2.0- and 1.3-fold, respectively, while it increases that of CER 4.4-fold [16, 77, 78]. The increase in the AUC of pravastatin can be partly explained by its reduced renal excretion and, therefore, the effect of GEM on the elimination of pravastatin in the liver is weaker [77]. The varied effects on different statins may be due to the fact that GEM and its metabolites inhibit both the uptake and CYP2C8-mediated metabolism of CER in the liver while they inhibit only hepatic uptake of pravastatin and pitavastatin and, on the other hand, CsA inhibited the hepatic uptake of these statins at the therapeutic concetrations. Indeed, the effect of GEM and GEM-1-O-glu on OATP2-mediated uptake was weak (Table 9).

In conclusion, GEM and GEM-1-O-glu are potent inhibitors of the CYP2C8-mediated metabolism and OATP2-mediated hepatic uptake of drugs. Their inhibition of the

CYP2C8-mediated metabolism of CER (mainly by GEM-1-O-glu) is a major mechanism which governs the clinically relevant DDI between CER and GEM, while their inhibition of the OATP2-mediated uptake of CER may also contribute to the DDI, but to a lesser extent.

[Section 2]

Comparative inhibitory effects of different inhibitors on rat Oatp1 (*Slc21a1*)- and Oatp2 (*Slc21a5*)-mediated transport. A search for specific inhibitors of these transporters

Previously, drug uptake studies have been performed in sinusoidal membrane vesicles and in isolated and cultured hepatocytes in order to characterize the transport properties of hepatocellular drug uptake [18, 97]. In isolated and primary cultured hepatocytes, it is also possible to predict the *in vivo* elimination rate of drugs from the initial uptake rate in isolated or primary cultured hepatocytes by considering the number of hepatocytes per g liver [18, 37]. More recent studies to investigate the molecular mechanism of hepatic drug uptake have shown that Oatp1 (*Slc21a1*), Oatp2 (*Slc21a5*), Oatp4 (*Slc21a10*) and Oat2 (*Slc22a7*) are involved in the hepatic uptake of anionic compounds from the sinusoidal membrane in rats [30-31].

Studies with cRNA-injected *Xenopus laevis* oocytes and cDNA-transfected mammalian cells have shown that many kinds of substrates, including organic anions [30, 35, 98, 99], steroids [31, 35, 100] and bulky organic cations [101], are transported by members of the Oatp family. Other studies show that taurocholate, triiodothyronine and thyroxine are common substrates of Oatp1, Oatp2 and Oatp4 [31, 102, 103], whereas bile acids, including cholate and glycocholate, organic anions, including estradiol 17β-D-glucuronide ($E_2$17 β G) and estrone 3-sulfate, ouabain and type II organic cations, including N-(4,4-azo-n-pentyl)-21-deoxyajmaline and rocuronium, are substrates of both Oatp1 and Oatp2 [101, 103]. In addition, digoxin is a specific substrate of Oatp2 [31, 32] and leucotriene C_4 is recognized as a substrate by Oatp1 and Oatp4, but not by Oatp2 [32, 46, 103]. These findings suggest that the hepatic transporters have a partially overlapping substrate specificity, i.e. some substrates are transported by more than one transporter.

Although some substrates are known to be taken up into hepatocytes by multiple cloned transporters, investigations of the relative contribution of individual transporters to the overall hepatic uptake have been rather limited until now. One of the methods to estimate their contribution is to inhibit a single or multiple transporter(s) using a specific inhibitor. Although the contribution of drug metabolizing enzymes (isoforms of cytochrome P450) has been examined in detail using this method [104], the contribution of transporters remains to be investigated.

In the present study, I focused particularly on the function of Oatp1 and Oatp2, and analyzed the comparative effect of inhibitors of these two transporters using Oatp1- and Oatp2-stably expressing LLC-PK_1 cells.

<Results>

Concentration-dependent uptake of $E_2$17βG and digoxin in Oatp1- and Oatp2-expressing LLC-PK_1 cells

The concentration-dependent uptake of $E_2$17βG and digoxin was examined in Oatp1- and Oatp2-expressing LLC-PK_1, respectively, to evaluate these experimental systems. Eadie-Hofstee plots of their uptake in transporter-expressing cells and mock transfected cells are shown in Fig. 28. As shown in Fig. 28, concentration-dependent uptake of the substrates was observed in transporter-expressing cells but not in mock-transfected cells (Fig. 28). The obtained K_m, V_{max} and P_{dif} values for the uptake of $E_2$17βG in Oatp1-expressing cells were 11.2 ± 4.7 μM, 114 ± 42 pmol/min/mg protein and 0.726 ± 0.479 μL/min/mg protein, respectively. The corresponding values for the uptake of digoxin in Oatp2-expressing cells were 279 ± 57 nM, 1.76 ± 0.33 fmol/min/mg protein and 0.856 ± 0.171 μL/min/mg protein.

Comparative effect of inhibitors on Oatp1- and Oatp2-mediated transport

In order to identify inhibitors which selectively inhibit Oatp1- or Oatp2-mediated transport, the inhibitory effects of a wide range of different compounds on the Oatp1-mediated transport of $E_2$17βG and the Oatp2-mediated transport of digoxin were compared. As shown in Table 10, seventeen compounds showed a concentration-dependent inhibition of both Oatp1 and Oatp2. In contrast, propionic acid (a monocarboxylate), α-ketoglutarate (a dicarboxylate) and *p*-aminohippurate inhibited neither Oatp1- nor Oatp2, even at concentrations as high as 1000 μM (Table 10). Some inhibitors showed a selective inhibition of Oatp1 or Oatp2: NSAIDs (indomethacin, ibuprofen, ketoprofen and naproxen), deoxycorticosterone and quinidine preferentially inhibited Oatp1-mediated transport, whereas rifampicin, digoxin and quinine preferentially inhibited Oatp2-mediated transport (Table 10). To investigate their selectivity for these transporters, more detailed studies of their inhibitory effects were performed.

Inhibitory effects of ibuprofen

The concentration-dependent inhibitory effect of ibuprofen on the Oatp1-mediated transport of $E_2$17βG and the Oatp2-mediated transport of digoxin are shown in Fig. 29. In this study, ibuprofen concentrations ranged from 0 to 3000 μM. Although ibuprofen inhibited both Oatp1 and Oatp2 in a concentration-dependent manner, it inhibited Oatp1 more potently at low concentrations (Fig. 29). In contrast, ibuprofen had no effect on nonsaturable uptake into vector-transfected cells (Fig. 29). The K_i values for Oatp1 and Oatp2 were 126 ± 77 μM and 2430 ± 1590 μM (mean ± computer calculated S.D. value), respectively, supporting its selective inhibitory effect on Oatp1 (Fig. 29).

Inhibitory effects of rifampicin

The concentration-dependent inhibitory effect of rifampicin on the Oatp1-mediated transport of $E_2$17βG and the Oatp2-mediated transport of digoxin is shown in Fig. 30. The concentration of rifampicin ranged from 0 to 300 and 0 to 500 μM for the inhibition of Oatp1 and Oatp2, respectively. Rifampicin preferentially inhibited Oatp2 rather than Oatp1 (Fig. 30). Its K_i values for Oatp1 and Oatp2 were 18.2 ± 11.2 μM and 1.46 ± 0.58 μM (mean ± computer calculated S.D. value), respectively.

Inhibitory effects of quinine and quinidine

We also investigated the inhibitory effects of quinine and its stereoisomer quinidine on Oatp1 and Oatp2. The concentrations of quinine and quinidine ranged from 0 to 1000 μM and from 0 to 400 μM, respectively. As shown in Fig. 31, although quinine inhibited Oatp2 more potently, its stereoisomer, quinidine, preferentially inhibited Oatp1. The K_i values of quinine for Oatp1 and Oatp2 were 76.7 ± 15.6 μM and 3.81 ± 1.36 μM (mean ± computer calculated S.D. value), respectively, and the corresponding values for quinidine were 9.27 ± 4.92 μM and 120 ± 27 μM (mean ± computer calculated S.D. value).

Inhibitory effect of digoxin

Although digoxin inhibited Oatp1-mediated transport only minimally, its inhibitory effect on Oatp2 was potent at 100 μM (Table 10). Based on these results, we focused on the inhibitory effect of digoxin at lower concentrations to examine its selectivity for Oatp2. Up to 10 μM, digoxin inhibited Oatp2 in a concentration-dependent manner without affecting Oatp1 (Fig. 32). 10 μM digoxin almost completely inhibited Oatp2-mediated transport without significantly inhibiting Oatp1-mediated transport, suggesting that digoxin is a selective inhibitor of Oatp2 (Fig. 32). The K_i value for the Oatp2-mediated transport was 0.196 ± 0.037 μM (mean ± computer calculated S.D. value), which is much smaller than that for Oatp1 (> 100 μM).

<Discussion>

In the present study, I investigated the effect of 20 compounds on Oatp1- and Oatp2-mediated transport in order to find a selective inhibitor of each of these transporters. As candidates for such selective inhibition, I chose compounds which (1) are actively taken up into rat hepatocytes, (2) are inhibitors of transporter-mediated uptake in rat hepatocytes and/or (3) are substrates or inhibitors of Oatp family transporters. Although many of them inhibited both Oatp1 and 2 to comparable degrees, some of them preferentially inhibited one transporter: NSAIDs, deoxycorticosterone and quinidine preferentially inhibited Oatp1, whereas digoxin, rifampicin and quinine preferentially inhibited Oatp2 (Table 10). These compounds may act as selective inhibitors at appropriate concentrations. Comparison of the K_i values of digoxin for Oatp1 and Oatp2 revealed that this cardiac glycoside acts as a selective inhibitor of Oatp2 over a wide range of concentrations (3.7 ~ 10 < μM). In contrast, the selectivity of the other inhibitors described above was not high; indeed there was only a 13- ~ 20-fold difference in K_i values between Oatp1 and Oatp2.

Kinetic analysis revealed that the K_m values for the uptake of $E_2$17βG and digoxin in Oatp1- and Oatp2-expressing LLC-PK_1 cells, respectively, were within the same range as the reported values [31, 48] and the P_{dif} for both substrates in transporter-expressing cells were close to their uptake clearance in mock transfected cells (Fig. 28). These results suggest that the saturable transport of each substrate is mediated mainly by Oatp1 or Oatp2 and the nonsaturable transport is due to passive diffusion, similarly to the passive diffusion in mock transfected cells. The uptake in mock transfected cells did not show any concentration-dependence, suggesting that LLC-PK_1 cells do not have any endogenous transporters which make a significantly contribution to any uptake. Therefore, most of the saturable transport seen in transporter-expressing cells can be regarded as being mediated by only a single transporter: Oatp1 or Oatp2.

The results of the present study should be discussed in relation to the previous findings in isolated hepatocytes. Kouzuki et al. (1999) have investigated the transport properties of

ibuprofen and indomethacin in primary cultured rat hepatocytes and COS-7 cells transiently expressing Oatp1, along with the inhibitory effect of indomethacin on the function of Oatp1 [48, 105]. Although both compounds were actively taken up into rat hepatocytes, this uptake was not mediated by Oatp1 [48, 105]. Indomethacin inhibited the function of Oatp1 in a concentration-dependent manner, with IC_{50} values of 10 - 100 μM (Table 10), which is within the same range as the estimated K_i value in an earlier report [106]. In addition, we have shown that both NSAIDs are able to inhibit the function of Oatp2, with higher K_i values than those for Oatp1 (Table 10 and Fig. 29).

I also found that rifampicin preferentially inhibited Oatp2-mediated transport (Table 10 and Fig. 30), which was consistent with the report by Fattinger et al. (2000) [107]. However, although these authors reported that 100 μM rifampicin minimally inhibited Oatp1-mediated transport (reduced to 94% of the control), the present results suggest that this concentration of rifampicin reduced the Oatp1-mediated transport of $E_2$17βG to 47% of the control (Table 10 and Fig. 30). This discrepancy may be due to the difference in the host cells: Fattinger et al. (2000) used cRNA-injected *Xenopus laevis* oocytes, whereas I used cDNA transfected LLC-PK_1 cells [107].

The present finding that quinine, but not quinidine, is a potent inhibitor of the Oatp2-mediated transport of digoxin supports the previous findings by Hedman and Meijer (1997) that the uptake of digoxin into isolated rat hepatocytes is potently inhibited by quinine, but not by quinidine [108]. However, Hedman and Meijer (1997) did not determine the K_i values of quinidine and quinine for the uptake of digoxin in isolated rat hepatocytes, although 25 and 50 μM quinine almost completely inhibited the saturable portion whereas 50 μM quinidine allowed more than half the activity to be retained [108]. This suggests that the K_i values for quinine and quinidine may be << 25 μM and >50 μM, respectively. These values are consistent with the K_i values determined in the present study (Fig. 31).

I also found that cimetidine, a type I organic cation, did not inhibit the function of either Oatp1 or Oatp2 at low concentrations (Table 10), which is consistent with the

previous report by van Montfoort et al. (1999) who showed that type I organic cations did not significantly interact with Oatp family proteins [101]. In contrast, I found that quinidine and quinine, type II organic cations, inhibited Oatp1 and Oatp2 function (Table 10 and Fig. 31). Although it is not yet known if these two compounds are transported by Oatp family proteins, van Montfoort et al. (1999) demonstrated that N-methyl-quinine is transported by Oatp1, but not by Oatp2, and that *N*-methyl-quinidine is not transported by either of these transporters [101].

Using a selective inhibitor, the contributions of transporter(s) to the hepatic uptake of drugs of interest can be estimated. Among the selective inhibitors examined in the present study, digoxin is the most useful for estimating the contribution of Oatp2 *in vitro* due to the large difference in K_i values between Oatp1 and Oatp2. This method should be discussed in relation to the method previously proposed.

Previously, Hagenbuch et al. (1996) estimated the contributions of Na^+-taurocholate transporting polypeptides (Ntcp) and Oatp1 to the uptake of taurocholate (TC) and sulfobromophthalein (BSP) using *Xenopus laevis* oocytes injected with total rat liver mRNA and antisense oligonucleotides [109]. Although this is a useful approach, the practical application of this method may be limited since there is often difficulty in observing a significant uptake of test compounds into oocytes injected with total rat liver mRNA. Kouzuki et al. (1999) have compared the uptake of compounds into cultured rat hepatocytes and COS-7 cells transiently expressing Ntcp and Oatp1 and estimated the relative contributions of Ntcp and Oatp1 to the total uptake in cultured rat hepatocytes by normalizing the uptake of test compounds with respect to that of representative substrates of these transporters [48, 60]. In determining the contribution of the cloned transporters to the cellular uptake, the use of selective inhibitors may be helpful, together with these previously proposed methods. Indeed, by comparing the uptake of temocaprilat into hepatocytes and Oatp1 expressing COS-7 cells, Ishizuka et al. suggested that approximately 50% of the uptake of this ACE inhibitor into rat hepatocytes might be

accounted for by Oatp1 [34]. This result is consistent with the finding that approximately 50% of temocaprilat uptake into rat hepatocytes is inhibited by an excess (up to 40 μM) of $E_2$17βG [34]. However, it is possible that the presence of other, as yet unidentified, transporters may also affect this kind of analysis. For accurate estimation of the contribution, molecular cloning of additional important transporters is required.

In conclusion, we have performed comparative studies of the inhibitory effects of a wide range of compounds on Oatp1- and Oatp2-mediated transport and found that ibuprofen and quinidine preferentially inhibit Oatp1, whereas digoxin and quinine preferentially inhibit Oatp2. At appropriate concentrations, they are able to act as selective inhibitors of Oatp1 or Oatp2. These inhibitors may be used to estimate the contribution of Oatp1 and Oatp2.

<Conclusion>

From the present analyses, I conclude that the clinically relevant DDI between CER and CsA is, at least partly, caused by transporter-mediated hepatic uptake while the DDI between CER and GEM is mainly caused by the inhibition of the metabolism of CER by one of the metabolites of GEM, GEM-1-O-glu. Although GEM itself also has an inhibitory effect on the metabolism of CER and, in addition, GEM and GEM-1-O-glu are inhibitors of OATP2-mediated hepatic uptake of CER, these effects possibly do not change the *in vivo* disposition of CER at clinically relevant concentrations. Although the clinically relevant DDI between CER and CsA could not be quantitatively explained by using the unbound concentration of CsA in the circulating blood, the unbound concentration of CsA in the blood at the inlet to the liver estimated by the method of Ito et al. (1998) [3, 4, 58]. The study using rats suggests that the DDI between CER and CsA can be fully explained only by inhibition of the hepatic uptake process of CER by CsA; data obtained, using the steady-state blood concentration of CsA after continuous intravenous infusion, also support this conclusion.

CsA is a well-known inhibitor of CYP3A4 and P-glycoprotein (P-gp) [110, 111]. The present finding suggests that CsA is an inhibitor of hepatic uptake transporters like OATP2 as well and, therefore, CsA possibly causes a transporter-mediated DDI. This fact suggests that many DDI caused by coadministration of CsA may be, at least partly, due to inhibition of transporter-mediated hepatic uptake.

On the other hand, GEM is reported to inhibit metabolic enzymes including CYP1A2, 2C8, 2C9 and 2C19 and UGT [80-82]. However, because of the high K_i or IC_{50} values, it is less likely that GEM alters the in vivo disposition of drugs which undergo the metabolism mediated by these enzymes, taking the unbound plasma concentration of GEM in clinical situations into consideration. Although GEM was shown to inhibit OATP2-mediated transport, the obtained IC_{50} value was also too high to produce a clinically relevant DDI. GEM-1-O-glu is also an inhibitor of the OATP2-mediated uptake and the metabolism of

CER with a lower IC_{50} value, however, its plasma unbound concentration in clinical situations is also too low to produce a DDI. However, this metabolite is thought to be actively taken up into the liver, and the concentrated GEM-1-O-glu may inhibt the metabolism of CER, leading to a severe interaction in clinical situations.

In the case of transporter-mediated DDI such as CER and CsA, isolated human hepatocytes are a good tool for quantitative prediction. However, due to the scarcity of human hepatocytes, their use is limited athough they are commercially available. Therefore, the expression systems of human transporters may be useful for the quantitative analysis of the hepatic uptake and transporter-mediated DDI with information about the contributions of transporters to the total uptake of drugs in the liver. In the present study, we compared the inhibitory effects of different compounds on rat Oatp1 and Oatp2, in an attempt to construct a method to estimate their contributions. We have found some inhibitors which can be used for the selective inhibition of each of these transporters to calculate their contributions. This method can be applied to the human transporters and, in the future, will be useful for the further analysis of drug transport and transporter-mediated DDI.

< Perspectives>

This study is the first report showing that inhibition of transporter-mediated hepatic uptake is the mechanism of a clinically relevant DDI. Although there have been many reports that therapeutic drugs are substrates or inhibitors of transporters [18, 19, 27, 112], my analysis is the first one which quantitatively demonstrated that a concomitantly administered drug possibly inhibits the transporter-mediated uptake of another drug in the liver at therapeutic concentrations. Until now, there have been few reports of clinically relevant DDI, clearly proved to be caused by a transporter-mediated uptake process. However, considering that many therapeutic drugs are substrates of transporter(s), many clinically relevant DDI could be, at least partly, caused by the transporter-mediated hepatic uptake process.

I believe this type of study, i.e. a quantitative analysis of the inhibitory effect of drugs and comparison with the therapeutic concentrations, will be needed for further studies of clinically relevant DDI. For the quantitative prediction of transporter-mediated DDI, cryopreserved human hepatocytes are very useful as shown in my present work. The transporter expression systems will also be a good tool for this purpose, with information about the contributions of each transporter to the total hepatic uptake. We proposed a method to estimate the contributions of transporter(s) by using specific or selective inhibitor for each transporter. Sugiyama et al. (2001) have used this method to estimate the contributions of rat Oatp and Oat family transporters to the efflux of $E_2$17βG in brain across the blood-brain barrier [113]. However, there are some reports which have proposed other methods to calculate the contribution of each transporter. Hagenbuch et al. (1996) proposed a method to estimate the contribution of each transporter by the coinjection of antisense DNA for the transporter in total liver cRNA injected *Xenopus leavis* oocytes [109]. Kouzuki et al. (1999) have proposed a relative contribution of each transporter relative to that of the reference compounds, which are assumed to be taken up by a specific transporter [60, 106]. Hasegawa et al. (2003) also used estimated the contributions of rat

Oat1 and 3 to the renal elimination of organic anions and nucleoside derivatives by using the relative contributions [114]. The method using total liver cRNA-injected oocytes coinjected with antisense DNA has a disadvantage that total liver cRNA-injected oocytes have only a limited uptake capacity for most of drugs and, therefore, it is difficult to detect their uptake and estimate the accurate contributions made by specific transporters. The estimation of the relative contribution is useful but it is necessary to find a good reference compound which is predominantly taken up by a specific transporter. However, the method using specific or selective inhibitors also has a disadvantage that no inhibitors of human transporters have been reported to be suitable for this analysis yet and further research to discover specific inhibitors will be required.

In the present study, the mechanism of the severe interaction between CER and GEM was analyzed. This interaction was not caused by the inhibition of the transporter-mediated uptake of CER, but by the inhibition of the metabolism of CER by one of the metabolites of GEM, GEM-1-O-glu. However, transporters play an important role even in this interaction because concentrated GEM-1-O-glu taken up into the liver via transporter(s) inhibited metabolism. As many conjugated metabolites are actively taken up into the liver via transporters, we should pay more attention to their inhibitory effects on the metabolism.

In the present study, I have reported novel mechanism of clinically relevant DDI and suggested methods for the quantitative prediction of them. To avoid such severe interactions, we should recognize the importance of transporters on the drug disposition and many DDI as well as the metabolism.

<Materials and Methods>

Section 1

Materials

[^{3}H]-$E_2$17βG was purchased from New England Nuclear (Boston, MA, USA). [^{14}C]-CER was kindly provided by Bayer AG (Wuppertal, Germany). Unlabeled $E_2$17βG and cyclosporin A were purchased from Sigma-Aldrich (St. Louis, MO, USA). All other reagents are of analytical grade. GEM was purchased from Sigma-Aldrich (St. Louis, MO). A metabolite of GEM, M3 was chemically synthesized in KNC Laboratories, Co. Ltd. (Kobe, Japan). GEM-1-O-glu was enzymatically synthesized from GEM using rat liver microsomes as the glucuronide-conjugate of GEM is mostly GEM-1-O-glu in rats [115, 116]. 2 mg/mL GEM was incubated at 37 ^{o}C with rat microsomes (3.6 mg protein/mL) and 5 mg/mL UDP glucuronic acid in 100 mM glycine-NaOH buffer (pH 8.5) supplemented with 20 % (w/v) glycerin for 27 h, followed by the addition of 1 N HCl to bring the pH to 4.0. This sample was chromatographed on an ODS column (Cosmosil 75C_{18}-PREP, 300 mL, Nakalai Tesque, Kyoto, Japan) with MeOH:H_2O (30:70 – 80:20, stepwise) as the mobile phase, followed by evaporation, to obtain GEM-1-O-glu. The purity was determined by HPLC-UV. The sample was separated on an ODS column (Inertsil ODS-2, ϕ4.6 mm x 150 mm, GL Sciences, Inc., Tokyo, Japan) with a mobile phase of 0.05 % trifluoroacetic acid/acetonitrile (53/47) at a flow rate of 1.0 mL/min. The product was detected by its absorbance at 254 nm. All other reagents were of analytical grade.

Human hepatocytes preparation

Cryopreserved human hepatocytes were kindly provided by In Vitro Technologies, Inc. (Baltimore, MD, USA). The human hepatocytes used in the study were isolated from human livers donated for transplantation purposes but not used for transplantation mainly due to the lack of appropriate recipients (Table 3). All livers were surgically removed from brain-dead donors whose hearts were functioning and who were free of known liver

diseases. All livers were stored for less than 24 hours in University of Wisconsin solution. Hepatocytes were isolated by perfusion using a two-step collagenase digestion procedure. After enzymatic dissociation, the hepatocytes were further separated from nonparenchymal cells by centrifugation through 30 % Percoll. Freshly isolated hepatocytes, before cryopreservation, were used within 4 hours of isolation. The cells were stored on ice in Krebs-Henseleit buffer. For the studies using cryopreserved hepatocytes, the purified hepatocytes were cryopreserved in liquid nitrogen until analysis. Immediately before the uptake studies, the hepatocytes (1 mL suspension) were thawed at 37 ^{o}C then immediately suspended in 10 mL ice-cold Krebs-Henseleit buffer and centrifuged (50 x *g*) for 2 minutes at 4 ^{o}C, followed by removal of the supernatant. This procedure was repeated once more to remove cryopreservation buffer and then cells were resuspended in the same buffer to give a designated cell density (2.0 x 10^6 viable cells/mL for all uptake studies of CER and the kinetic analysis of $E_2$17βG and 4.0 x 10^6 viable cells/mL for the time-course of uptake of $E_2$17βG).

Rat hepatocytes preparation

Rat hepatocytes were prepared from 7-week-old Sprague-Dawley (SD) rats by the method previously described by Yamazaki et al. (1993) [117]. The abdomen of 7-week-old SD rats was opened under light anesthesia. A cannula was inserted into the portal vein and, simultaneously, perfusion of the liver was started with the following medium adjusted to pH 7.2: 137 mM NaCl, 5.4 mM KCl, 0.5 mM NaH_2PO_4, 0.42 mM Na_2HPO_4, 4 mM $NaHCO_3$, 5 mM glucose, 10 mM HEPES and 0.5 mM EGTA. The medium was aerated with 95 % O_2/5 % CO_2 and the temperature was 37 ^{o}C. After insertion of the cannula, liver was excised and the perfusion was continued for 20 min. After 20-min perfusion, the perfusate was replaced with the following medium (pH 7.5): 137 mM NaCl, 5.4 mM KCl, 0.5 mM NaH_2PO_4, 0.42 mM Na_2HPO_4, 4 mM $NaHCO_3$, 10 mM HEPES, 1 mM $CaCl_2$, 0.5 g/L collagenase and 0.05 g/L trypsin inhibitor. After an additional 20 min, the tissue was very

soft and tended to fall apart and then it was transferred to ice cold Krebs-Henseleit buffer (pH 7.3) in a 100-mL beaker, followed by separation by rotation for several minutes. The contents of the beaker were poured through a nylon mesh (150 mesh) without exerting any pressure, followed by centrifugation at 50 x *g* for 2 min at 4 ^{o}C. The cells were washed again with ice cold Krebs-Henseleit buffer and adjusted to 4.0 x 10^6 cells/mL or 2.0 x 10^7 cells/mL for the uptake study in the absence and presence of 90 % rat plasma, respectively. Cells were stored on ice until the uptake study.

Uptake study into isolated hepatocytes

Prior to starting the uptake studies, 120-500 μL of the cell suspensions was prewarmed in an incubator at 37 ^{o}C for 3 minutes. In a pilot experiment, a 3-minute preincubation was confirmed to be sufficiently long to raise the temperature of cells to 37 ^{o}C and longer preincubation, for up to 30 min, did not alter the uptake rate of $E_2$17βG (data not shown). The uptake studies were initiated by adding an equal volume of substrate solution to the cell suspension. At a designated time, the reaction was terminated by separating the cells from the substrate solution by centrifugal filtration. An aliquot of 100 μL incubation mixture was collected and placed in a centrifuge tube (450 μL) containing 50 μL 2 N NaOH under a layer of 100 μL oil (density = 1.015, a mixture of silicone oil and mineral oil, Sigma-Aldrich). The sample tube was then centrifuged for 10 sec using a tabletop centrifuge (10,000 x *g*: Beckman Microfuge E^{TM}, Beckman Coulter, Fullerton, CA) during which the hepatocytes passed through the oil layer into the alkaline solution. After an overnight incubation in alkali to dissolve the hepatocytes, the centrifuge tube was cut and each compartment was transferred to a scintillation vial. The compartment containing the dissolved cells was neutralized with 50 μL 2 N HCl, mixed with scintillation cocktail and the radioactivity was counted using a liquid scintillation counter (LS6000SE, Beckman Coulter). For the uptake study in the presence of 90 % rat plasma, 270 μL substrate solution prepared from rat plasma was added to 30 μL cell suspension.

Uptake of [^{14}C]-CER in OATP2-expressing cells

OATP2-expressing MDCK II cells were constructed and kindly provided by Mr. Makoto Sasaki at the University of Tokyo [118]. The construction and culture of OATP2-expressing cells have been described previously [118]. For the uptake study of [^{14}C]-CER, MDCKII cells transfected with OATP2 or vector only as a control were seeded on a Cell Culture Insert^{TM} (BD Biosciences, Bedford, MA, USA). After 2 days, the culture medium was replaced with one containing 10 mM Na^+ butyrate for the induction of OATP2 [118, 119]. After culturing for a further day, the culture medium was replaced with ice-cold Krebs-Henseleit buffer, washed twice with the same buffer, then preincubated at 37^{o}C. The uptake study was initiated by replacing the buffer on the basal side of the cells with that containing [^{14}C]-CER in the presence or absence of unlabeled CER or CsA. At designated times, the reaction was terminated by aspirating the incubation buffer and washing 4 times with ice-cold buffer. Subsequently, the cells were dissolved in 0.75 mL 0.1 N NaOH overnight, followed by neutralization with 0.75 mL 0.1 N HCl. Then, 1.3 mL aliquots were transferred to scintillation vials and the radioactivity associated with the cells and that in the medium was determined in a liquid scintillation counter (LS6000SE). The remaining 0.1 mL aliquots of the cell lysate were used for protein assay by the Lowry method with bovine serum albumin as a standard [120].

Uptake of [^{14}C]-CER in Oatp1-expressing cells.

Oatp1-expressing HEK293 cells were constructed and kindly provided by Ms. Wakaba Yamashiro and Mr. Kazuya Maeda at the Univ. of Tokyo. The construction of rat Oatp1 expression vector has previously been described [48]. Rat Oatp1 expressing-HEK293 cells and control cells were constructed by the transfection of expression vector and control pcXN2 vector [121], respectively, into cells using FuGENE6 (Roche Diagnostics, Indianapolis, IN), according to the manufacturer's instruction and

selection by 800 μg/mL antibiotic G418 sulfate (Promega, Madison, WI) for 3 weeks. Oatp1-expressing cells and control cells were cultured in Dulbecco's modified Eagle's medium (Invitrogen, Carlsbad, CA) supplemented with 10 % FBS and 200 mg/L G418 sulfate. For the uptake study, cells were seeded on 12-well culture plates coated by poly-L-lysine/poly-L-ornithine at 1.2 x 10^5 cells/well. After 2 days, culture medium was replaced with the same medium containing 10 mM sodium butyrate (Sigma-Aldrich) and cultured overnight to induce the transporters [119]. Prior to initiation of the uptake study, cells were washed twice with Krebs-Henseleit buffer and preincubated in 0.5 mL of the same buffer at 37°C. The uptake study was initiated by replacing the Krebs-Henseleit buffer with 0.5 mL of the same buffer containing radiolabeled substrates and incubated at 37°C. Uptake studies were initiated by the addition of [^{14}C]-CER and the incubation period was 5 minutes. Then, 5 minutes after the initiation of the uptake study, buffer was removed to terminate the reaction and the cells were washed 4 times with ice cold Krebs-Henseleit buffer. The cells were then dissolved in 0.5 mL 0.1 N NaOH overnight, followed by neutralization with an equal volume of 0.1N HCl. Then, 0.8 mL aliquots were transferred to scintillation vials and the radioactivity associated with cells and medium was determined in a liquid scintillation counter (LS6000SE; Beckman Coulter, Fullerton, CA, USA). The remaining 0.1 mL aliquots of cell lysate were used to assay protein using the Lowry method [120] with bovine serum albumin as a standard.

Metabolism of [^{14}C]-CER and testosterone in human and rat liver microsomes

To measure the effect of CsA on the metabolism of [^{14}C]-CER and testosterone, its *in vitro* metabolism in human and rat liver microsomes (BD Gentest, Woburn, MA) was examined while, to measure the effect of GEM and its metabolites, its *in vitro* metabolism in human liver microsomes was examined. For the estimation of the contribution by CYP2C8, human liver microsomes were preincubated with a specific inhibitory Ab against CYP2C8 (BD Gentest) at 4 °C for 20 min. To estimate the contribution by CYP3A4,

ketoconazole, a potent CYP3A4 inhibitor, was used. Prior to the metabolism study, human or rat liver microsomes (final 0.2 mg protein/mL, for the effect of GEM and its metabolites and to estimate the contributions by CYP2C8 and 3A4 and final 0.5 mg protein/mL for the effect of CsA) were incubated at 37 ^{o}C for 10 min in 100 mM potassium phosphate buffer (pH 7.4) containing 3.3 mM $MgCl_2$, 3.3 mM glucose-6-phosphate, 0.4 U/mL glucose-6-phosphate dehydrogenase, 1.3 mM NADPH and 0.8 mM NADH. A 500 μL-volume of incubation mixture was transferred to a polyethylene tube and [^{14}C]-CER (final 0.25 μM, for the effect of GEM and its metabolites and to estimate the contributions by CYP2C8 and 3A4 and final 1 μM for the effect of CsA) or testosterone (final 30 μM) were added to initiate the reaction with or without inhibitors. After incubation for a designated time, the reaction was terminated by the addition of 500 μL ice-cold acetonitrile and 200 μL ice-cold methanol for the metabolism of [^{14}C]-CER and testosterone, respectively, followed by centrifugation. To measure the metabolic rate of [^{14}C]-CER, the supernatant was collected and concentrated to approximately 20 μL in a centrifugal concentrator (VC-36N, TAITEC, Saitama, Japan), followed by TLC. The analytes were separated on silica-gel 60F_{254} (Merck KGaA, Darmstadt, Germany) using a mobile phase (toluene / acetone / acetic acid, 70 : 30 : 5, v/v/v). The intensity of the bands of intact [^{14}C]-CER and its metabolites separated by TLC was determined by the BAS 2000 system (Fuji Film, Tokyo, Japan). To measure the metabolic rate of testosterone, 6β- and 16α-hydroxytestosterone (16α- only for the metabolism in rat liver microsomes) in the incubation mixture were determined by an HPLC-UV detection method. To a 100 μL-volume of supernatant, 100 μL internal standard (10 μg/mL phenacetin) was added and subjected to HPLC (VP-5, Shimadzu, Kyoto, Japan). The analyte was separated on a C18 column (Cosmosil 5C18-AR, 5mm, 4.6 mm i.d. x 250 mm, Nakalai Tesque, Kyoto, Japan) at 45 ^{o}C. The mobile phase consisted of solvent A (20% THF, 80% water) and solvent B (methanol). A 20-min linear gradient from 20% B to 30% B was applied at a flow rate of 1.0 mL per min. The product was detected by its absorbance at 254 nm and quantitated by comparison with

a standard curve constructed using 6β-hydroxytestosterone.

Metabolism of [^{14}C]-CER in human CYP2C8 and 3A4 expression systems

To measure the effect of GEM and its metabolites on the metabolism of [^{14}C]CER its in vitro metabolism was also examined in CYP2C8 and 3A4 expressing insect cells supplemented with the expressions of human CYP reductase and cytochrome b5 (Supersome®; BD Gentest). The metabolism of [^{14}C]-CER was examined by the method described above.

Protein binding of GEM and its metabolites

To estimate the fraction unbound to human serum protein, GEM, M3 and GEM-1-O-glu were added to human serum (Nissui Pharmaceuticals, Inc., Tokyo, Japan) buffered with 50 mM potassium phosphate at 37^{o}C and incubated for 2 minutes. After that, the sample underwent ultrafiltration (Amicon Centrifree, Millipore, Billerica, MA) and the GEM and its metabolites in the filtrate were determined by HPLC-UV. To 0.5 mL filtrate, 0.5 mL phosphate buffered saline containing 5 μL 1 mM ibuprofen (internal standard) and 20 μL formic acid were added, followed by vigorous shaking. Subsequently, the sample was extracted with 5 mL ethyl acetate/cyclohexane (20/80), then 4 mL of the organic phase was collected and evaporated. The obtained sample was dissolved in 0.5 mL acetonitrile and separated on an ODS column (Super ODS column, ϕ4.6 mm x 150 mm, Tosoh, Tokyo, Japan). The mobile phase for GEM was 10 mM acetate buffer (pH 4.7) / acetonitrile (55/45) while that for M3 and GEM-1-O-glu was a mixture of 10 mM acetate buffer (pH4.7) and acetonitrile with a linear gradient from 70 % to 55 % acetate buffer for 30 min. The flow rate was 1.0 mL/min. The absorbance was measured at 254 nm and quantitation carried on by comparison with the absorbance of a standard curve for each compound.

***In vivo* study: Analysis of CER plasma concentrations in rats**

The studies were carried out in accordance with *the Guide for the Care and Use of Laboratory Animals* as adopted and promulgated by the National Institutes of Health. CER (640 and 2400 ng/mL for administration by bolus and infusion, respectively) was dissolved in saline. CsA was dissolved in a mixture of Cremophor EL (Sigma-Aldrich) and 94 % ethanol (Wako, Osaka, Japan) (containing 0.65 g Cremophor EL/ mL), and subsequently diluted with 10 volumes of saline. Under light ether anesthesia, the right and left femoral veins of 7-week-old SD rats were cannulated with polyethylene tubing (PE-50: BD, Franklin Lakes, NJ). To avoid enterohepatic recirculation, which increases the inhibitor concentration in the portal vein and at the inlet to the liver, the bile duct was also cannulated with polyethylene tubing (PE-10: BD). CER (640 ng/kg) and CsA (0, 1.4 and 4.8 mg/kg) were administered as a bolus via both femoral veins, followed by infusion of CER (2.4 μg/h/kg) and CsA (0, 0.21 and 0.72 mg/h/kg). At 5 h after infusion, 400 μL blood was collected from the tail vein and EDTA (1 mg/mL) was added. At this time-point, it was confirmed that the plasma and blood concentrations of both CER and CsA had reached steady-state (data not shown). The samples were stored at –20^{o}C until analysis. Plasma concentrations of CER were determined by a validated method using atmospheric pressure ionization liquid chromatography-tandem mass spectrometry (LC/MS/MS). To a 50 μL sample, 500 μL 1 M phosphate buffer (pH 5.5) and 5 mL diethyl ether/dichloromethane (2:1) were added, the sample was shaken for 10 min and centrifuged. Then, the organic layer was evaporated to dryness under N_2 gas at 40°C and the residue was dissolved in 200 μL mobile phase. A 20 μL portion of each sample was then subjected to LC/MS/MS. A Shimadzu 10A HPLC system (Shimadzu, Kyoto, Japan) combined with a Model API 365 MS/MS (Applied Biosystems/MDS Sciex, Quebec, Canada) equipped with a Turbo IonSpray™ probe was used. The analytes were separated on an Inertsil ODS-3 column (5 μm, 2.1 mm i.d.×150 mm, GL Sciences Inc., Tokyo, Japan) using a mobile phase (acetonitrile /0.2% formic acid, 60:40, v/v) at a flow rate of 0.2 mL/min. Selected reaction monitoring was used to detect the analytes and internal standard (positive mode, m/z

460.6/356.1). Blood concentrations of CsA were determined by radioimmunoassay using CYCLO-Trac^{R} (DiaSorin, Stillwater, MN).

In vivo liver uptake index (LUI) method

Under light ether anesthesia, the femoral veins of 7-8 week-old SD rats were cannulated with polyethylene tubing (PE-50). Prior to the LUI study, a 2mL/kg bolus of CsA (0, 2.4, 4.8 and 9.6 mg/kg) was administered via the femoral vein. At 5 min after i.v. administration of CsA, [^{14}C]-CER and [^{3}H]-inulin dissolved in rat plasma (approximately 18.5 and 100 kBq/mL/kg for [^{14}C]-CER and [^{3}H]-inulin) containing a 1:1500 dilution of CsA solution, which was used for the bolus i.v. administration, were rapidly injected in the portal vein just after ligation of the hepatic artery. After 18 sec of bolus administration of radiolabeled compounds, which is long enough for the bolus to pass completely through the liver but short enough to prevent recirculation of the isotope [122)], the portal vein was cut and the liver was excised. The radioactivity taken up by the liver and in the injectate was counted in a liquid scintillation counter (LS6000SE).

Data analysis

The time-courses of the uptake of CER into isolated hepatocytes and OATP2-expressing cells were expressed as the uptake volume (μL/10^{6} cells or μL/mg protein) for the radioactivity taken up into cells (dpm/10^{6} cells or dpm/mg protein) divided by the concentration of radioactivity in the incubation medium (dpm/μL). The initial velocity uptake of each drug into isolated hepatocytes was calculated using the uptake volumes obtained at 0.5 and 2 min and expressed as the uptake clearance (CL_{uptake}: μL/min/10^{6} cells). The metabolic rate constant of [^{14}C]CER was calculated by the decrease of unchanged [^{14}C]CER or the synthesis of its metabolites, M1 and M23 by the following equation:

$$X(t) = X(0) \cdot \exp(-k \cdot t) \quad \ldots(8)$$

or

$$M(t) = X(0) \cdot \exp(-k \cdot t) \quad \ldots(9)$$

where, X(t) and M(t) represent the amount of unchanged CER and its metabolite at time = t, respectively, and k represents the metabolic rate constants based on the degradation of [^{14}C]CER or the syntheses of its metabolites.

The kinetic parameters for the uptake of CER were calculated using equation (10):

$$v_0 = \frac{V_{max} \cdot S}{K_m + S} + P_{dif} \cdot S \qquad (10)$$

where v_0 is the initial uptake rate (pmol/min/10^6 cells), S is the substrate concentration (μM), K_m is the Michaelis constant (μM), V_{max} is the maximum uptake rate (pmol/min/10^6 cells) and P_{dif} is the nonsaturable uptake clearance (μL/min/10^6 cells).

The following equation was fitted to the obtained data in the inhibition study for the uptake of CER into isolated hepatocytes to calculate the IC_{50} values.

$$CL_{uptake}(+\text{inhibitor}) = \frac{CL_{uptake}(\text{control}) - CL_{uptake}(\text{resistant})}{1 + I/IC_{50}} + CL_{uptake}(\text{resistant}) \quad \ldots(11)$$

where CL_{uptake}(+inhibitor) is the CL_{uptake} estimated in the presence of inhibitors, CL_{uptake}(control) is the CL_{uptake} estimated in the absence of inhibitors, CL_{uptake}(resistant) is the CL_{uptake} which is not affected by inhibitors and I is the inhibitor concentration.

For the estimation of the IC_{50} value for the uptake in OATP2-expressing cells, the following equation was fitted to the obtained data:

$$\Delta CL_{uptake}(+\text{inhibitor}) = \frac{\Delta CL_{uptake}(\text{control})}{1 + I/IC_{50}} \qquad \ldots(12)$$

where ΔCL_{uptake} is CL_{uptake} for OATP2-mediated uptake, which is the CL_{uptake} of [^{14}C]CER minus that estimated in the presence of excess unlabeled CER, ΔCL_{uptake}(+inhibitor) and ΔCL_{uptake}(control) are the ΔCL_{uptake} values estimated in the presence and absence of inhibitors, respectively, I is the inhibitor concentrations.

For the inhibitory effects of GEM and its metabolites on the metabolism of [^{14}C]CER in

CYP2C8 and 3A4 expression systems, the IC_{50} values (IC_{50_CYP2C8} and IC_{50_CYP3A4}, respectively) were calculated from the following equation:

$$k(+\text{inhibitor}) = \frac{k(\text{control})}{1 + I/IC_{50}} \qquad \ldots(13)$$

where k(+inhibitor) and k(control) are the metabolic rate constants (k) of CER in the presence and absence of inhibitors, respectively.

The above equations were fitted to the uptake data by a nonlinear least-squares method using a computer program, MULTI [66] and WinNonlin® (Pharsight, Mountain View, CA) to obtain the kinetic parameters.

The data obtained in the LUI study of CER in rats were expressed as a %LUI [%], which represents the ratio of the hepatic extraction of [^{14}C]-CER to that of [^{3}H]-inulin. The %LUI was obtained by the following equation:

$$\%\,\text{LUI} = \frac{([^{14}\text{C}]\text{ counts taken by liver} / [^{3}\text{H}]\text{ counts taken by liver})}{([^{14}\text{C}]\text{ counts in injectate} / [^{3}\text{H}]\text{ counts in injectate})} \times 100\,[\%] \qquad \ldots(14)$$

Section 2

Materials

[^{3}H]$E_2$17βG (1628 GBq/mmol) and [^{3}H]digoxin (703 GBq/mmol) were purchased from New England Nuclear (Boston, MA). Unlabeled $E_2$17βG, digoxin, quinidine and quinine were purchased from Sigma-Aldrich (St. Louis, MO, USA). Ibuprofen and indomethacin were purchased from Wako Pure Chemicals (Tokyo, Japan). All other chemicals were commercially available and of analytical grade.

Construction of Oatp1- and Oatp2-expressing LLC-PK$_1$ cells

The construction of the Oatp1-expression vector is described by Kouzuki et al [48]. Full length cDNA for Oatp2 was initially cloned in the plasmid pBluescript SK(-) (Stratagene, La Jolla, CA)[31]. Oatp2 cDNA was excised with *EcoR*V and *Hinc*II (Takara, Shiga, Japan) and subcloned into the *Xho*I site in the pCXN$_2$ vector [121] after converting to blunt ends. For the control study, pCXN$_2$ alone was used (vector-transfected). For transfection, LLC-PK$_1$ cells were cultured in 6-well culture plates in medium 199 (Sigma-Aldrich) supplemented with 10% fetal bovine serum and an antibiotic-antimycotic agent (Invitrogen, Grand Island, NY). At 30% confluence, cells were exposed to serum-free medium 199 containing plasmid (1 μg/mL) and lipofectAMINE^{TM} (10 μg/mL) (Invitrogen). At 8 hr after transfection, the medium containing plasmid and lipofectAMINE^{TM} was replaced with culture medium containing 10 % fetal bovine serum. Then, 2 days after transfection, 800 μg/mL G418 sulfate (Promega, Madison, WI) was added to the medium followed by culturing for a further 2 weeks to allow the selection of transfected cells. Expression levels of transporters were determined by Northern blot analysis and cells with the highest expression levels were selected and used for all further studies.

Uptake study

For the uptake study, cells were seeded on 12-well culture plates at 1.2 x 10^5

cells/well. After 2 days, culture medium was replaced with the same medium containing 4 mM sodium butyrate (Sigma-Aldrich) and cultured overnight to induce the transporters [119]. Prior to initiation of the uptake study, cells were washed twice with Krebs-Henseleit buffer and preincubated in 0.5 mL of the same buffer at 37°C. The uptake study was initiated by replacing the Krebs-Henseleit buffer with 0.5 mL of the same buffer containing radiolabeled substrates and incubated at 37°C. In all uptake studies, [^{3}H]-$E_2$17βG and [^{3}H]-digoxin were used as radiolabeled substrates for Oatp1- and Oatp2-expressing cells, respectively, because their uptakes were sufficiently high to detect the effects of inhibitors. For the inhibition study, inhibitors and radiolabeled substrates were added simultaneously. The incubation period was 2 min and 5 min for the uptake of [^{3}H]-$E_2$17βG in Oatp1-expressing cells and [^{3}H]-digoxin in Oatp2-expressing cells, respectively, because preliminary experiments had shown that the transport rate was linear over these time-periods (data not shown). At designated times, buffer was removed to terminate the reaction and the cells were washed 4 times with ice cold Krebs-Henseleit buffer. Then, the cells were dissolved in 0.5 mL 0.1 N NaOH overnight, followed by neutralization with an equal volume of 0.1N HCl. Then, 0.8 mL aliquots were transferred to scintillation vials and the radioactivity associated with cells and medium was determined in a liquid scintillation counter (LS6000SE; Beckman Coulter, Fullerton, CA, USA). The remaining 0.1 mL aliquots of cell lysate were used to assay protein using the Lowry method [120] with bovine serum albumin as a standard.

Data analysis

The uptake of [^{3}H]-$E_2$17βG and [^{3}H]-digoxin was expressed as the uptake volume [μL/mg protein], defined as the amount of isotopes taken up into cells [dpm/mg protein] divided by their concentration in the incubation medium [dpm/μL]. The initial uptake rate of substrates was expressed as an uptake clearance (CL_{uptake}) [μL/min/mg protein], defined as the initial velocity of uptake divided by the incubation time.

The kinetic parameters for the uptake of [^{3}H]-$E_2$17βG and [^{3}H]-digoxin in the transporter expressing cells were obtained from equation (10). When the substrate concentration is much lower than the K_m value, the data obtained in the inhibition study of the uptake in transporter-expressing cells regardless of inhibitor type (i.e. competitive or non-competitive inhibitor) can be fitted to the following equation (15) to calculate the inhibition constant (K_i).

$$CL_{uptake}(+inhibitor) = \frac{CL_{uptake}(control) - CL_{uptake}(resistant)}{1 + I/K_i} + CL_{uptake}(resistant) \quad \ldots(15)$$

These equations were fitted to the data from the uptake or inhibition study using the nonlinear least-squares method by means of the computer program, MULTI [66], to obtain the required parameters. The input data were weighed as the reciprocal of the observed values and the Damping Gauss Newton method was used as the fitting algorithm.

All results from the inhibition experiments are given as a % of the control. As the number of cell passages increased, the contribution of transporter-mediated uptake to the total uptake into the transfected cells and fell from 87.4 to 51.9 % for Oatp1 and from 79.7 to 59.3 % for Oatp2, presumably due to a reduction in the level of expression. However, we found that none of the inhibitors affected the uptake into vector-transfected LLC-PK_1 cells.

<Acknowledgement>

I would like to express my deepest thanks to Professor Yuichi Sugiyama at the University of Tokyo for his kind advice and valuable discussions throughout the entire period of the research. I also would like to thank Professor Tomoo Itoh at Kitasato University and Professor Hitoshi Sato at Showa University for their encouragement during the study.

I am very greatful to Dr. Hiroshi Suzuki and Dr. Yukio Kato for their kind help and valuable discussions. I am also grateful to Dr. Peter J. Meier and Dr. Takaaki Abe for providing cDNA for rat Oatp1 and Oatp2, respectively. I am also grateful to Dr. Albert P. Li and Mr. Makoto Sasaki for providing cryopreserved human hepatocytes and human OATP2-expressing MDCK II cells, respectively.

I would aldo like to express my thanks to all members of the Department of Molecular Pharmacokinetics, Graduate School of Pharmaceutical Sciences, the University of Tokyo for helpful discussions. I also would like to thank colleagues at Kitasato University and Showa University.

In addition, I would like to express my deep appreciation to my wife, Mikiko for her support during this study and to my son, Akito for his encouragement.

<References>

1) Hansten PD (2002) Clinically important drug interactions, in Preclinical and clinical evaluation of drug-drug interactions (Li AP and Sugiyama Y eds) pp 1-29, ISE Press, Baltimore.

2) Okuda H, Nishiyama T, Ogura K, Nagayama S, Ikeda K, Yamaguchi S, Nakamura Y, Kawaguchi Y and Watabe T (1998) Lethal drug interactions of sorivudine, a new antiviral drug, with oral 5-fluorouracil prodrugs. Drug Metab Dispos 25: 270-273.

3) Ito K, Iwatsubo T, Kanamitsu S, Nakajima Y and Sugiyama Y (1998a) Quantitative prediction of in vivo drug clearance and drug interactions from in vitro data on metabolism, together with binding and transport. Annu Rev Pharmacol Toxicol 38: 461-499.

4) Ito K, Iwatsubo T, Kanamitsu S, Ueda K, Suzuki H and Sugiyama Y (1998b) Prediction of pharmacokinetics alterations caused by drug-drug interactions: metabolic interaction in the liver. Pharmacol Rev 50: 387-411.

5) Kanamitsu S, Ito K, Okuda H, Ogura K, Watabe T, Muro K and Sugiyama Y (2000) Prediction of in vivo drug-drug interaction from in vitro data: Inhibition of 5-fluorouracil metabolism by (E)-5-(2-bromovinyl) uracil. Drug Metab Dispos 28: 467-474.

6) Ohno Y (2002) A draft of Japanese guidance for drug interactions (DI); in vitro and in vivo assessment (version #13), in Preclinical and clinical evaluation of drug-drug interactions (Li AP and Sugiyama Y eds) pp 296-312, ISE Press, Baltimore.

7) 薬物相互作用の検討方法について（医薬審第 813 号）(2001) 各都道府県衛生主管部(局)長

8) Moghadasian MH (1999) Clinical pharmacology of 3-hydroxy-3-methylglutaryl coenzyme A reductase inhibitors. Life Sci 65: 1329-1337.

9) Mück W (1998) Rational assessment of the interaction profile of cerivastatin supports its low propensity for drug interactions. Drugs 56 Suppl. 1: 15-23.

10) Mück W (2000) Clinical pharmacokinetics of cerivastatin. Clin Pharmacokinet 39: 99-116.

11) Mück W, Ochmann K, Rohde G, Unger S and Kuhlmann J. (1998) Influence of erythromycin pre- and co-treatment on single-dose pharmacokinetics of the HMG-CoA reductase inhibitor cerivastatin. Eur J Clin Pharmacol 53: 469-473.

12) Kantola T, Kivistö KT and Neuvonen PJ (1999) Effect of itraconazole on cerivastatin pharmacolinetics. Eur J Clin Pharmacol 54: 851-855.

13) Mück W (2000) Metabolic interactions between mibefradil and HMG-CoA reductase inhibitors: linking in vitro with in vivo information [Letter]. Br J Clin Pharmacol 49: 87-90.

14) Mück W, Mai I, Fritsche L, Ochmann K, Rohde G, Unger S, Johne A, Bauer S, Budde K, Roots I, Neumayer H-H and Kuhlmann J (1999) Increase in cerivastatin systemic exposure after single and multiple dosing in cyclosporin-treated kidney transplant recipients. Clin Pharmacol Ther 65: 251-261.

15) Mueck W, Frey R, Boix O and Voith B (2001) Gemfibrozil/Cerivastatin Interaction.

AAPS PharmSci 3 (suppl.): abstract No. 3566

16) Backman JT, Kyrklund C, Neuvonen M and Neuvonen PJ (2002) Gemfibrozil greatly increases plasma concentrations of cerivastatin. Clin Pharmacol Ther. 72: 685-691.

17) Campana C, Regazzi MB, Buggia I and Molinaro M (1996) Clinically significant drug interactions with cyclosporin. An update. Clin Pharmacokinet 30: 141-79.

18) Nakai D, Nakagomi R, Furuta Y, Tokui T, Abe T, Ikeda T and Nishimura K (2001) Human liver-specific organic anion transporter, LST-1, mediates uptake of pravastatin by human hepatocytes. J Pharmacol Exp Ther 297: 861-867.

19) Hsiang B, Zhu Y, Wang Z, Wu Y, Sasseville V, Yang WP and Kirchgessner TG (1999) A novel human hepatic organic anion transporting polypeptide (OATP2). Identification of a liver-specific human organic anion transporting polypeptide and identification of rat and human hydroxymethylglutaryl-CoA reductase inhibitor transporters. J Biol Chem 274: 37161-37168.

20) Yamazaki M, Suzuki H and Sugiyama Y (1996) Recent advances in carrier-mediated hepatic uptake and biliary excretion of xenobiotics. Pharm Res 13: 497-513.

21) Kusuhara H and Sugiyama Y (2001) Drug-drug interactions involving the membrane transport process, in Drug-Drug Interacions (Rodrigues AD eds) pp123-188, Marcel Dekker, New York.

22) Mizuno N and Sugiyama Y (2002) Drug Transporters: Their Role and Importance in New Drug Selection and Development. Drug Metabol Phamacokin 17: 93-108.

23) Mizuno N, Niwa T, Yotsumoto Y and Sugiyama Y (2003) Impact of drug transporter studies on drug discovery and development. Pharmacol Rev 55: 425-461.

24) Kusuhara H and Sugiyama Y (2001) Efflux transport systems for drugs at the blood-brain barrier and blood-cerebrospinal fluid barrier (Part 1). Drug Discovery Today 6: 150–156.

25) Abe T, Kakyo M, Tokui T, Nakagomi R, Nishio T, Nakai D, Nomura H, Unno M, Suzuki M, Naitoh T, Matsuno S and Yawo H (1999) Identification of a novel gene family encoding human liver-specific organic anion transporter LST-1. J Biol Chem 274: 17159-17163.

26) König J, Cui, Y, Nies AT and Keppler D (2000) A novel human organic anion transporting polypeptide localized to the basolateral hepatocyte membrane. Am J Physiol 278: G156-G164.

27) König J, Cui Y, Nies AT and Keppler D (2000) Localization and genomic organization of a new hepatocellular organic anion transporting polypeptide. J Biol Chem 275: 23161-23168.

28) Kok LD, Siu SS, Fung KP, Tsui SK, Lee CY and Waye MM (2000) Assignment of liver-specific organic anion transporter (SLC22A7) to human chromosome 6 bands p21.2-->p21.1 using radiation hybrids. Cytogenet Cell Genet 88: 76-77.

29) Tamai I, Nezu J, Uchino H, Sai Y, Oku A, Shimane M and Tsuji A (2000) Molecular identification and characterization of novel members of the human organic anion transporter (OATP) family. Biochem Biopys Res Com 273: 251-260.

30) Jacquemin E, Hagenbuch B, Stieger B, Wolkoff AW and Meier PJ (1994) Expression cloning of a rat liver Na+-independent organic anion transporter. Proc Natl Acad Sci USA. 91: 133-137.

31) Noé B, Hagenbuch B, Stieger B and Meier PJ (1997) Isolation of multispecific organic anion and cardiac glycoside transporter from rat brain. Proc Natl Acad Sci USA 94: 10346-10350.

32) Cattori V, Hagenbuch B, Hagenbuch N, Stieger B, Ha R, Winterhalter KE and Meier PJ (2000) Identification of organic anion transporting polypeptide 4 (Oatp4) as a major full-length isoform of the liver-specific transporter-1 (rlst-1) in rat liver. FEBS letters 474: 242-245.

33) Sekine T, Cha SH, Tsuda M, Apiwattanakul N, Nakajima N, Kanai Y and Endou H (1998) Identification of multispecific organic anion transporter 2 expressed predominantly in the liver. FEBS letters 429: 179-182.

34) Ishizuka H, Konno K, Naganuma H, Nishimura K, Kouzuki H, Suzuki H, Stieger B, Meier PJ and Sugiyama Y (1998) Transport of temocaprilat into rat hepatocytes: Role of organic anion transporting polypeptides. J. Pharmacol. Exp. Ther. 287: 37-42.

35) Meier PJ, Eckhardt U, Schroeder A, Hagenbuch B and Stieger B (1997) Substrate specificity of sinusoidal bile acid and organic anion uptake systems in rat and human liver. Hepatology 26: 1667-1677.

36) Kusuhara H and Sugiyama Y (2002) Role of transporters in the tissue-selective

distribution and elimination of drugs: transporters in the liver, small intestine, brain and kidney. J Controlled Release 78: 43-54.

37) Ishigami M, Tokui T, Komai T, Tsukahara K, Yamazaki M and Sugiyama Y (1995) Evaluation of the uptake of pravastatin by perfused rat liver and primary cultured rat hepatocytes. Pharm Res 12: 1741-1745.

38) Li AP, Roque MA, Beck DJ and Kaminsli DL (1992) Isolation and culturing of hepatocytes from human liver. J Tissue Culture Meth 14: 139-146.

39) Li AP, Lu C, Brendt JA, Fackett A, Ruegg CE and Silber PA (1999) Cryopreserved human hepatocytes: Characterization of drug-metabolizing enzyme activities and applications in higher throughput screening assays for hepatotoxicity, metabolic stability, and drug-drug interaction potential. Chem-Biol Interact 121: 17-35.

40) Madan A, DeHaan R, Mudra D, Carroll K, LeCluyse E and Parkinson A (1999) Effect of cryopreservation on cytochrome P-450 enzyme induction in cultured rat hepatocytes. Drug Metab Dispos 27: 327-35.

41) Yamazaki M, Akiyama S, Nishigaki R and Sugiyama Y (1996) Uptake is the rate-limiting step in the overall hepatic elimination of pravastatin at steady state in rats. Pharm Res 13: 1559-1564.

42) Tirona RG, Leake BF, Merino G and Kim RB (2001) Polymorphisms in OATP-C. Identification of multiple allelic variants associated with altered transport activity among European- and American-Americans. J Biol Chem 276: 35669-35675.

43) Michalski C, Cui Y, Nies AT, Nuessler AK, Neuhaus P, Zanger UM, Klein K, Eichelbaum M, Keppler D and König J (2002) A naturally occuring mutation in the SLC21A6 gene causing impaired localization of the hepatocyte uptake transporter. J Biol Chem 277: 43058-43063.

44) Niinuma K, Kato Y, Suzuki H, Tyson CA, Weizer V, Dabbs JE, Froehlich R, Green CE and Sugiyama Y (1999) Primary active transport of organic anions on bile canalicular membrane in humans. Am J Physiol 27: G1153-G1164.

45) Li L, Lee TK, Meier PJ and Ballatori N (1998) Identification of glutathione as a driving force and leucotriene C4 as a substrate for oatp1, the sinusoidal organic solute transporter. J Biol Chem 273: 16184-16191.

46) Li L, Meier PJ and Ballatori N (2000) Oatp2 mediated bidirectional organic solute transport: a role for intracellular glutathione. Mol Phamacol 58: 335-340.

47) Sandker GW, Weert B, Olinga P, Wolter H, Slooff MJH, Meijer DKF and Groothuis GMM (1994) Characterization of transport in isolated human hepatocytes: A study with the bile acid taurocholic acid, the unchanged ouabain and the organic cations vecuronium and rocuronium. Biochem Pharmacol 47: 2193-2200.

48) Kouzuki H, Suzuki H, Ito K, Ohashi R and Sugiyama Y (1999) Contribution of organic anion transporting polypeptide to uptake of its possible substrates into rat hepatocytes. J Pharmacol Exp Ther 288: 627-634.

49) Zachoval R, Gerbes AL, Schwandt P and Parhofer KG (2001) Short-term effects of statin therapy in patients with hyperlipoprotienemia after liver transplantation: results of

randomized cross-over trial. J Hepatol 35: 86-91.

50) Deseger J-P and Horsmans Y (1996) Clinical pharmacokinetics of 3-hydroxy-3-methylglutaryl-coenzyme A reductase inhibitors. Clin Pharmacokinet 31: 348-371.

51) Kanamitsu S, Ito K, Green CE, Tyson CA, Shimada N and Sugiyama Y (2000) Prediction of in vivo interaction between triazolam and erythromycin based on in vitro studies using human liver microsomes and recombinant human CYP3A4. Pharm Res 17: 419-426.

52) Regazzi MB, Campana IC, Raddato V, Lesi C, Perani G, Gavazzi A and Vigano M (1993) Altered disposition of pravastatin following concomitant drug therapy with cyclosporin A in transplant recipients. Transplant Proc 25: 2732-2734.

53) Hirayama M, Yoshimura Y and Moriyasu M (2000) Carrier-mediated uptake of cerivastatin in primary cultured rat hepatocytes. Xenobio Metabol Dispos 15: 219-225.

54) Komai T, Shigehara E, Tokui T, Ishigami M, Kuroiwa C and Horiushi S (1992) Carrier-mediated uptake of pravastatin by rat hepatocytes in primary culture. Biochem Pharmacol 43: 667-670.

55) Ohyama K, Nakajima M, Nakamura S, Shimada N, Yamazaki H and Yokoi T (2000) A significant role of human cytochrome P450 2C8 in amiodarone N-deethylation: An approach to predict the contribution with relative activity factor. Drug Metab Dispos 28: 1303-1310.

56) Kawahara I, Kato Y, Suzuki H, Achira M, Ito K, Crespi CL and Sugiyama Y (2000) Selective inhibition of human cytochrome P450 3A4 by N-[2(R)-hydroxy-1(S)-indanyl]-5-[2(S)-(1, 1-dimethylethylaminocarbonyl)-4-[(furo[2, 3-B]pyridin-5-yl)methyl]piperazin-1-yl]-4(S)-hydroxy-2(R)-phenylmethy lpentanamide and P-glycoprotein by valspodar in gene transfectant systems. Drug Metab Dispos 28: 1238-1243.

57) Lemaire M. and Tillement JP (1982) Role of lipoproteins and erythrocytes in the in vitro binding and distribution of cyclosporin A in the blood. J Pharm Pharmacol 34: 715-718.

58) Ito K, Chiba K, Horikawa M, Ishigami M, Mizuno N, Aoki J, Gotoh Y, Iwatsubo T, Kanamitsu S, Kato M, Kawahara I, Niinuma K, Nishino A, Sato N, Tsukamoto Y, Ueda K, Itoh T and Sugiyama Y (2002) Which concentration of the inhibitor should be used to predict in vivo drug interactions from in vitro data? AAPS PharmSci 4: article 25 (http://www.aapspharmsci.org/)

59) Sugiyama Y, Kato Y and Ito K (2002) Quantitative prediction: metabolism, transport in the liver, in Preclinical and clinical evaluation of drug-drug interactions (Li AP and Sugiyama Y eds) pp 108-124, ISE Press, Baltimore.

60) Kouzuki H, Suzuki H, Ito K, Ohashi R and Sugiyama Y (1999) Contribution of sodium taurocholate co-transporting polypeptide to the uptake of its possible substrates into rat hepatocytes. J Pharmacol Exp Ther 286: 1043-1050.

61) Ueda K, Kato Y, Komatsu K and Sugiyama Y (2001) Inhibition of biliary excretion of methotrexate by probenecid in rats: quantitative prediction of interaction from in vitro data. J Pharmacol Exp Ther 297:1036-1043.

62) Ong CE, Coulter S, Birkett DJ, Bhasker CR and Miners JO (2000) The xenobiotic inhibitor profile of cytochrome P4502C8. Br J Clin Pharmacol 50: 573-580.

63) Rahman A, Korzekwa KR, Grogan J, Gonzalez FJ and Harris JW (1994) Selective biotransformation of taxol to 6 α-hydroxytaxol by human cytochrome P450 2C8. Cancer Res 54: 5543-5546.

64) Kanamitsu S, Ito K and Sugiyama Y (2000) Quantitative prediction of in vivo drug-drug interactions from in vitro data based on physiological pharmacokinetics: Use of maximum unbound concentration of inhibitor at the inlet to the liver. Pharm Res 17: 336-343.

65) Hirota N, Ito K, Iwatsubo T, Green CE, Tyson CA, Shimada N, Suzuki H and Sugiyama Y (2001) In vitro/in vivo scaling of alprazolam metabolism by CYP3A4 and CYP3A5 in humans. Biopharm Drug Dispos 22: 53-71.

66) Yamaoka K, Tanigawara Y, Nakagawa T and Uno T (1981) A pharmacokinetic analysis program (MULTI) for microcomputer. J Pharmacobio-Dyn 4: 879-885.

67) Boberg M, Angerbauer R, Kanhai WK, Karl W, Kern A, Radtke M and Steinke W (1998) Biotransformation of cerivastatin in mice, rats, and dogs in vivo. Drug Metab Dispos 26: 640-652.

68) Miyauchi S, Sawada Y, Iga T, Hanano M and Sugiyama Y (1993) Comparison of the hepatic uptake clearances of fifteen drugs with a wide range of membrane permeabilities in isolated rat hepatocytes and perfused rat livers. Pharm Res 10: 434-440.

69) Wierzbicki AS, Mikhalidis DP, Wray R, Schacter M, Cramb R, Simpson WG and Byrne CB (2003) Curr Med Res Opin 19: 155-168.

70) Moghadasian MH, Mancini GB and Frohlich JJ (2000) Pharmacotherapy of hypercholesterolaemia: statins in clinical practice. Expert Opin Pharmacother 1: 683-695.

71) Abdul-Ghaffar NU and El-Sonbaty MR (1995) Pancreatitis and rhabdomyolysis associated with lovastatin-gemfibrfozil therapy. J Clin Gastroenterol 21: 340-341.

72) Bruce-Joyce J, Dugas JM and MacCausland OE (2001) Cerivastatin and gemfibrozil-associated rhabdomyolysis. Ann Pharmacother 35: 1016-1019.

73) Roca B, Calvo B and Monferrer R (2002) Severe rhabdomyolysis and cerivastatin-gemfibrozil combination therapy. Ann Pharmacother 36: 730-731.

74) Kyrklund C, Backman JT, Kivistö KT, Neuvonen M, Latila J, Neuvonen PJ (2001) Plasma concentrations of active lovastatin acid are markedly increased by gemfibrozil but not by bezafibrate. Clin Pharmacol Ther 69: 340-345.

75) Matzno S, Tazuya-Murayama K, Tanaka H, Yasuda S, Mishima M, Uchida T, Nakabayashi T and Matsuyama K (2003) Evaluation of the synergistic adverse effects of concomitant therapy with statins and fibrates on rhabdomyolysis. J Pharm Pharmacol 55: 795-802.

76) Backman JT, Kyrklund C, Kivistö KT, Wang J-S, Neuvonen PJ (2000) Plasma concentrations of active simvastatin acid are increased by gemfibrozil. Clin Pharmacol Ther 68: 122-129.

77) Kyrklund C, Backman JT, Neuvonen M and Neuvonen PJ (2003) Gemfibrozil increases plasma pravastatin concentrations and reduces pravastatin renal clearance. Clin Pharmacol Ther 73: 538-544.

78) Mathew P (2003) ピタバスタチン(NK-104)のフィブラート系薬剤（フェノフィブラート、ゲムフィブロジル）併用時における薬物動態試験　診療と新薬 40: 779-785

79) Staffa JA, Chang J and Green G (2002) Cerivastatin and reports of ftal rhabdomyolysis. N Engl J Med 346: 539-540.

80) Wang J-S, Neuvonen M, Wen X, Backman JT and Neuvonen PJ (2002) Gemfibrozil inhibits CYP2C8-mediated cerivastain metabolism in human liver microsomes. Drug Metab Dispos 30: 1352-1356.

81) Wen X, Wang J-S, Backman JT, Kivistö KT and Neuvonen PJ (2001) Gemfibrozil is a potent inhibitor of human cytochrome P450 2C9. Drug Metab Dispos 29: 1359-1361.

82) Prueksaritanont T, Zhao JJ, Ma B, Roadcap BA, Tang C, Qiu Y, Liu L, Lin JH, Pearson G and Baillie TA (2002) Mechanistic studies on metabolic interactions between gemfibrozil and statins. J Pharmacol Exp Ther 301: 1042-1051.

83) Prueksaritanont T, Tang C, Qiu Y, Mu L, Subramanian R and Lin JH (2002) Effects of fibrates on metabolism of statins in human hepatocytes. Drug Metab Dispos 30: 1280-1287.

84) Prueksaritanont T, Subramanian R, Fang X, Ma B, Qiu Y, Lin JH, Pearson PG and Baillie TA (2002) Glucuronidation of statins in animals and humans: a novel mechanism of

statin lactonization. Drug Metab Dispos 30: 505-512.

85) Todd PA and Ward A (1988) Gemfibrozil: a review of its pharmacodynamic and pharmacokinetic properties, and therapeutic use in dyslipidaemia. Drugs 36: 314-339.

86) Nakagawa A, Shigeta A, Iwabuchi H, Horiguchi M, Nakamura K and Takahagi H (1991) Simultaneous determination of gemfibrozil and its metabolites in plasma and urine by a fully automated high performance liquid chromatographic system. Biochem Chromatogr 5: 68-73.

87) Okerholm RA, Keeley FJ, Peterson FE and Glazko AJ (1976) The metabolism of gemfibrozil. Proc roy Soc Med 69 (suppl. 2): 11-14.

88) Hengy H and Kölle EU (1985) Determination of gemfibrozil in plasma by high performance liquid chromatography. Arzneimittelforschung 35: 1637-1639.

89) Sallustio BC, Fairchild BA, Shanahan K, Evans AM and Nation RL (1996) Disposition of gemfibrozil and gemfibrozil acyl glucuronide in the rat isolated perfused liver. Drug Metab Dispos 24: 984-989.

90) Sabordo L, Sallutio BC, Evans AM and Nation RL (1998) Hepatic disposition of the acyl glucuronide1-O-gemfibrozil β-D-glucuronide: Effects of dibromosulfophthalein on membrane transport and aglycone formation. J Pharmacol Exp Ther 288: 414-420.

91) Sabordo L, Sallustio BC, Evans AM and Nation RL (2000) Hepatic disposition of the acyl glucuronide 1-O-gemfibrozil-β-D-glucuronide: Effects of clofibric acid, acetaminophen, and acetaminophen glucuronide. J Pharmacol Exp Ther 295: 44-50.

92) Cui Y, König J, Leier I, Buchholz U and Keppler D (2001) Hepatic uptake of bilirubin and its conjugates by the human organic anion transporter SLC21A6. J Biol Chem 276: 9626-9630.

93) Spence JD, Munoz CE, Hendricks L, Latchinian L and Khouri HE (1995) Pharmacokinetics of the combination of fluvastatin and gemfibrozil. Am J Cardiol 76: 80A-83A.

94) Fujino H, Yamada I, Shimada S, Yoneda M and Kojima J (2003) Metabolic fate of pitavastatin, a new inhibitor of HMG-CoA reductase: human UDP-glucuronosyltransferase enzymes involved in lactonization. Xenobiotica 33: 27-41.

95) Hirano M, Maeda K and Sugiyama Y (2003) Hepatic uptake mechanism of pitavastatin in humans: involvement of OATP family transporters. Abstract for Molecular Biopharmaceutics –A new era in drug absorption transport and delivery- p.72.

96) 蓮沼智子、中村正彦、矢地孝、有沢紀子、福島邦昭、飯島肇、齋藤康 (2003) 新規HMG-CoA 還元酵素阻害薬ピタバスタチン(NK-104)の薬物間相互作用—シクロスポリンのピタバスタチン血漿中濃度に及ぼす影響— 臨床医薬 19: 381-389

Hasunuma T,Nakamura M, Yachi T, Arisawa N, Fukushima K and Iijima H (2003) The drug-drug interactions of pitavstatin (NK-104), a novel HMG-CoA reductase inhibitor and cyclosporine. J Clin Ther Med 19: 381-389.

97) Deseger J-P and Horsmans Y (1996) Clinical pharmacokinetics of 3-hydroxy-3-methylglutaryl-coenzyme A reductase inhibitors. Clin Pharmacokinet 31: 348-371.

98) Kim AE, Dintaman JM, Waddell DS and Silverman JA (1998) Saquinavir, an HIV protease inhibitor, is transported by P-glycoprotein. J Pharmacol Exp Ther 286: 1439-1445.

99) Takenaka O, Horie T, Suzuki H and Sugiyama Y (1996) Carrier-mediated active transport of the glucuronide and sulfate of 6-hydroxy-5,7-dimethyl-2-methylamino-4-(3-pyridylmethyl) benzothiazole (E3040) into rat liver: Quantitative comparison of permeability in isolated hepatocytes, perfused liver and liver in vivo. J Pharmacol Exp Ther 280: 948-958.

100) Kanai N, Lu R, Wolkoff AW and Schuster VL (1996) Transient expression of oatp organic anion transporter in mammalian cells: identification of candidate substrates. Am J Physiol 270: F319-F325.

101) Eckhardt U, Schroeder A, Stieger B, Höchli M, Landmann L, Tynes R, Meier PJ and Hagenbuch B (1999) Polyspecific substrate uptake by the hepatic organic anion transporter Oatp1 in stably transfected CHO cells. Am J Physiol 276: G1037-G1042.

102) Kanai N, Lu R, Bao Y, Wolkoff AW, Vore M and Schuster VL. Estradiol 17β-D-glucuronide is a high-affinity substrate for oatp organic anion transporter. Am J Physiol 270: F326-F331.

103) van Montfoort JE, Hagenbuch B, Fattinger KE, Müller M, Groothuis GMM, Meijer DKF and Meier PJ (1999) Polyspecific organic anion transporting polypeptides mediate hepatic uptake of amphipathic type II organic cations. J Pharmacol Exp Ther 291: 147-152.

104) Abe T, Kakyo M, Sakagami H, Tokui T, Nishio T, Tanemoto M, Nomura H, Hebert SC,

Matsuno S, Kondo H and Yawo H (1998) Molecular characterization and tissue distribution of a new organic anion transporter subtype (oatp3) that transports thyroid hormones and taurocholate and comparison with oatp2. J Biol Chem 273: 22395-22401.

105) Reichel C, van Montfort CE, Cattori V, Rahner C, Stieger B, Kamisako T and Meier PJ (1999) Localization and function of the organic anion-transporting polypeptide oatp2 in rat liver. Gastroenterol 117: 688-695.

106) Bertz RJ and Granneman GR (1997) Use of in vitro and in vivo data to estimate the likelyhood of metabolic pharmacokinetic interactions. Clin Pharmacokinet 32: 210-258.

107) Kouzuki H, Suzuki H and Sugiyama Y (2000) Pharmacokinetic study of the hepatobiliary transport of indomethacin. Pharm Res 17:432-438.

108) Kouzuki H, Suzuki H, Stieger B, Meier PJ and Sugiyama Y (2000) Characterization of the transport properties of organic anion transporting polypeptide 1 (oatp1) and Na+/taurocholate Cotransporting polypeptide (Ntcp): Comparative studies on the inhibitory effect of their possible substrates in hepatocytes and cDNA-transfected COS-7 cells. J Pharmacol Exp Ther 292: 505-511.

109) Fattinger K, Cattori V, Hagenbuch B, Meier PJ and Stieger B (2000) Rifamycin SV and rifampicin exhibit differential inhibition of the hepatic rat organic anion transporting polypeptides, Oatp1 and Oatp2, Hepatology 32: 82-86.

110) Hedman A and Meijer DKF (1997) Stereoselective inhibition by the diastereomers quinidine and quinine of uptake of cardiac glycosides into isolated rat hepatocytes. J Pharm Sci 87: 457-461.

111) Hagenbuch B, Scharschmidt BF and Meier PJ (1996) Effect of antisense oligonucleotides on the expression of hepatocellular bile acid and organic anion uptake systems in Xenopus laevis oocytes. Biochem J 316: 901-904.

112) Ishizuka H, Konno K, Naganuma H, Nishimura K, Kouzuki H, Suzuki H, Stieger B, Meier PJ and Sugiyama Y (1998) Transport of temocaprilat into rat hepatocytes: role of organic anion transporting polypeptide. J Pharmacol Exp Ther 287: 37-42

113) Sugiyama D, Kusuhara H, Shitara Y, Abe T, Meier PJ, Sekine T, Endou H, Suzuki H and Sugiyama Y (2001) Characterization of the efflux transporter of 17β-estradiol-D-17β-glucuronide from the brain across the blood-brain barrier. *J Pharmacol Exp Ther* 298: 316-322.

114) Hasegawa M, Kusuhara H, Endou H and Sugiyama Y (2003) Contribution of organic anion transporters to the renal uptake of anionic compounds and nucleoside derivatives in rat. J Pharmacol Exp Ther 305: 1087-1097.

115) Curtis CG, Danaher TM, Hibbert EA, Morris CL, Scott AM, Woolcott BA and Powell GM (1985) The fate of gemfibrozil and its metabolites in the rat. Biochem Soc Trans 13: 1190-1191

116) Thomas BF, Burgess JP, Coleman DP, Scheffler NM, Jeffcoat AR and Dix KJ (1999) Isolation and identification of novel metabolites of gemfibrozil in rat urine. Drug Metab Dispos 27: 147-157.

117) Yamazaki M, Suzuki H, Hanano M and Sugiyama Y (1993) Different relationships

between cellular ATP and hepatic uptake among taurocholate, cholate and organic anions. Am J Physiol 264: G693-G701.

118) Sasaki M, Suzuki H, Ito K, Abe T and Sugiyama Y (2002) Transcellular transport of organic anions across double-transfected MDCKII cell monolayer expressing both human organic anion transporting polypeptide (OATP2/SLC21A6) and multidrug resistance associated protein 2 (MRP2/ABCC2). J Biol Chem 277: 6497-6503.

119) Schroeder A, Eckhardt U, Stieger B, Tynes R, Schteingart CD, Hofmann AF, Meier PJ and Hagenbuch B (1998) Substrate specificity of the rat liver Na+-bile salt cotransporter in Xenopus laevis oocytes and in CHO cells. Am J Physiol 274: G370-G375.

120) Lowry OH, Rosebrough NJ, Farr AL and Randal RJ (1951) Protein measurement with the Folin phenol reagent. J Biol Chem 193: 265-275.

121) Niwa H, Yamamura K and Miyazaki J (1991) Efficient selection for high-expression transfectants with a novel eukaryotic vector, Gene 108: 193-200.

122) Partridge WM, Premachandra BN and Fierer G (1985) Transport of thyroxine bound to human prealbumin into rat liver. Am J Physiol 248: G545-G550.

Tables and Figures

Table 1

Comparison of uptake clearance for $E_2$17βG in freshly isolated and cryopreserved human hepatocytes.[a]

	freshly isolated [μL/min/10^6 cells]	cryopreserved [μL/min/10^6 cells]	cryopreserved/fresh ratio	
HH-093	4.29 ± 1.15	3.43 ± 0.69	0.80 ± 0.27	
HH-097	21.5 ± 14.1	14.5 ± 2.0	0.67 ± 0.45	
HH-099	15.7 ± 2.4	5.97 ± 1.25	0.38 ± 0.10	*[b]
HH-105	14.9 ± 1.2	6.84 ± 0.93	0.46 ± 0.07	**
HH-106	5.94 ± 2.64	11.6 ± 3.35	1.95 ± 1.04	
mean[c]	12.5 ± 7.2	8.47 ± 4.49		

a) Uptake clearances were calculated as described in the Methods section. All uptake clearances mean transporter-mediated uptake clearances. All studies were carried out in triplicate and data are represented by mean ± S.D..

b) *…$p<0.05$, **…$p<0.01$: significantly different between in freshly isolated and cryopreserved hepatocytes by Dunnet's test

c) mean ± S.D. of 5 lot

Table 2

Kinetic parameters for the uptake of $E_2$17βG in cryopreserved human hepatocytes.[a]

Substrate	Lot No.	Km [μM]	Vmax [pmol/min/10^6 cells]	Vmax/Km [μL/min/10^6 cells]	Pdif [μL/min/10^6 cells]
$E_2$17βG	HH-063	3.09 ± 2.64	18.8 ± 11.5	6.08 ± 6.41	3.74 ± 0.46
	HH-068	11.5 ± 10.1	38.3 ± 33.1	3.33 ± 4.11	3.18 ± 0.51
	HH-069	6.31 ± 6.44	22.1 ± 19.3	3.50 ± 4.71	3.47 ± 0.45
	HH-088	18.1 ± 10.2	60.2 ± 35.1	3.33 ± 1.87	1.49 ± 0.39
	HH-117	3.21 ± 2.27	26.0 ± 12.5	8.10 ± 5.73	0.688 ± 0.33
average		8.44 ± 2.86	33.1 ± 7.5	4.87 ± 0.96	2.51 ± 0.60
	rat[b, c]	12.9 ± 1.3	1300 ± 100	101 ± 13	

a) Kinetic parameters were obtained from the uptake studies shown in Fig. 8. All data are shown as mean ± computer calculated S.E. values.

b) V_{max} and V_{max}/K_m are expressed as pmol/min/mg protein and μL/min/mg protein, respectively [102].

c) 1-mg-protein rat hepatocytes correspond to approximately 10^6 cells in our studies.

Table 3

Background information on donors

Lot No. (Donor ID)	Age (years)	Sex	Race[a]	Tobacco Use	Alcohol Use	Substance Use	Viability[b] [%]
HH-063	33	male	C	yes	no	no	75
HH-068	44	female	C	no	yes	no	70
HH-069	63	female	C	yes	yes	no	89
HH-088	84	female	C	no	no	no	92
HH-093	68	female	C	no	no	no	93
HH-097	47	male	C	no	no	no	71
HH-099	74	female	C	no	no	no	69
HH-105	59	male	C	yes	yes	no	57
HH-106	59	female	C	no	no	no	58
HH-117	47	female	C	no	no	no	90

a) C…Caucasian

b) Cell viability was confirmed by trypan blue exclusion test.

Table 4

Kinetic parameters for the uptake of cerivastatin in cryopreserved human hepatocytes.

Lot No.	K_m [μM]	V_{max} [pmol/min/10^6 cells]	V_{max}/K_m [μL/min/10^6 cells]	P_{dif} [μL/min/10^6 cells]
HH-088	18.3 ± 6.9	5200 ± 1970	284 ± 108	70.2 ± 13.9
HH-106	2.61 ± 1.48	553 ± 161	212 ± 62	65.1 ± 8.3
HH-117	3.72 ± 1.29	362 ± 120	97.3 ± 32.3	41.7 ± 3.4

Table 5

Plasma concentration of cerivastatin and blood concentration of CsA after i.v. infusion in rats.[a)]

	concentration of cerivastatin [nM]		concentration of cyclosporin A [μM]
control	3.28 ± 0.12		–
low dose	4.58 ± 0.52	*[b)]	1.24 ± 0.02
high dose	4.73 ± 0.29	**[b)]	3.02 ± 0.22

a) Plasma and blood concentrations of CER and CsA, respectively, were measured at 5 hours after intravenous administration of both compounds. All data are mean ± S.E. (n=3-4)

b) Statistically significant difference from control by Student's t-test (*…p<0.05, **…p<0.01)

Table 6

Inhibitory effects of CsA on the Oatp1-mediated uptake of [^{14}C]CER.

Concentration of CsA [μM]	Oatp1-mediated uptake of [^{14}C]CER [μL/5min/mg protein]
0	29.7 ± 5.0
0.1	18.3 ± 1.4
1	18.2 ± 4.5
10	8.92 ± 3.16

Table 7

IC_{50} values of GEM and its metabolites on the OATP2-mediated uptake and the metabolism of [^{14}C]CER[a)].

	GEM [μM]	M3 [μM]	GEM-1-O-glu [μM]
OATP2-mediated uptake	72.4 ± 28.4	323 ± 108	24.3 ± 19.8
CYP2C8-mediated metabolim			
total metabolism	28.8 ± 4.8	no inhibition	4.25 ± 1.39
M1 formation	37.2 ± 5.5	no inhibition	5.45 ± 1.34
M23 formation	48.0 ± 10.8	no inhibition	5.26 ± 2.73
CYP3A4-mediated metabolism			
total metabolism	361 ± 88	no inhibition	235 ± 51
M1 formation	398 ± 94	no inhibition	260 ± 54

a) All data are represented as mean ± computer-calculated S.D.

Table 8

The contributions by CYP2C8 and 3A4 on the total metabolism of [^{14}C]CER in pooled HLM.

		CYP2C8	CYP3A4
Total[a)]	[%][c)]	61	37
	[pmol/min/mg protein HLM][d)]	*7.01*	*4.26*
		(11.5 ± 0.4)[e)]	
M1 formation[b)]	[%][c)]	55	45
	[pmol/min/mg protein HLM][d)]	*4.04*	*3.31*
		(7.35 ± 0.26)[e)]	
M23 formation	[%][c)]	100	0
	[pmol/min/mg protein HLM][d)]	*2.68*	*0*
		(2.68 ± 0.14)[e)]	

a) The contributions by CYP2C8 and 3A4 on the total metabolism of [^{14}C]CER (including the formations of M1, M23 and other minor metabolites) in pooled HLM.

b) The contributions by CYP2C8 and 3A4 on the M1 formation in pooled HLM. The contributions were calculated by the following equations:

$$R_{CYP2C8} \times \left(\frac{\text{M1 formation}}{\text{total metabolism}} \text{ in CYP2C8 expression system} \right)$$ and

$$R_{CYP3A4} \times \left(\frac{\text{M1 formation}}{\text{total metabolism}} \text{ in CYP3A4 expression system} \right)$$ for the contributions by CYP2C8 and 3A4, respectively.

c) The contributions by CYP2A8 and 3A4 are represented as % of the total metabolism.

d) CYP2C8- and 3A4-mediated metabolic rates in pooled HLM are represented.

e) Metabolic rates in pooled HLM obtained in the present study are represented.

Table 9

Plasma and liver concentrations of GEM and its metabolites, and their estimated inhibitory effects on the elimination of CER in the liver in clinical situations.

	GEM	M3	GEM-1-O-glu	total[h)]
C_{max}[a)] [μM]	100 - 150	50	20	
$1+I/IC_{50\_OATP2}$[b)]	2.4 - 3.1	1.2	1.8	
$1+I/IC_{50\_metabolism}$[c)]	2.2 - 2.6	no inhibition	2.1	
maximum inhibition[d)]	5.3 - 8.1	1.2	3.9	25 - 38
f_u[e)] [%]	0.648	1.23	11.5	
$C_{max,u}$[f)] [μM]	0.65 - 0.97	0.62	2.3	
$1+I/IC_{50\_OATP2}$[b)]	1.0	1.0	1.1	
$1+I/IC_{50\_metabolism}$[c)]	1.0	no inhibition	1.3	
maximum inhibition[d)]	1.0	1.0	1.4	1.4
$C_{max,u,liver}$[g)] [μM]	-	-	81 - 97	
$1+I/IC_{50\_OATP2}$[b)]			1.1	
$1+I/IC_{50\_metabolism}$[c)]	-	no inhibition	3.1 - 3.3	
maximum inhibition[d)]	-	-	3.4 - 3.6	> 3.4 - 3.6

a) All values are reported by Backman et al. (2002) [16)] and Okelhelm et al. (1976) [87)].

b) $1+I/IC_{50\_OATP2}$ represents the extent of DDI caused by the transporter-mediated hepatic uptake process, as reported by Ito et al., (1998)[3), 4)].

c) $IC_{50\_metabolism}$ is calculated by the equation (7). $1+I/IC_{50\_metabolism}$ represents the extent of DDI caused by microsomal metabolism, as reported by Ito et al. (1998) [3), 4)].

d) $(1+I/IC_{50\_OATP2})$ X $(1+I/IC_{50\_metabolism})$

e) Serum protein unbound fraction obtained in the present study.

f) $C_{max,u}$ is the maximum plasma concentration multiplied by the serum protein unbound fraction (f_u) obtained in the present study.

g) $C_{max,u,liver}$ is the unbound plasma concentration ($C_{max,u}$) multiplied by liver/perfusate concentration ratio reported by Sallustio et al., (1996) [89)].

h) Overall inhibition on the transporter-mediated hepatic uptake and the metabolism of CER is shown.

Table 10

Oatp1-mediated transport of $E_2$17βG and Oatp2-mediated transport of digoxin in the presence of inhibitors.[a)]

Inhibitors	oatp1-mediated transport[b)] [% of control]	oatp2-mediated transport[b)] [% of control]	
indomethacin			
1000 μM	1.16 ± 3.87	14.3 ± 2.6	
100 μM	13.6 ± 5.0	92.5 ± 10.1	**[c)]
10 μM	78.7 ± 6.0	106 ± 15.6	
ibuprofen			
1000 μM	10.0 ± 3.5	57.0 ± 3.6	**
100 μM	69.7 ± 13.3	93.9 ± 2.1	
10 μM	116 ± 8	74.7 ± 4.9	
ketoprofen			
1000 μM	6.89 ± 2.94	30.2 ± 1.7	**
100 μM	64.8 ± 2.4	96.7 ± 7.0	*
10 μM	79.1 ± 1.2	75.2 ± 11.6	
naproxen			
1000 μM	19.9 ± 1.8	52.2 ± 1.1	**
100 μM	87.4 ± 2.2	93.9 ± 2.0	
10 μM	87.9 ± 5.2	72.9 ± 10.2	
corticosterone			
100 μM	14.3 ± 2.5	32.9 ± 4.8	
10 μM	43.4 ± 2.9	65.7 ± 10.9	
deoxycorticosterone			
100 μM	1.34 ± 2.26	13.6 ± 7.1	
10 μM	20.6 ± 5.5	75.3 ± 12.7	*
digoxin			
100 μM	71.6 ± 12.7	8.57 ± 4.77	*
10 μM	105 ± 6	13.3 ± 0.97	**
methotrexate			
1000 μM	82.9 ± 3.0	77.7 ± 7.5	
100 μM	111 ± 8	97.6 ± 8.2	
10 μM	135 ± 5	124 ± 15	
penicillin G			
1000 μM	55.3 ± 6.2	81.0 ± 4.3	
100 μM	110 ± 1	109 ± 12	
10 μM	115 ± 9	90 ± 9.1	
verapamil			
1000 μM	-3.93 ± 3.89	4.12 ± 1.56	
100 μM	7.04 ± 8.28	14.0 ± 3.81	
10 μM	99.6 ± 11.0	87.5 ± 16.3	
cyclosporin A			
30 μM	27.6 ± 3.4	27.4 ± 13.8	
3 μM	88.1 ± 2.9	60.1 ± 5.9	*
0.3 μM	87.0 ± 4.6	91.6 ± 12.0	
tolbutamide			
1000 μM	32.9 ± 3.9	47.3 ± 10.7	
100 μM	101 ± 3	99.2 ± 4.9	
10 μM	94.4 ± 3.6	108 ± 6	

Table 10 continued

glibenclamide			
1000 μM	2.33 ± 2.80	1.61 ± 1.20	
100 μM	5.55 ± 6.37	22.2 ± 5.8	
10 μM	27.1 ± 6.5	64.7 ± 9.4	
rifampicin			
1000 μM	10.9 ± 3.3	5.64 ± 9.73	
100 μM	46.6 ± 3.4	17.9 ± 9.7	
10 μM	106 ± 10	32.0 ± 6.8	*
cimetidine			
1000 μM	79.4 ± 4.4	54.0 ± 5.8	
100 μM	90.9 ± 13.6	94.9 ± 6.2	
quinidine			
400 μM	20.6 ± 9.3	26.4 ± 4.1	
100 μM	8.36 ± 23.76	90.6 ± 10.4	
25 μM	47.3 ± 7.5	129 ± 11	*
quinine			
400 μM	1.13 ± 1.83	2.14 ± 13.64	
100 μM	40.4 ± 3.4	11.2 ± 14.4	
25 μM	97.9 ± 5.1	28.4 ± 11.2	**
a-ketoglutarate			
1000 μM	100 ± 5	84.6 ± 3.1	
propionic acid			
1000 μM	89.4 ± 1.8	121 ± 6	
***p*-aminohipprate**			
1000 μM	144 ± 9	124 ± 17	
100 μM	118 ± 6	139 ± 21	

a) Substrate uptake was measured by incubating cells with 0.1μM $E_2$17βG or 50nM digoxin in the presence or absence of inhibitors.

b) Values are CL_{uptake} in cDNA transfected cells minus that in mock-transfected cells, normalized by their control estimated in the absence of inhibitors and expressed as mean ± S.E. of 3 separate studies.

c) Statistically significant difference between Oatp1- and Oatp2-mediated transport by Dunnet's test. (*…$p < 0.05$, **…$p < 0.01$)

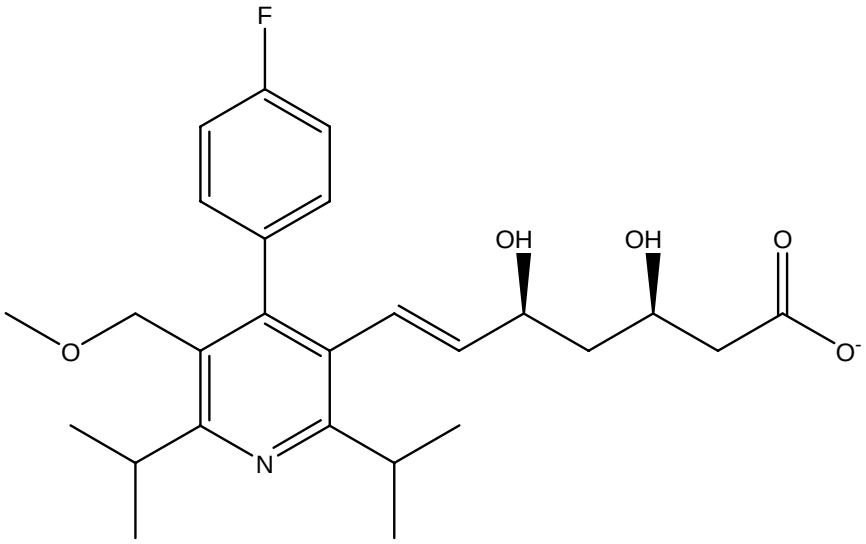

Figure 1

Chemical structure of CER.

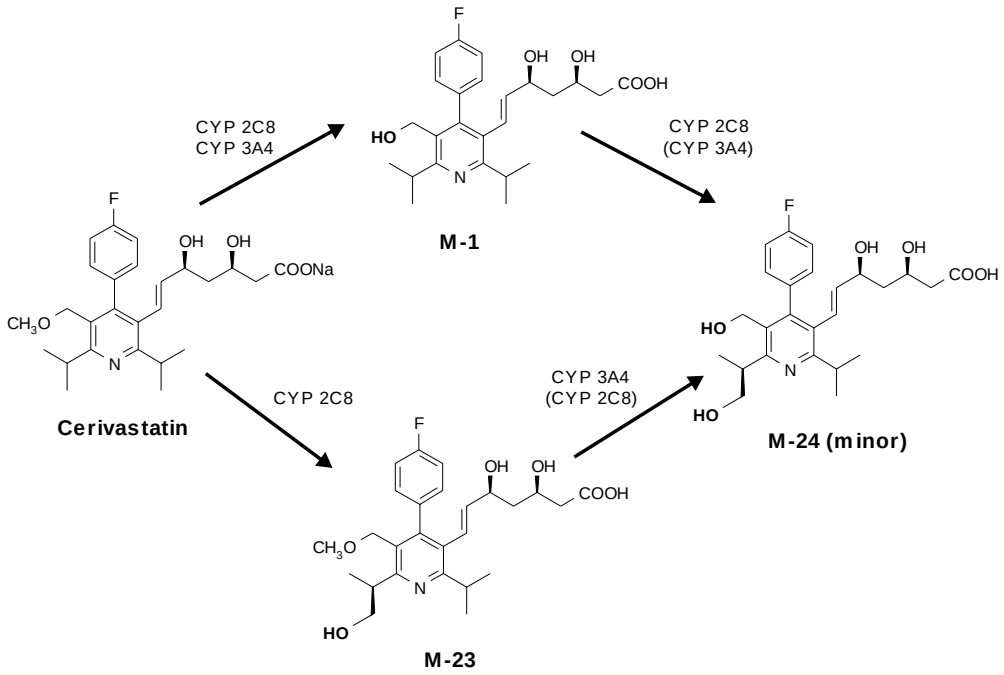

Figure 2

Metabolic pathway of CER.

CYP2C8 mediates the metabolism of CER into M-1 and M-23 while CYP3A4 mediates that into M-1. Both CYPs mediate the metabolism into M-24, however, it is minor metabolite and is minimally detected in human plasma and urine.

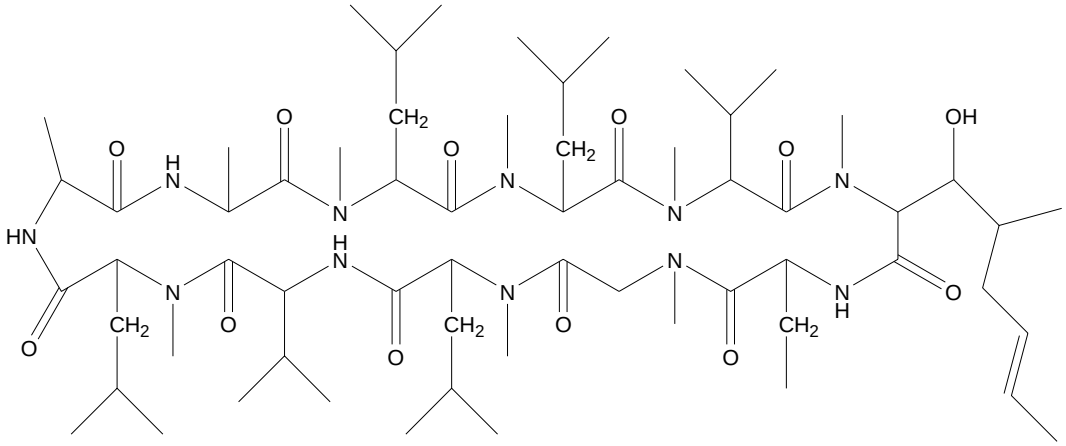

Figure 3

Chemical structure of CsA.

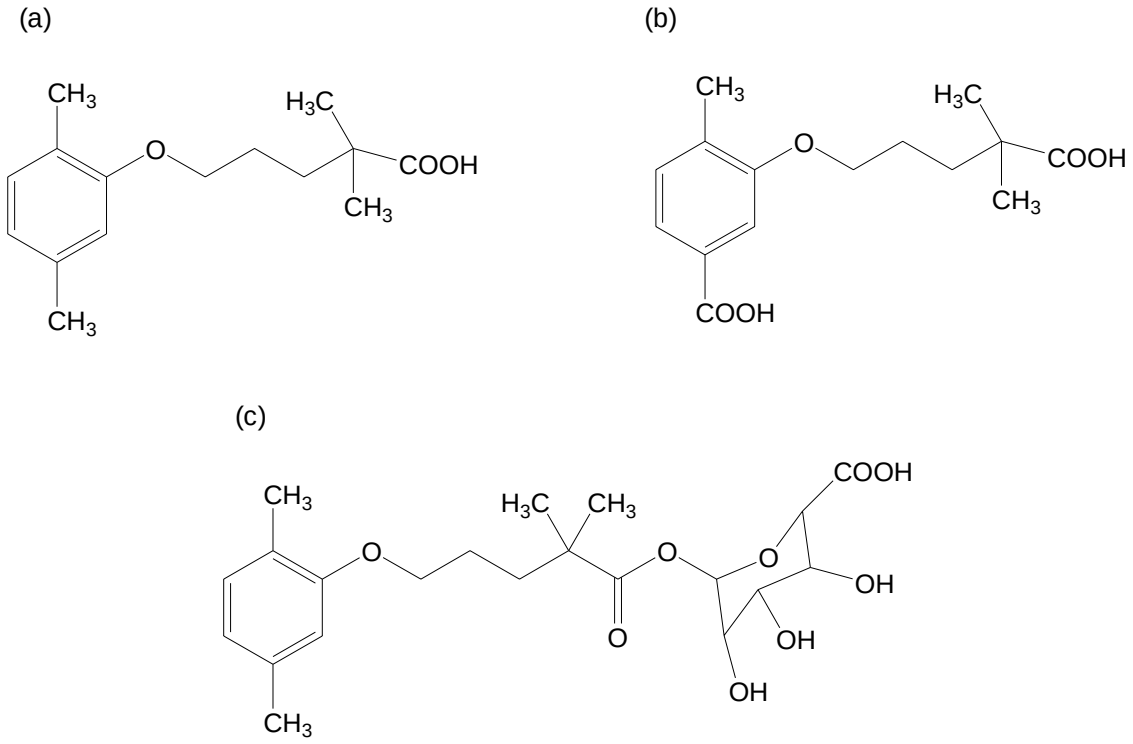

Figure 4

Chemical structure of GEM (a), M3 (b) and GEM-1-O-glu (c).

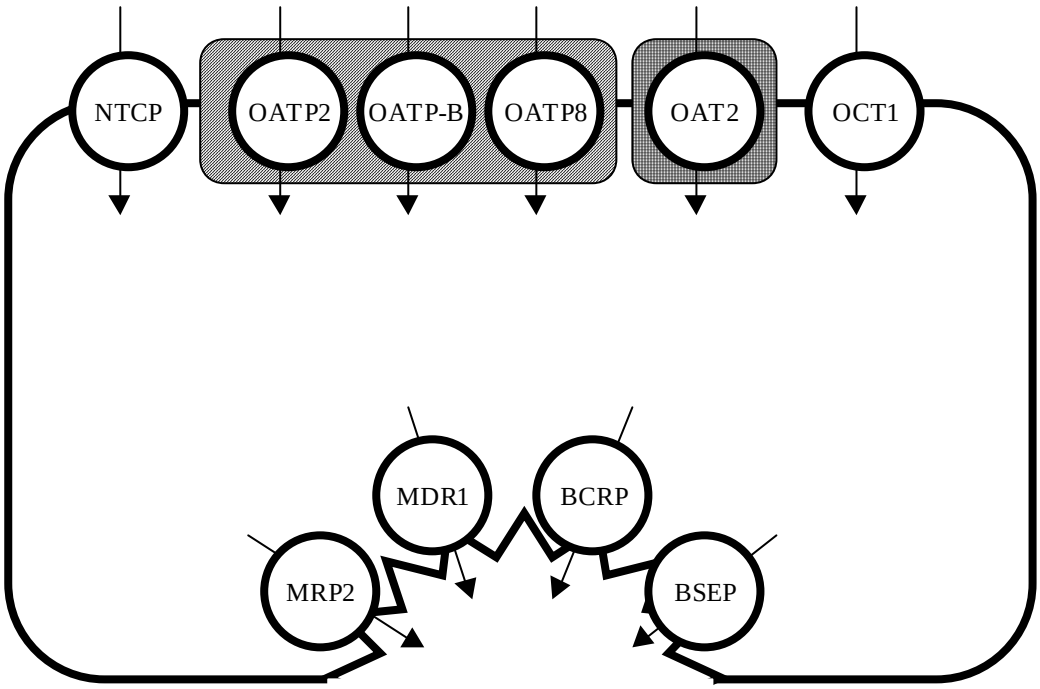

Figure 5

Transporters on human hepatocytes.

▨ : OATP family transporters, ▦ : OAT family transporters

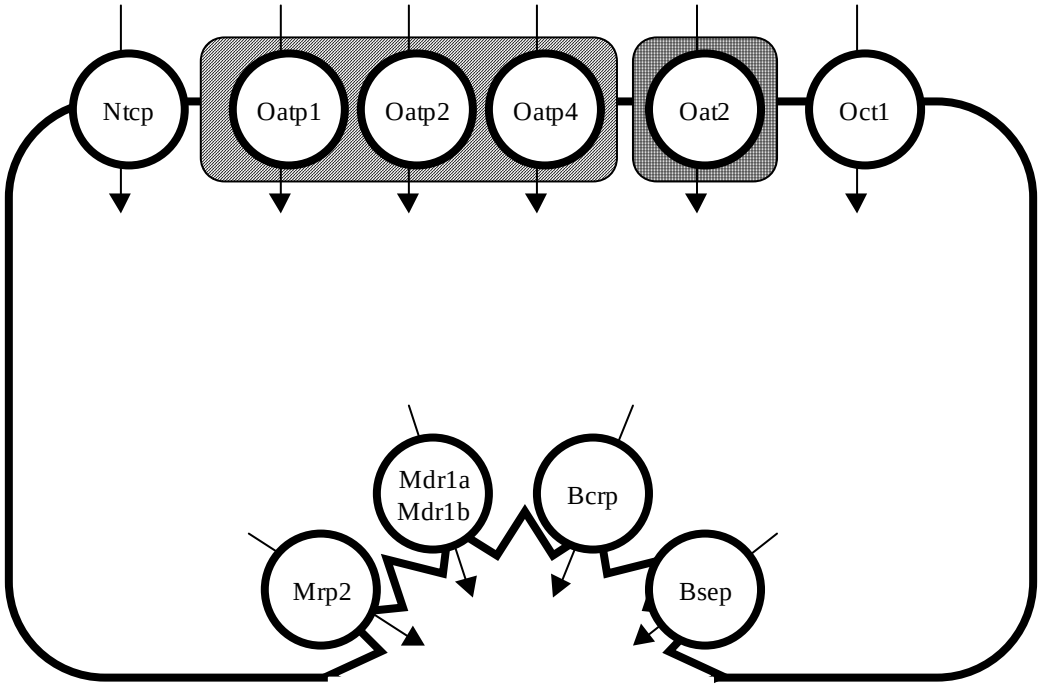

Figure 6

Transporters on rat hepato

▨ : OATP family transporters, ▦ : OAT family transporters

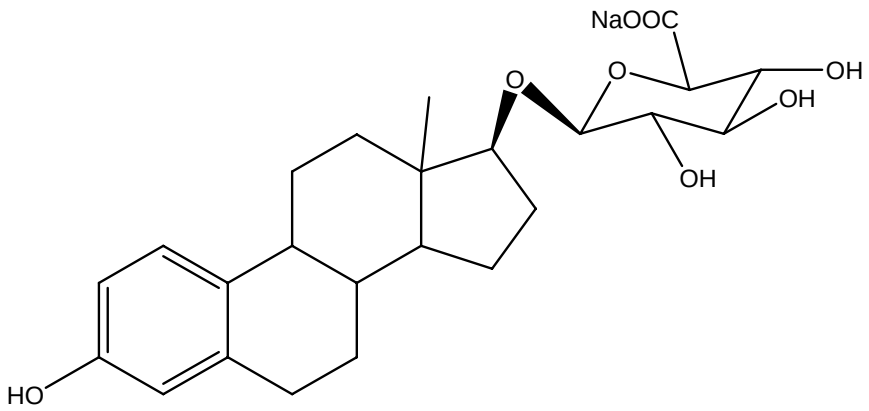

Figure 7

Chemical structure of $E_2$17βG.

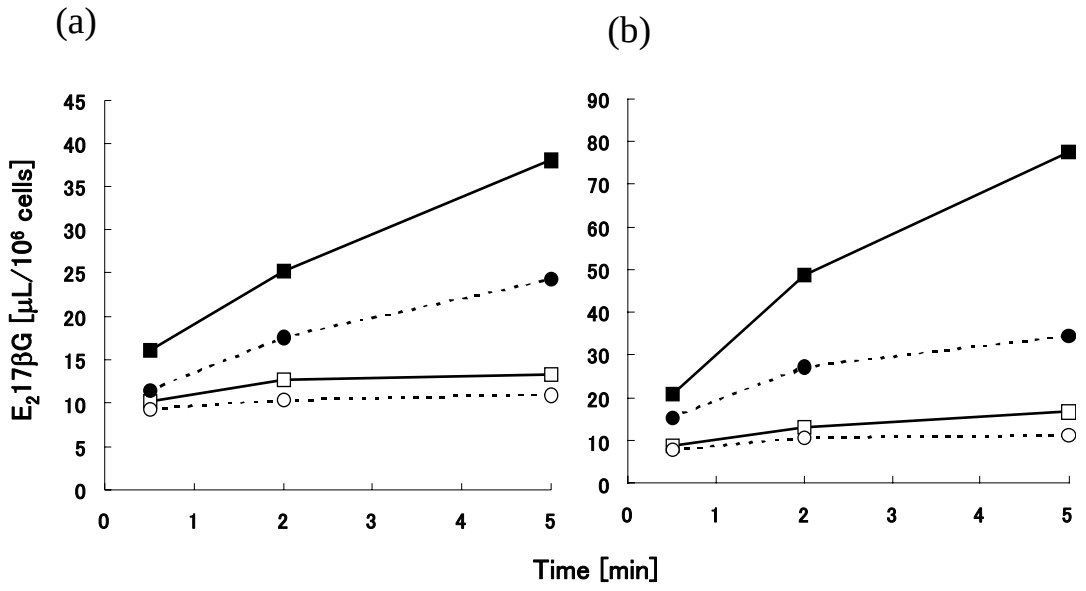

Figure 8

Time profile for the uptake of $E_2$17βG in freshly isolated or cryopreserved human hepatocytes.

Uptake of $E_2$17βG in freshly isolated hepatocytes (■, □) or cryopreserved hepatocytes (●, ○) was measured by incubating cells with 1 μM (●, ■) or 100 μM (○, □) $E_2$17βG at 37 ^oC in Krebs-Henseleit buffer. The uptake in lot No. HH-093 (a) and HH-099 (b) is shown here and other results are summarized in Table 1. Each point and bar represents mean ± S.E. of 3 separate determinations.

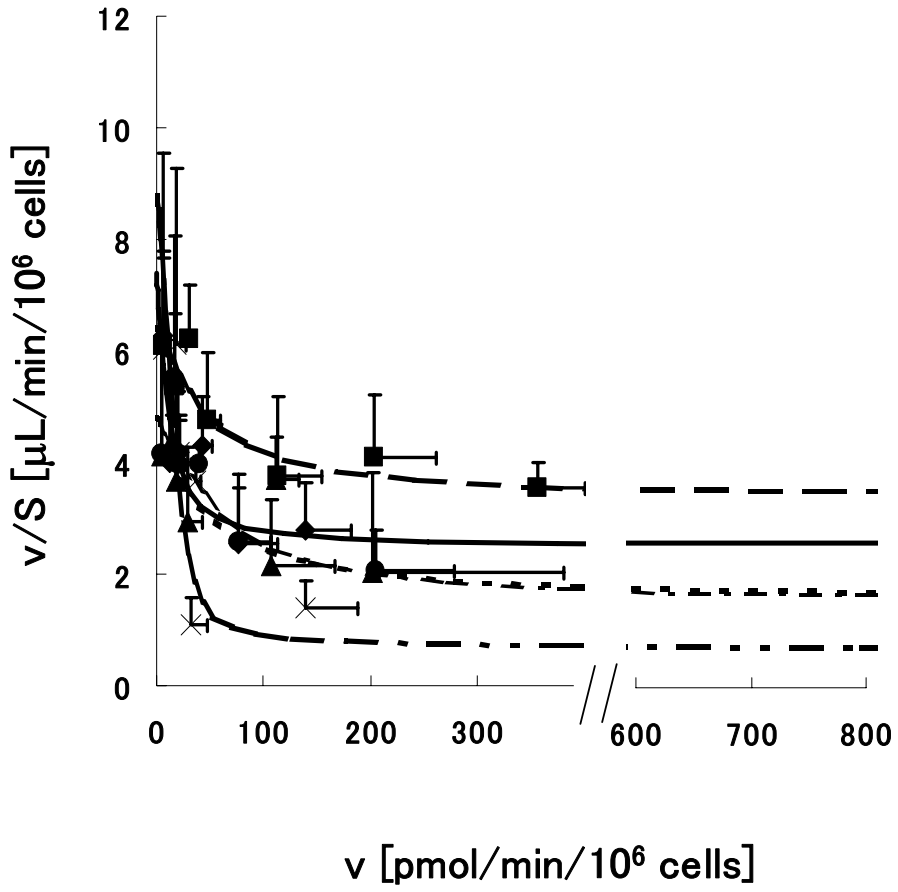

Figure 9

Eadie-Hofstee plots for the uptake of estradiol 17β-D-glucuronide ($E_2$17 β G) (b) in cryopreserved human hepatocytes, HH-063 (◆), HH-068 (■), HH-069 (▲), HH-088 (●) and HH-117 (×).

Uptake of $E_2$17 βG by cryopreserved hepatocytes was measured at concentrations of 1, 3, 5, 10, 30, 50, and 100 μM. Each point and bar represents mean ± S.E. of 3 separate determinations. In each graph, the lines represent the fitted curves obtained using equation (10).

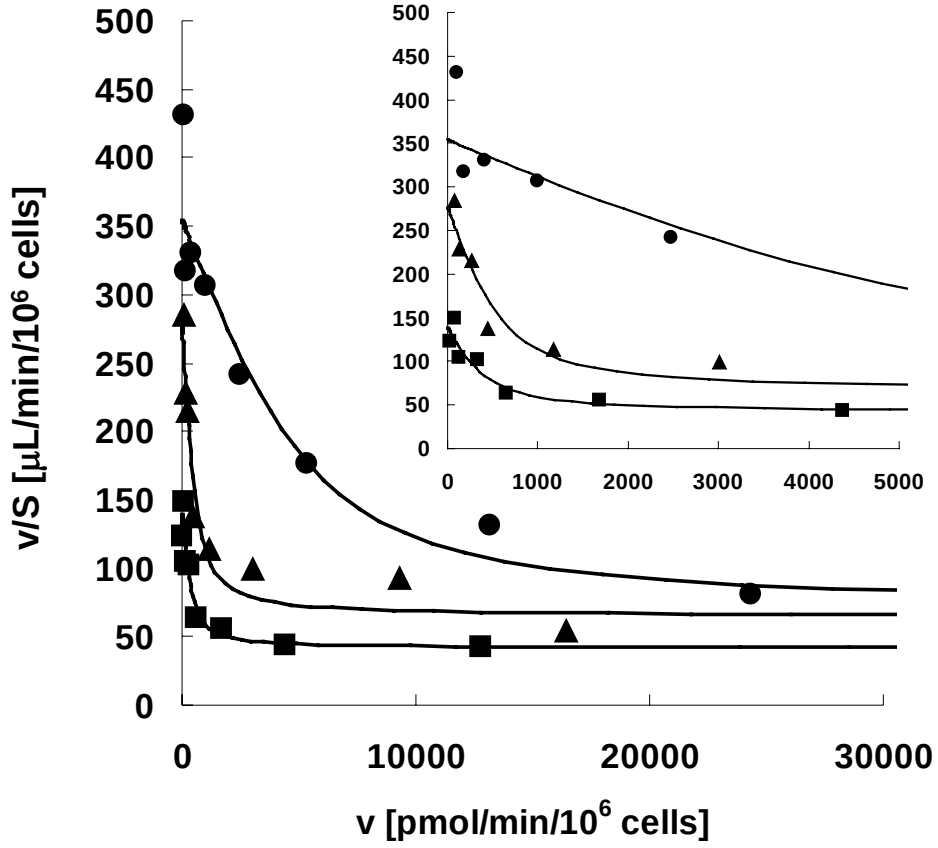

Figure 10

Eadie-Hofstee plot of the uptake of [^{14}C]-CER in cryopreserved human hepatocytes.

The uptake of [^{14}C]-CER was examined in 3 lots of cryopreserved human hepatocytes. Closed circles, triangles and squares (●, ▲, ■) represent the data for lot numbers HH-088, -106, and -117, respectively. Each symbol represents the mean value of 2 independent experiments. Solid lines represent the fitted lines.

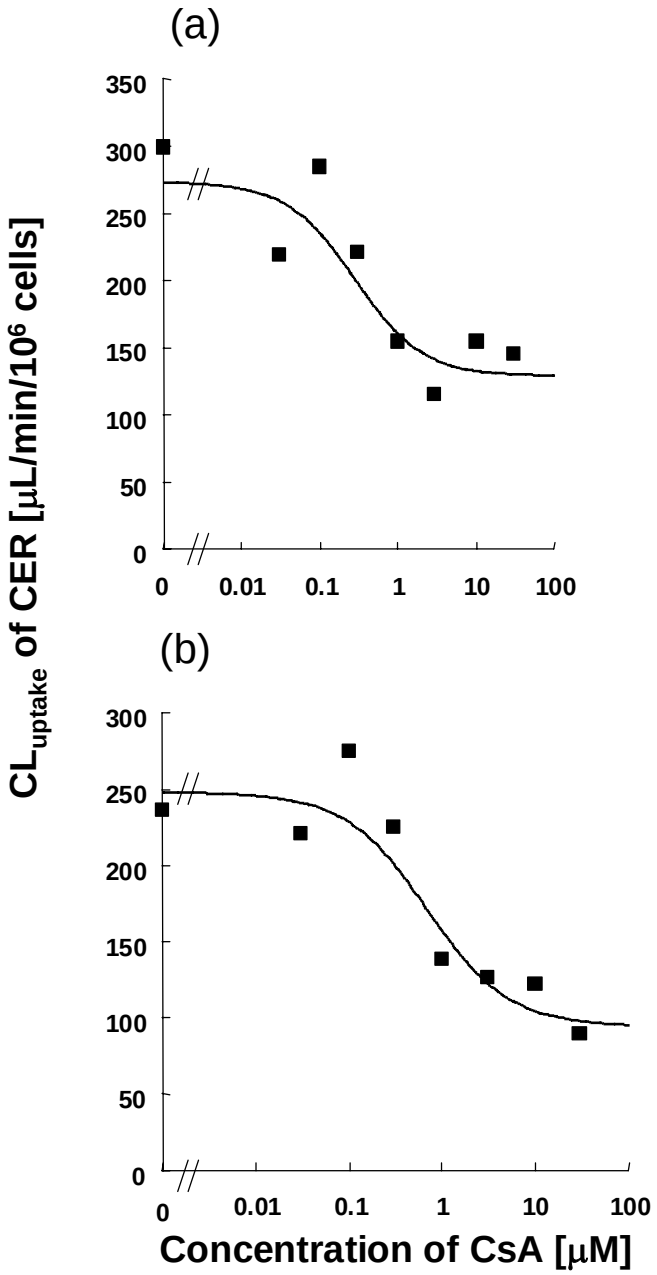

Figure 11

Inhibitory effect of CsA on the uptake of [^{14}C]-CER in cryopreserved human hepatocytes.

The inhibitory effect of CsA on the uptake of [^{14}C]-CER in lot numbers HH-088 (a) and HH-117 (b) of cryopreserved human hepatocytes was examined. Each symbol represents the mean value of 2 independent experiments. Solid lines represent the fitted lines.

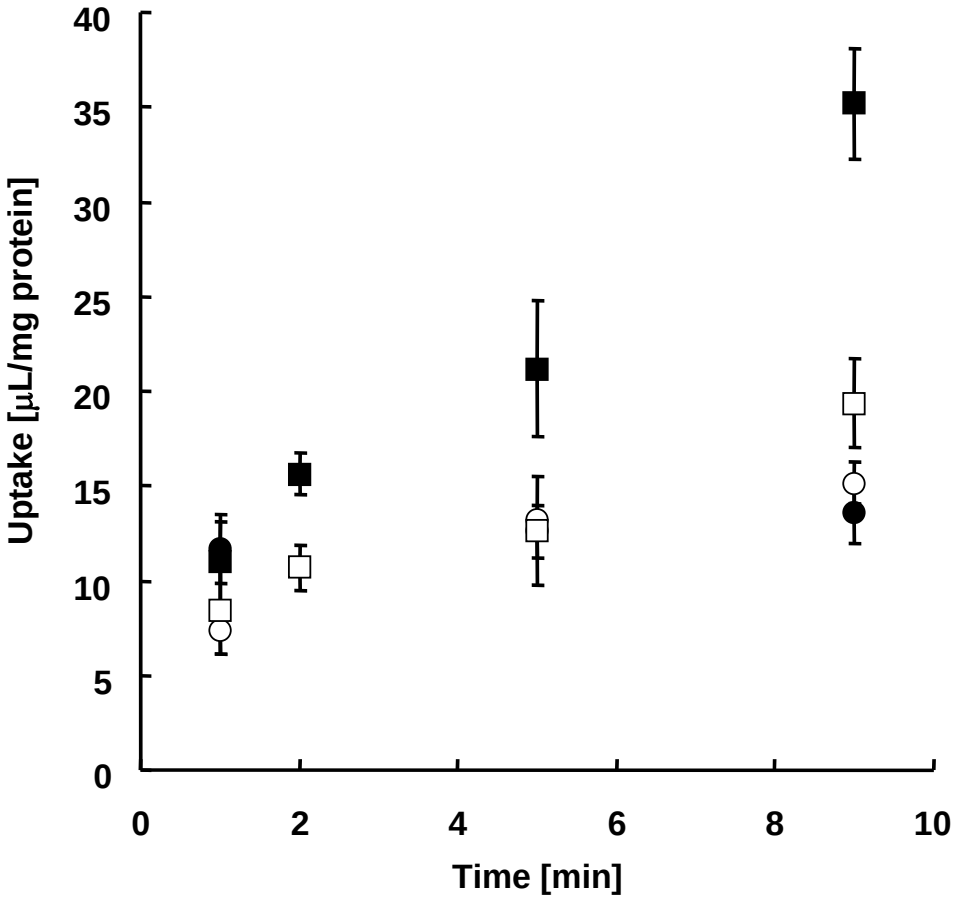

Figure 12

Uptake of [^{14}C]-CER in OATP2-expressing MDCKII cells.

The uptake of [^{14}C]-CER in MDCKII cells transfected with human OATP2 (■, □) or vector as a control (●, ○) was examined. The initial concentration of CER on the basal side of cells was 0.25 (■, ●) and 30 μM (□, ○). Each symbol represents the mean value ± S.E. of 3 independent experiments.

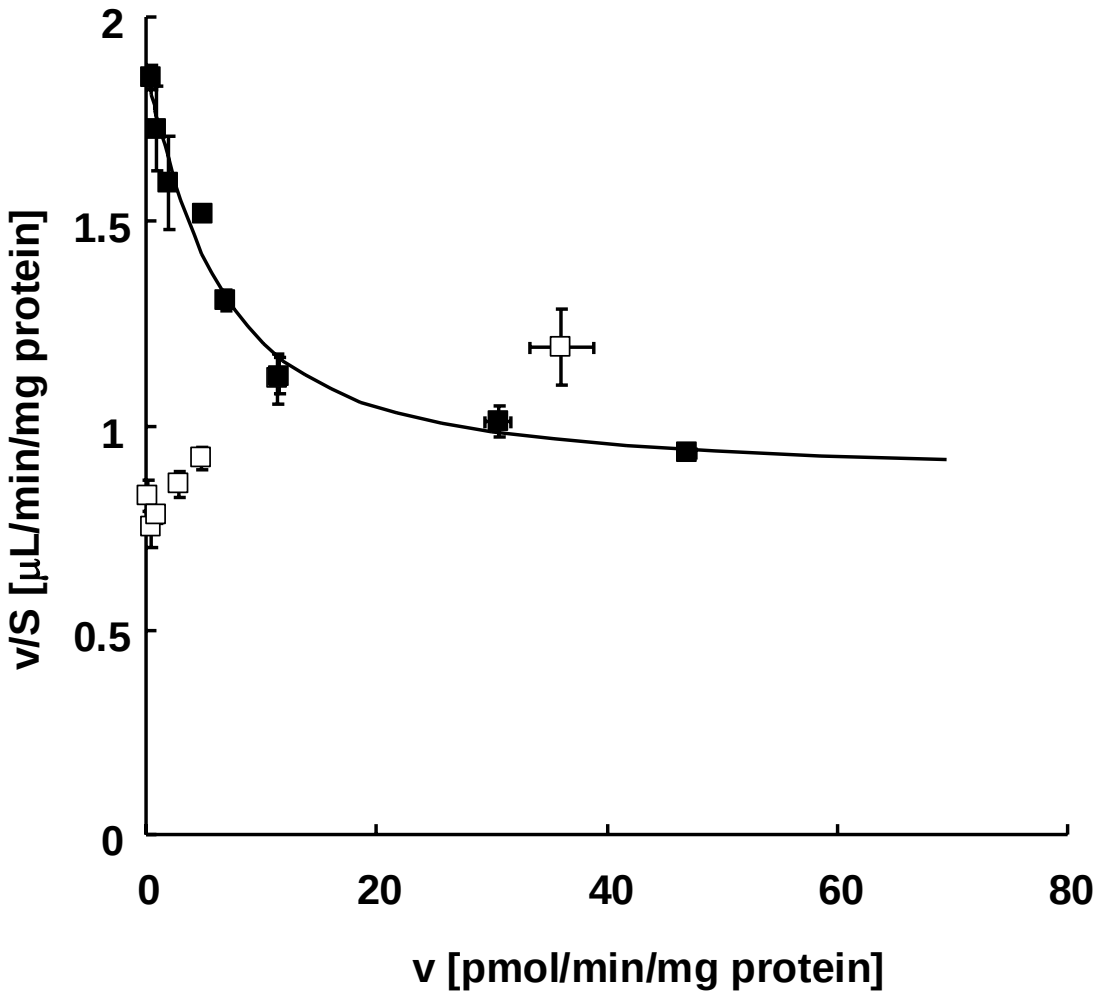

Figure 13

Eadie-Hofstee plot of the uptake of [^{14}C]-CER in OATP2-expressing and control MDCK cells.

The uptake of [^{14}C]-CER was examined in OATP2-expressing ( ) and control ( ) MDCK cells. Each symbol represents the mean value ± S.E. of 3 independent experiments. Solid line represents a fitted line.

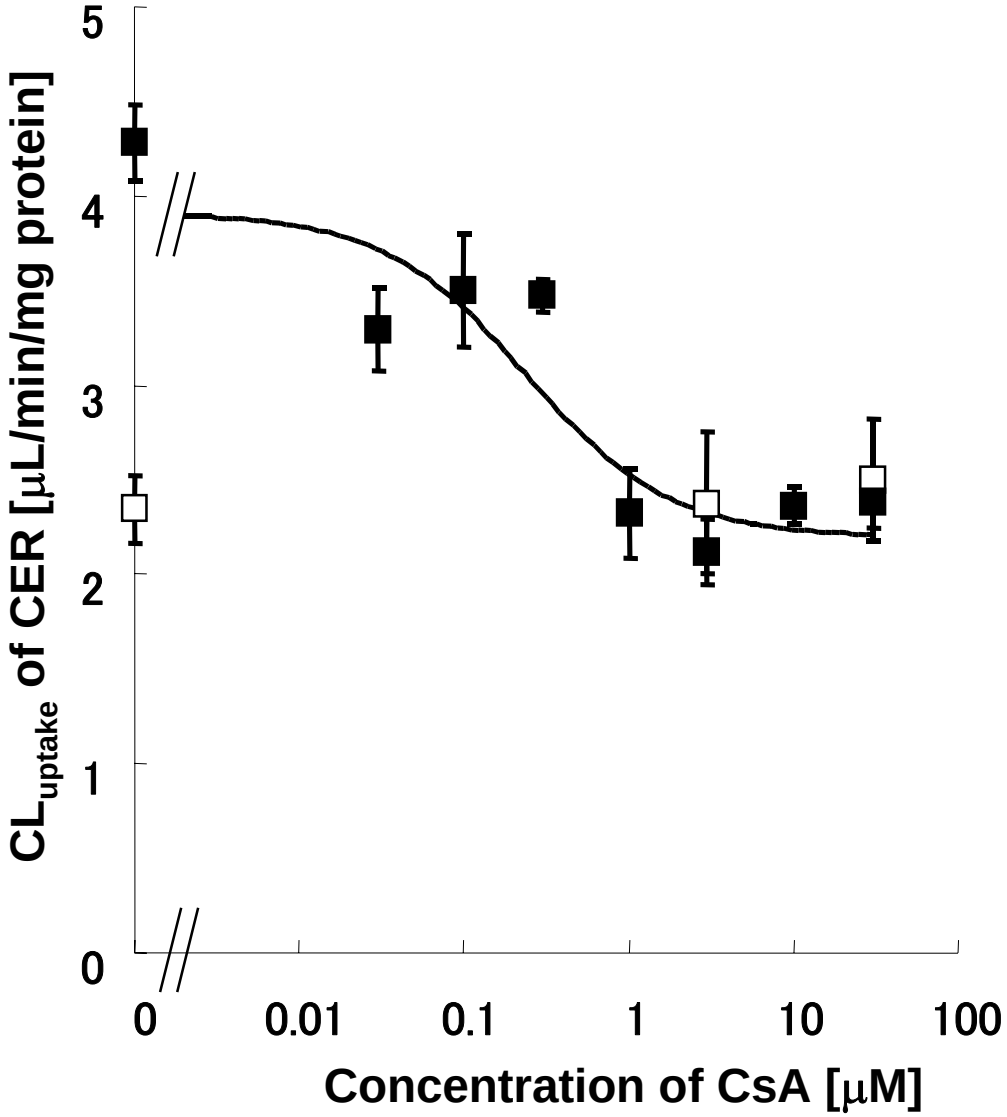

Figure 14

Inhibitory effect of CsA on OATP2-mediated uptake of [^{14}C]-CER.

The inhibitory effect of CsA on the uptake of [^{14}C]-CER in MDCKII cells transfected with human OATP2 (■) or vector (□) was examined. Each symbol represents the mean ± S.E. of 3 independent experiments. A solid line represents the fitted line for OATP2-mediated uptake of CER.

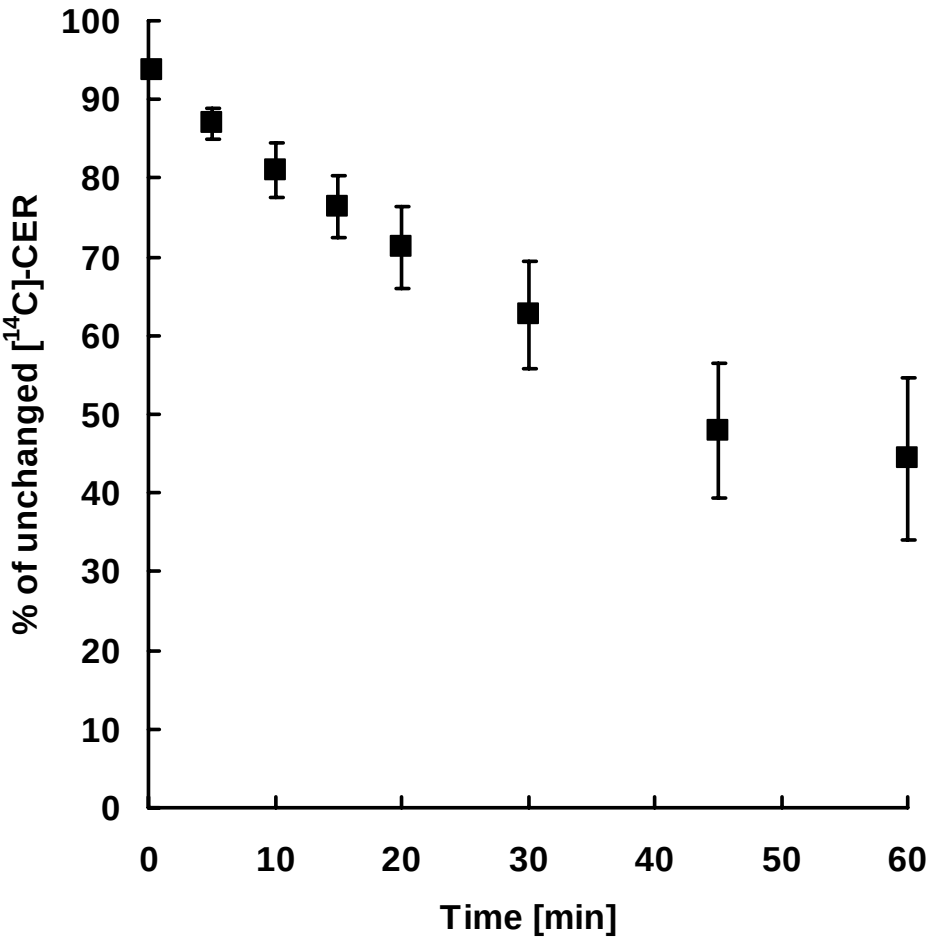

Figure 15

Metabolic stability of [^{14}C]-CER in pooled human microsomes.

The metabolism of [^{14}C]-CER was examined in pooled human microsomes at 37 ^{o}C for 60 min. Data are shown as the % unchanged [^{14}C]-CER with respect to the total radioactivity. Each point represents the mean ± S.E. of 3 independent experiments.

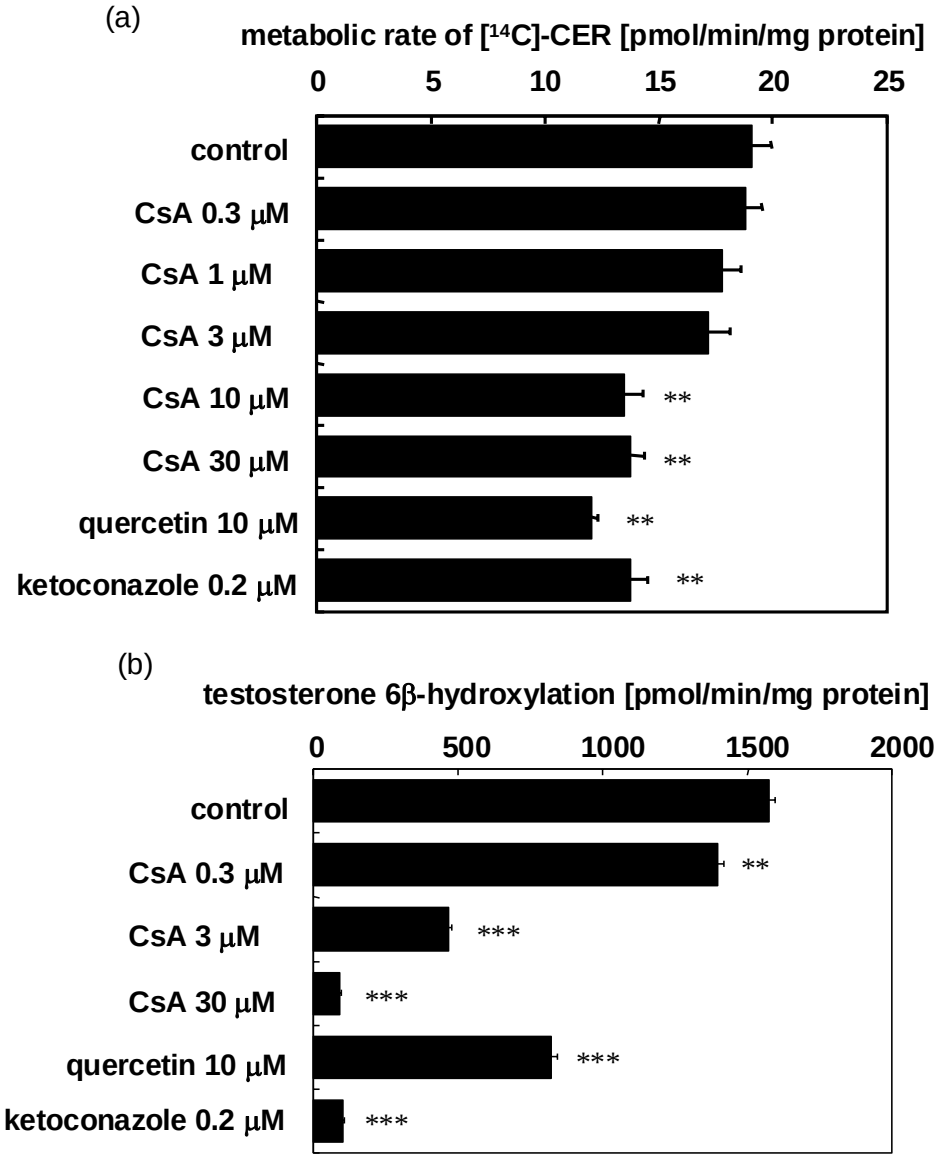

Figure 16

The effect of CsA and other inhibitors on the metabolic rate of [^{14}C]-CER (a) and testosterone 6β-hydroxylation (b).

The metabolic rates of [^{14}C]-CER (a) and testosterone 6β-hydroxylation in the absence or presence of CsA (0.3-30 μM), quercetin (10 μM) and ketoconazole (0.2 μM) were examined. Each bar represents the mean ± S.E. of 3 independent experiments. **…significant difference, $p < 0.01$, ***…$p < 0.001$ by the Student's t-test.

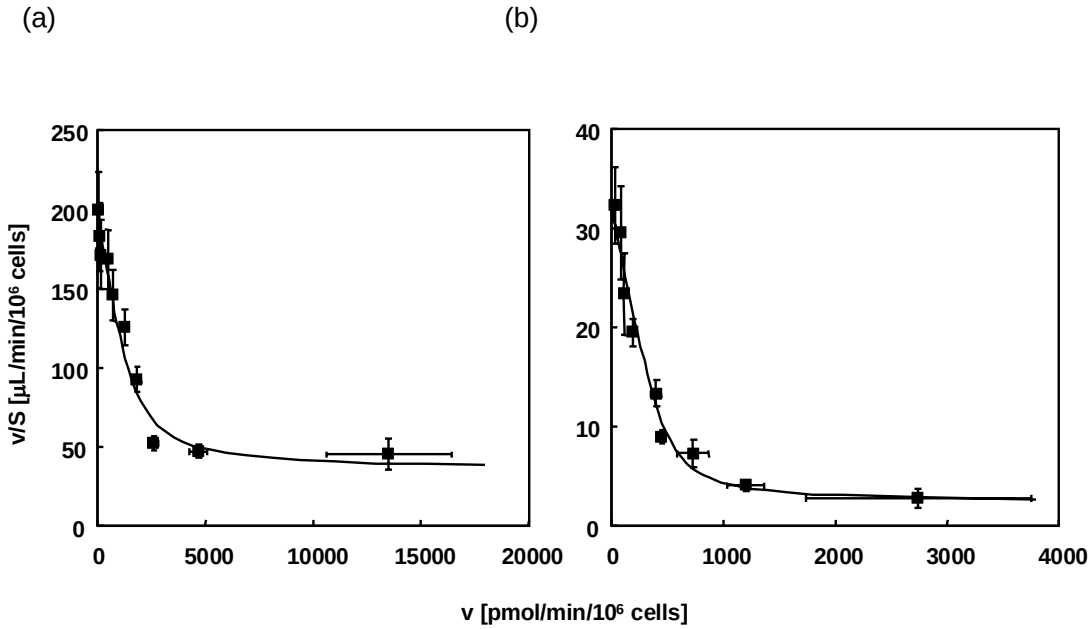

Figure 17

Eadie-Hofstee plot of the uptake of cerivastatin (CER) in isolated rat hepatocytes in the absence (a) or presence (b) of 90 % rat plasma.

Uptake of CER in isolated rat hepatocytes was examined in Krebs Henseleit buffer (a) or 90 % rat plasma containing buffer (b). Each point represents the mean ± S.E. (n = 3 x 3 cell preparations). Solid lines represent the fitted lines.

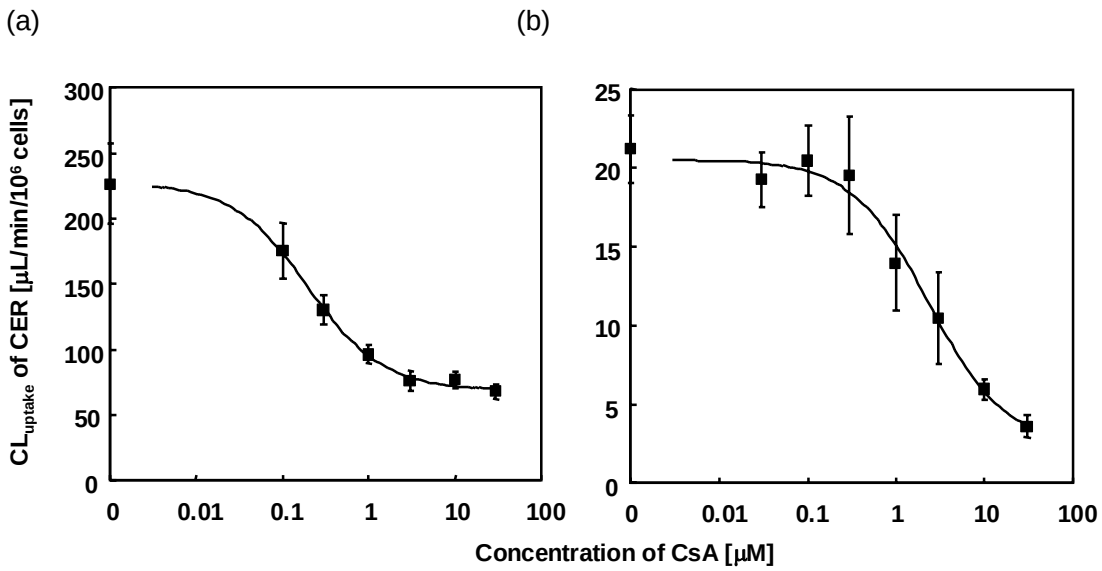

Figure 18

Inhibitory effect of cyclosporin A (CsA) on the uptake of cerivastatin (CER) in isolated rat hepatocytes.

Inhibitory effect of CsA on the uptake of CER in isolated rat hepatocytes was examined in the absence (a) or presence (b) of 90 % rat plasma. Each point represents the mean ± S.E. (n = 3 x 3 cell preparations). Solid lines represent the fitted lines.

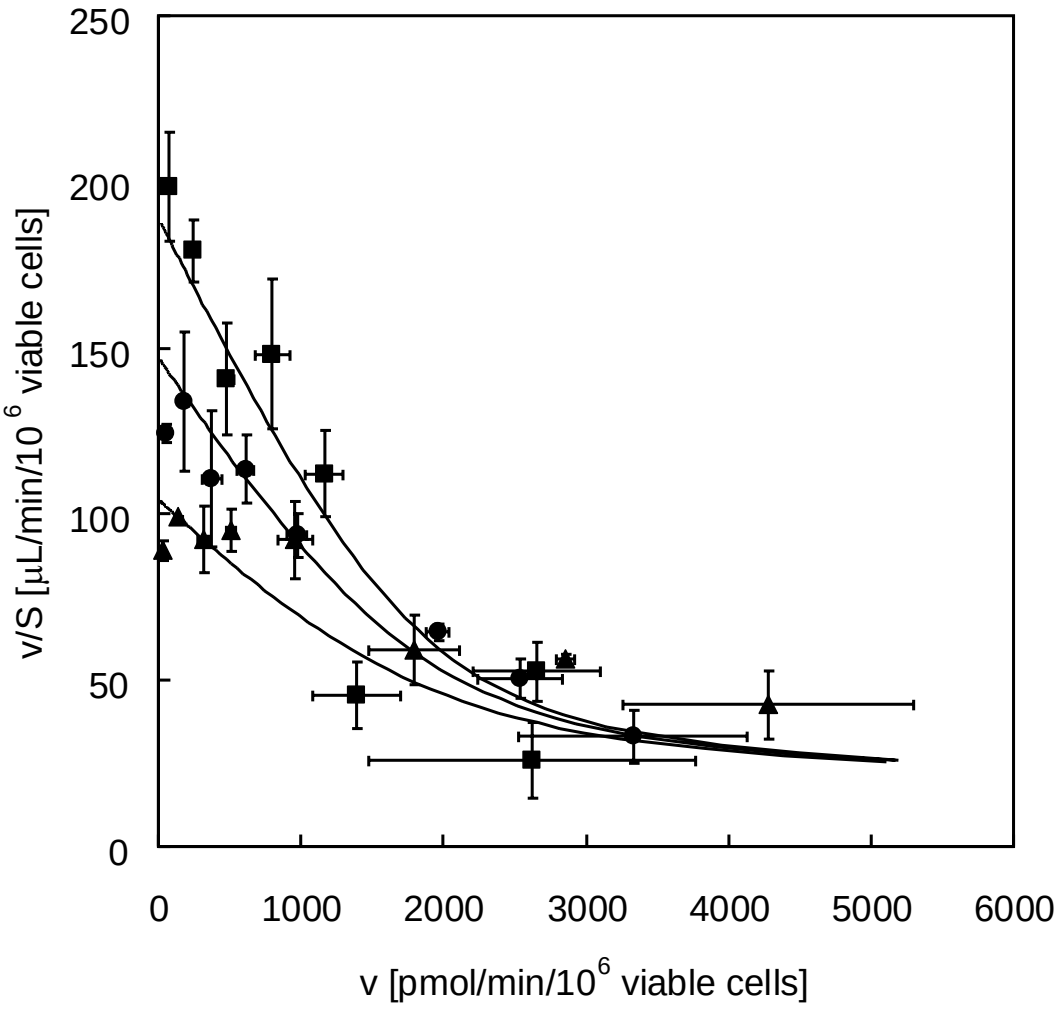

Figure 19

Eadie-Hofstee plot of the uptake of [^{14}C]-CER in the presence or absence of CsA.

Uptake of [^{14}C]-CER in isolated rat hepatocytes were examined in the presence of■ ( ), 0● ( ) and 0.▲( ) μM CsA. Each symbol represents mean ± S.E. of 3 independent experiments. Solid line represents a fitted line.

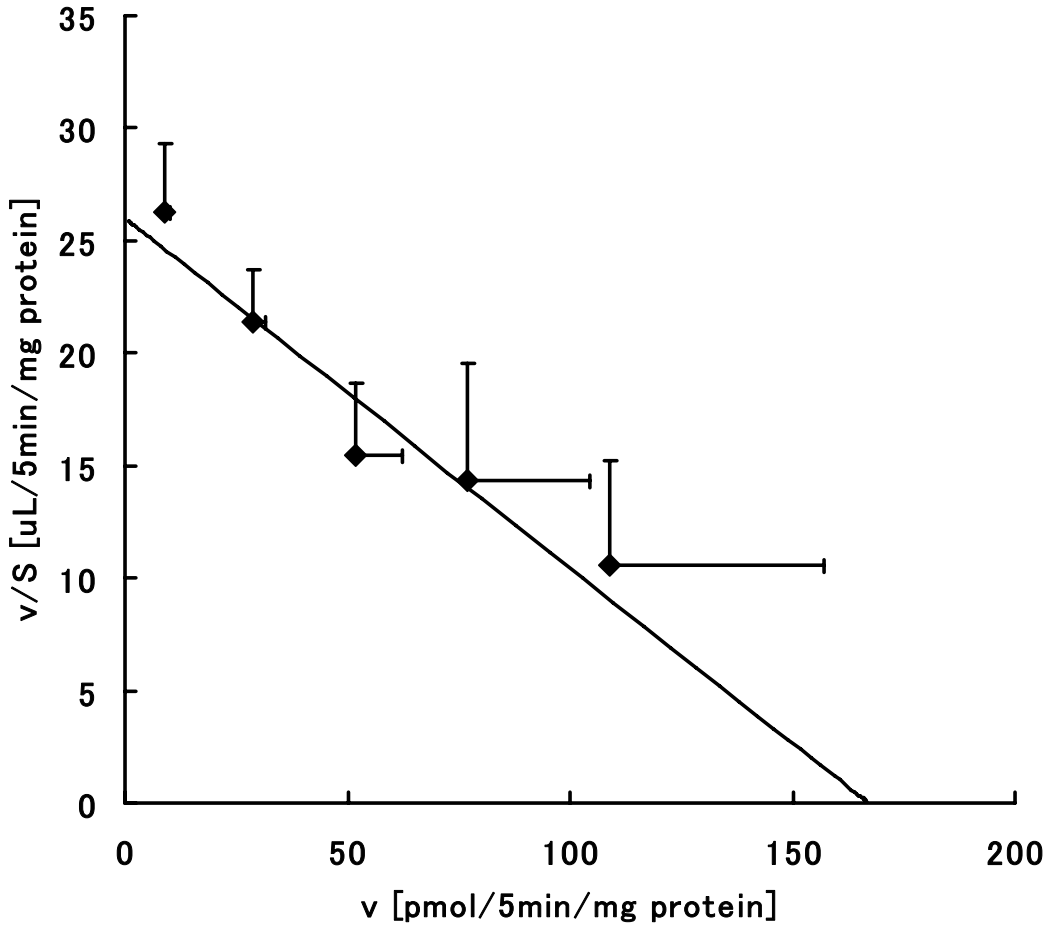

Figure 20

Eadie-Hofstee plot of the rat Oatp1-mediated uptake of [^{14}C]-CER.

Rat Oatp1-mediated uptake of [^{14}C]-CER, which represented the uptake in Oatp1-expressing cells minus that in control cells were plotted. Each symbol represents mean ± S.E. of 3 independent experiments. Solid line represents the fitted line.

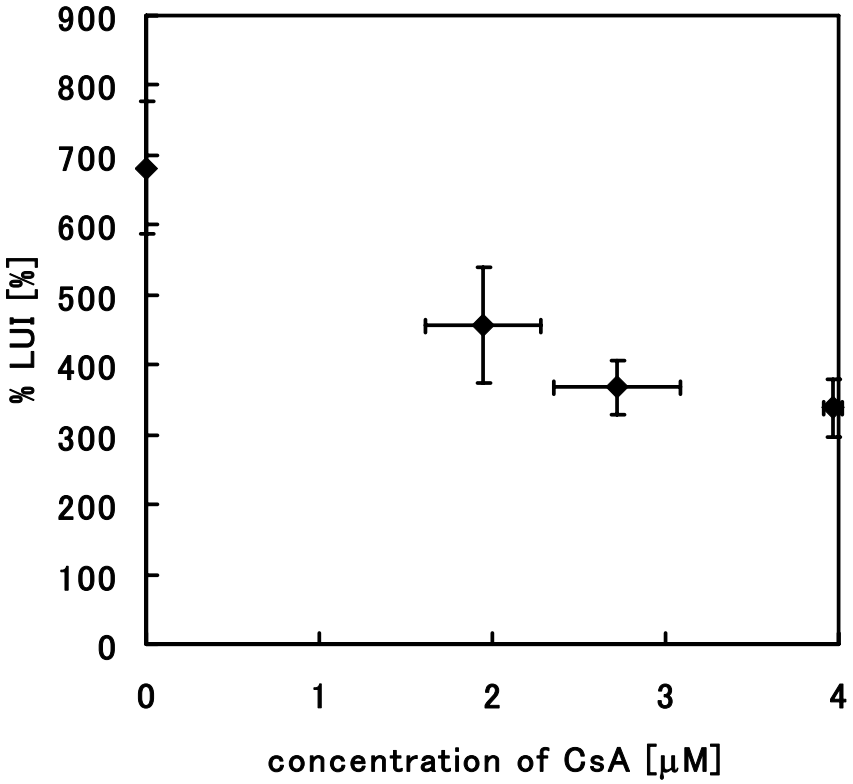

Figure 21

Inhibitory effect of cyclosporin A (CsA) on the hepatic uptake of cerivastatin (CER) in rats *in vivo*.

Inhibitory effect of CsA on the hepatic extraction of cerivastatin normalized by that of inulin (%LUI) during a single pass after p.v. bolus injection in rats was examined. %LUI was calculated from Eq. (14). Each point represents the mean ± S.E. (n = 4 and 8, with and without co-administration of CsA, respectively).

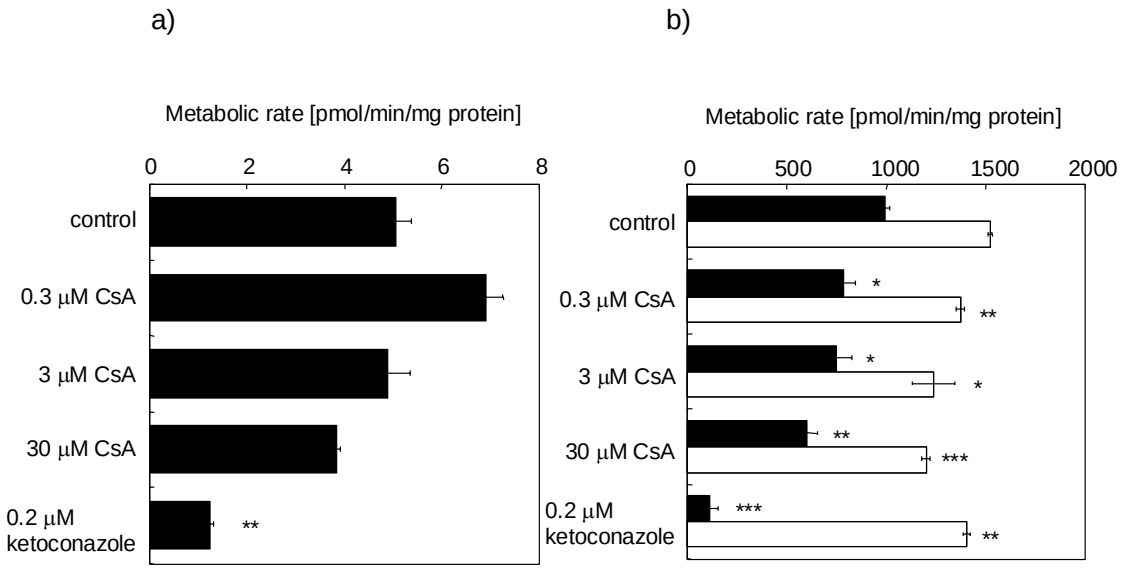

Figure 22

Metabolic stability of cerivastatin (CER) (a) and testosterone 6β- and 16α-hydroxylation (b) in rat liver microsomes in the presence or absence of cyclosporin A (CsA) or ketoconazole.

The effect of CsA and ketoconazole on the metabolic stability of CER and testosterone 6β-(■) and 16α-hydroxylation ▒) in rat liver microsomes was examined. The metabolic rate in the presence or absence of inhibitors is shown. Each bar represents the mean ± S.E. (n=3). *… $p < 0.05$, **…$p<0.01$, ***…$p<0.001$ (Student's *t*-test)

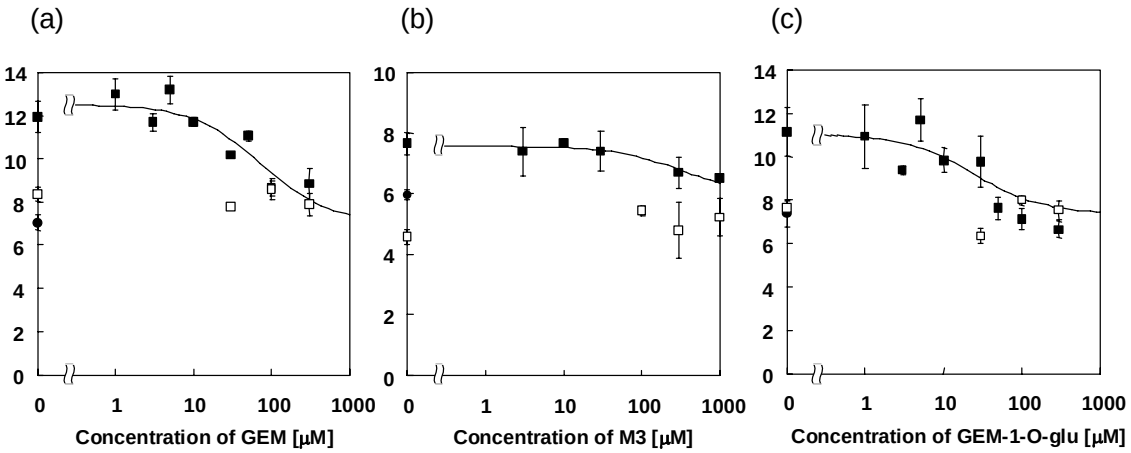

Figure 23

Effect of GEM and its metabolites on the OATP2-mediated uptake of [^{14}C]CER.

The inhibitory effects of GEM (a), M3 (b) and GEM-1-O-glu (c) on the OATP2-mediated uptake of [^{14}C]CER were examined. Uptake of [^{14}C]CER in OATP2-expressing (■) and vector-transfected cells (□) in the presence of GEM and its metabolites are represented. Uptake of [^{14}C]CER in the presence of excess unlabeled CER (30 μM) were also examined (●). Each symbol represents the mean value of three independent experiments ± S.E. and solid lines represent the fitted lines.

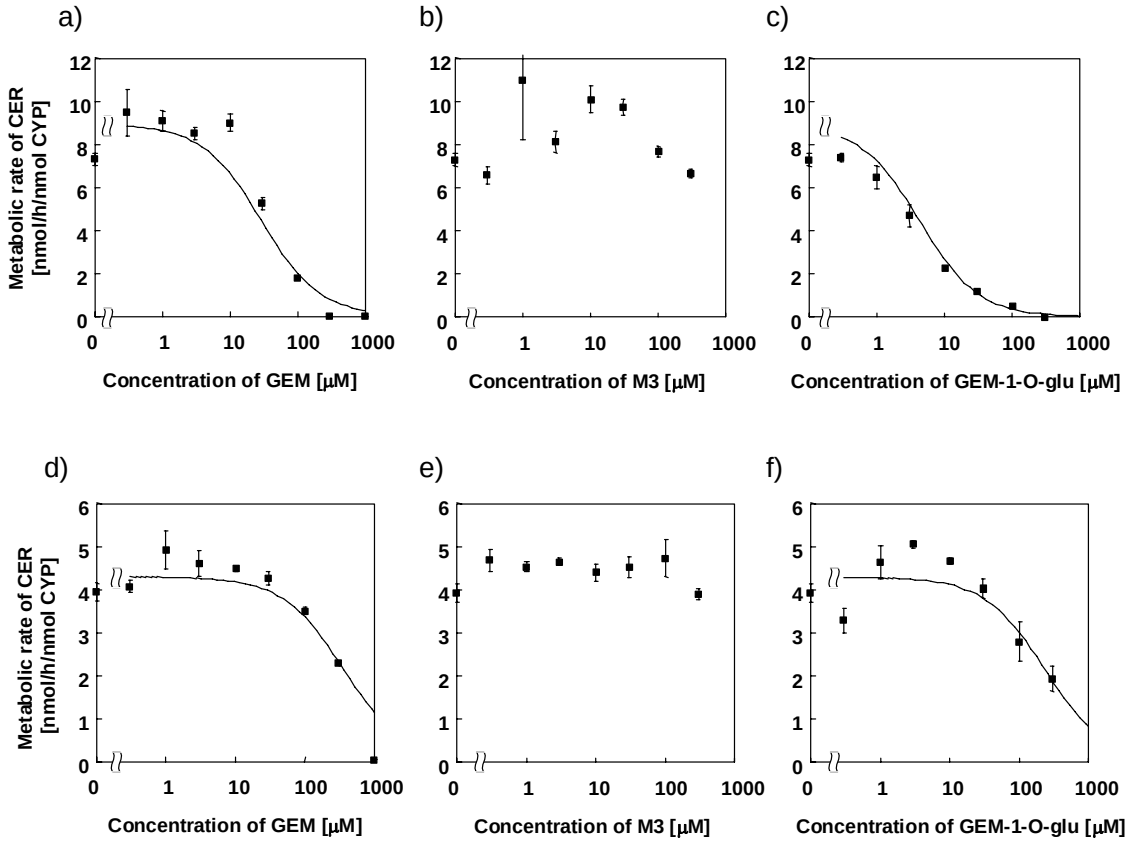

Figure 24

Effect of GEM and its metabolites on the CYP2C8- and 3A4-mediated metabolism of [^{14}C]CER.

Inhibitory effects of GEM (a, d), M3 (b, e) and GEM-1-O-glu (c, f) on the metabolism of [^{14}C]-CER in CYP2C8- (a, b, c) and 3A4- (d, e, f) expression systems were examined. Each symbol represents the mean value of three independent experiments ± S.E. and solid lines represent the fitted lines.

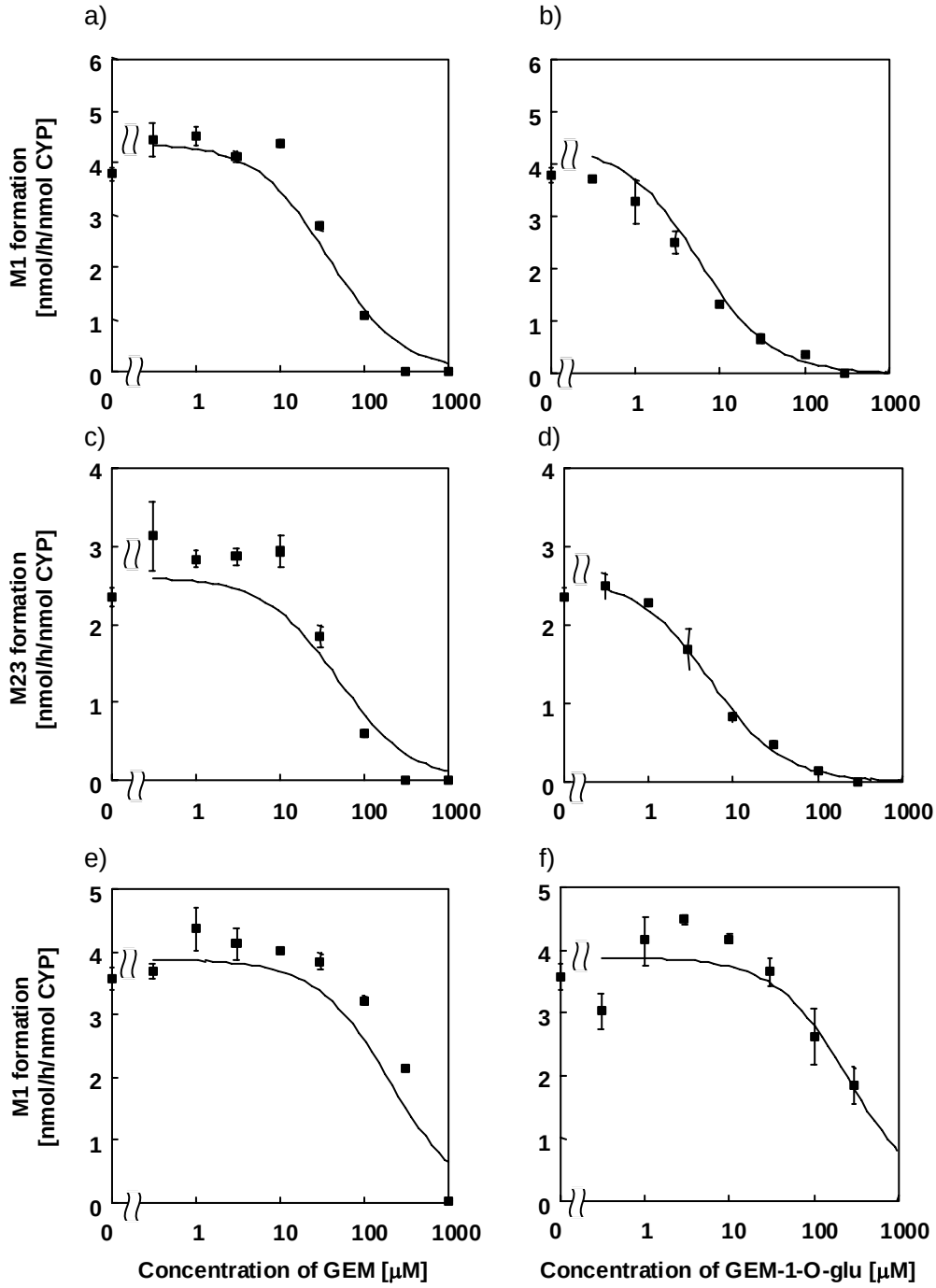

Figure 25

Effect of GEM and GEM-1-O-glu on the CYP2C8- and 3A4-mediated M1 and M23 formation of [^{14}C]CER.

Inhibitory effects of GEM (a, c, e) and GEM-1-O-glu (b, d, f) on the CYP2C8-mediated M1 formation (a, b), M23 formation (c, d) and 3A4-mediated M1 formation (e, f) in CYP expression systems were examined. Each symbol represents the mean value of three independent experiments ± S.E. and solid lines represent the fitted lines.

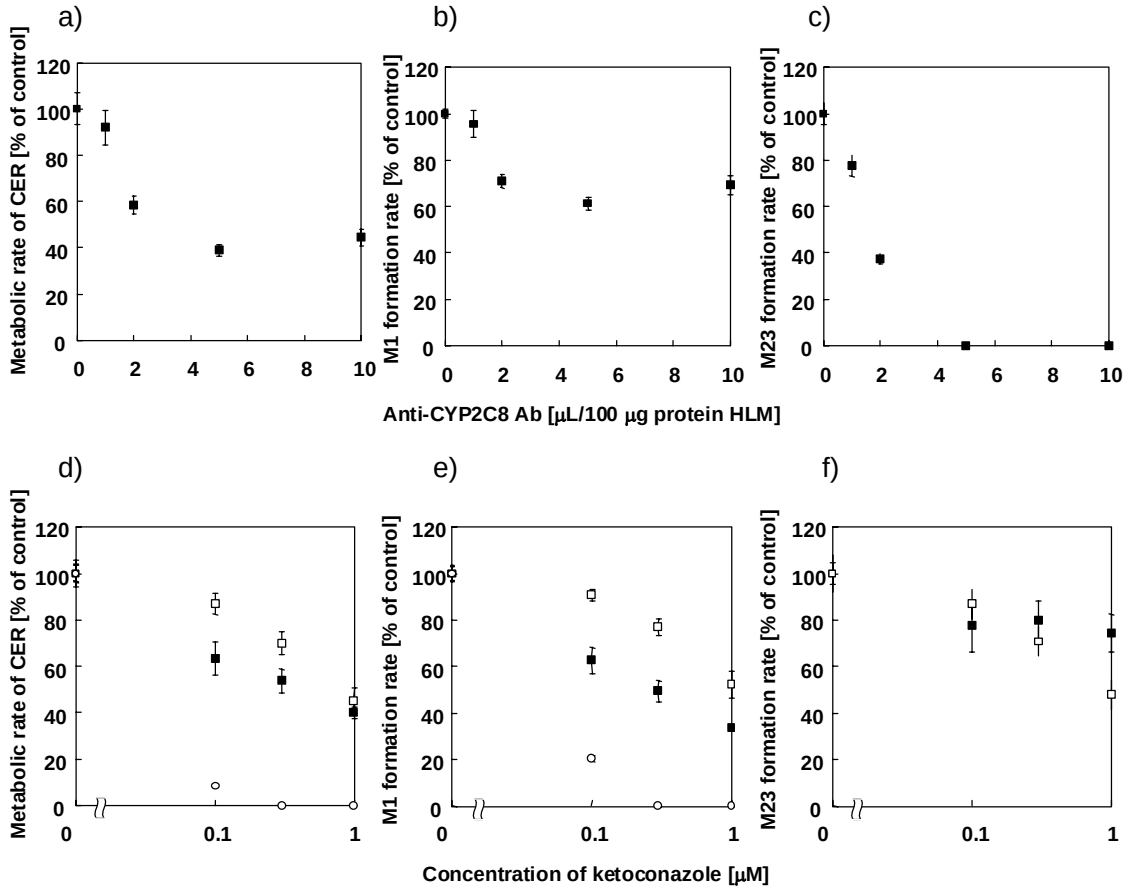

Figure 26

Effect of specific inhiitory antibody against CYP2C8 (anti-CYP2C8 Ab) and ketoconazole on the metabolism of CER in HLM.

The inhibitory effects of anti-CYP2C8 Ab (a) and ketoconazole, a potent CYP3A4 inhibitor, (d) on the metabolism of [^{14}C]CER in the pooled HLM (■) were examined. Their effects on M1 formation (b, e) and M23 formation (c, f) are also represented. Effect of ketoconazole on the metabolism of [^{14}C]-CER in CYP2C8- (□) and CYP3A4- (○) expression systems were also examined. Each symbol represents the mean value of three independent experiments ± S.E. and solid lines represent the fitted lines.

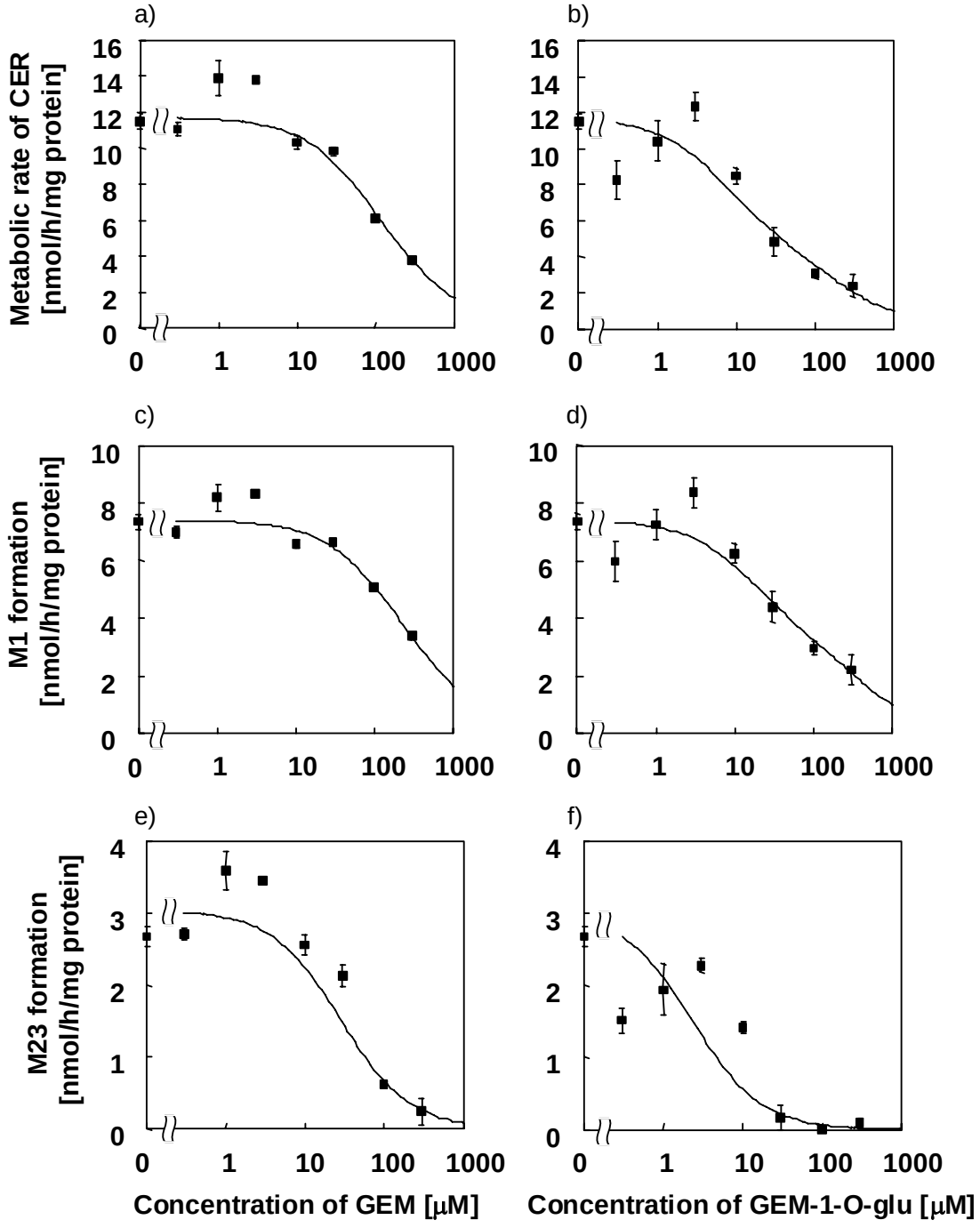

Figure 27

Effect of GEM and its metabolites on the metabolism of [^{14}C]-CER in HLM.

The inhibitory effects of GEM (a, c, e) and GEM-1-O-glu (b, d, f) on the metabolism of

[^{14}C]-CER (a, b) and the formation of M1 (c, d) and M23 (e, f) in pooled HLM were examined. Each symbol represents the mean value of three independent experiments ± S.E. Solid lines represent simulated lines based on the following equation using the contributions of CYP2C8 and 3A4 (R_{CYP2C8} and R_{CYP3A4}, respectively, Table 8) and IC_{50} values for CYP2C8- and 3A4-mediated metabolism in the CYP expression systems (IC_{50_CYP2C8} and IC_{50_CYP3A4}, Table 7).

$$k(+\text{inhibitor}) = k(\text{control}) \times \left(\frac{R_{CYP2C8}}{1 + I/IC_{50\_CYP2C8}} + \frac{R_{CYP3A4}}{1 + I/IC_{50\_CYP3A4}} \right) \quad \ldots(16)$$

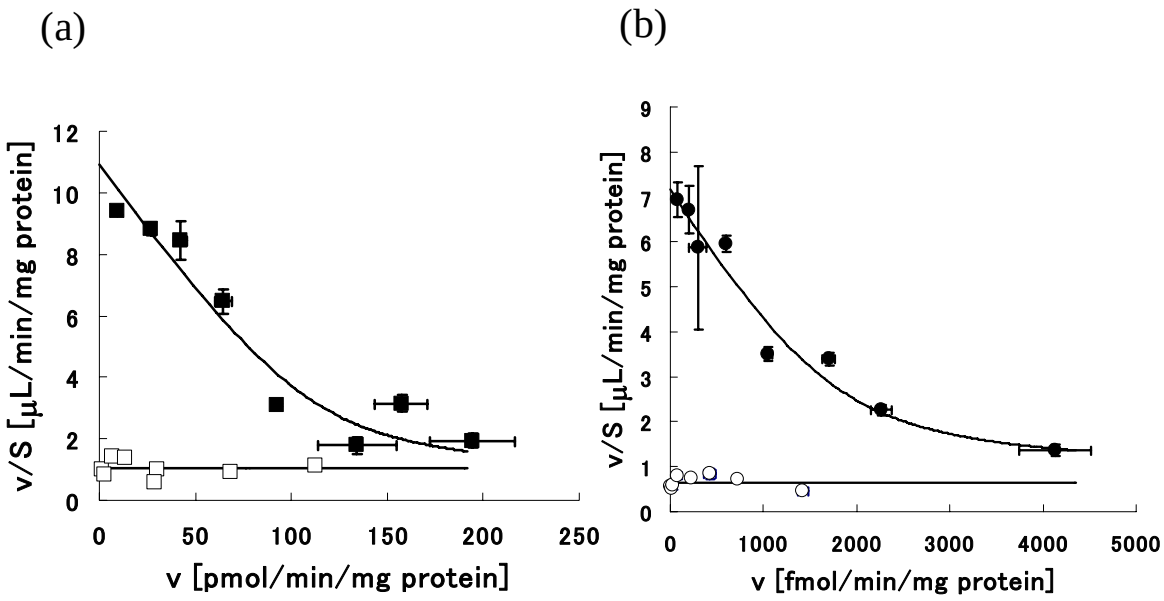

Figure 28

Eadie-Hofstee plots of the uptake of $E_2$17βG into Oatp1-expressing LLC-PK1 cells (a) and digoxin into Oatp2-expressing LLC-PK1 cells (b).

Uptake of 1 μM [^{3}H]-$E_2$17βG (■) or 0.1 μM [^{3}H]-digoxin (●) by oatp1 and oatp2 expressing LLC-PK_1 cells, respectively, was examined in the presence of various concentrations of unlabeled substrates. Uptake of $E_2$17βG (□) and digoxin (○) by vector-transfected cells is also shown in this figure. Each point and bar represents the mean ± S.E. (n =3). The solid lines represent the fitted lines.

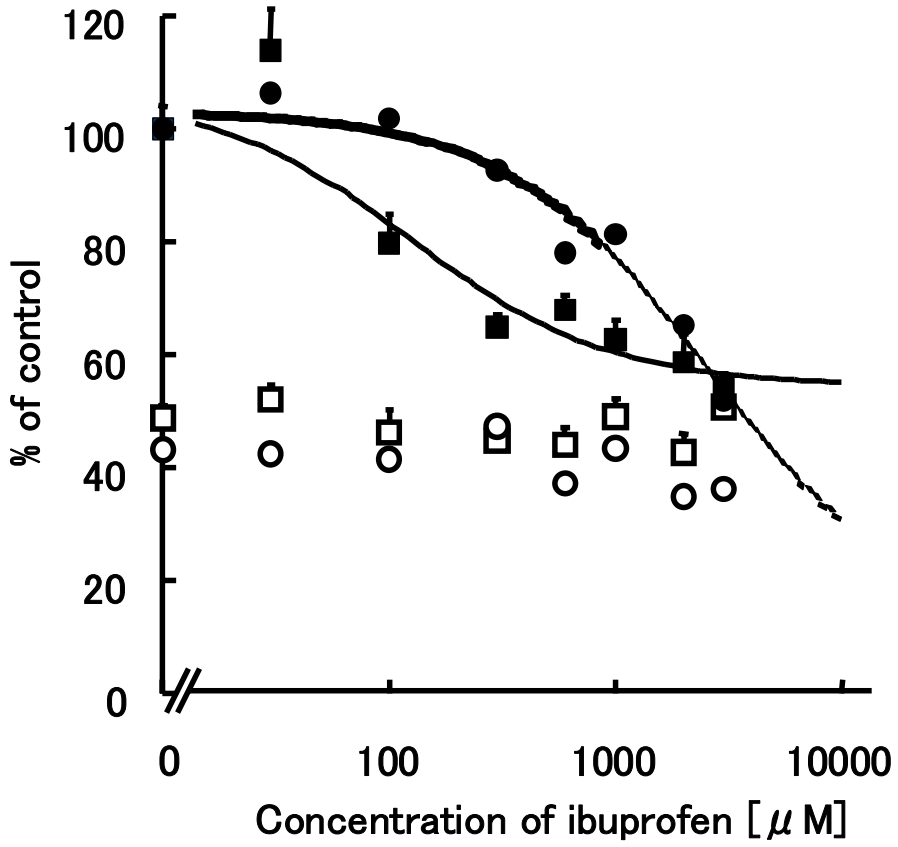

Figure 29

Concentration-dependent effect of ibuprofen on the function of Oatp1 and Oatp2.

Uptake of 0.1 μM [^{3}H]-$E_2$17βG (■) or 50nM [^{3}H]-digoxin (●) by Oatp1 and Oatp2 expressing LLC-PK_1 cells, respectively, was examined in the presence or absence of ibuprofen. Uptake of $E_2$17βG (□) and digoxin (○) in vector-transfected cells is also shown in this figure. Results are given as a % of the control. Each point and bar represents the mean ± S.E. (n = 9 from 3 independent cell preparations). The solid and dotted lines represent the fitted line for the Oatp1-mediated uptake of $E_2$17βG and Oatp2-mediated uptake of digoxin, respectively.

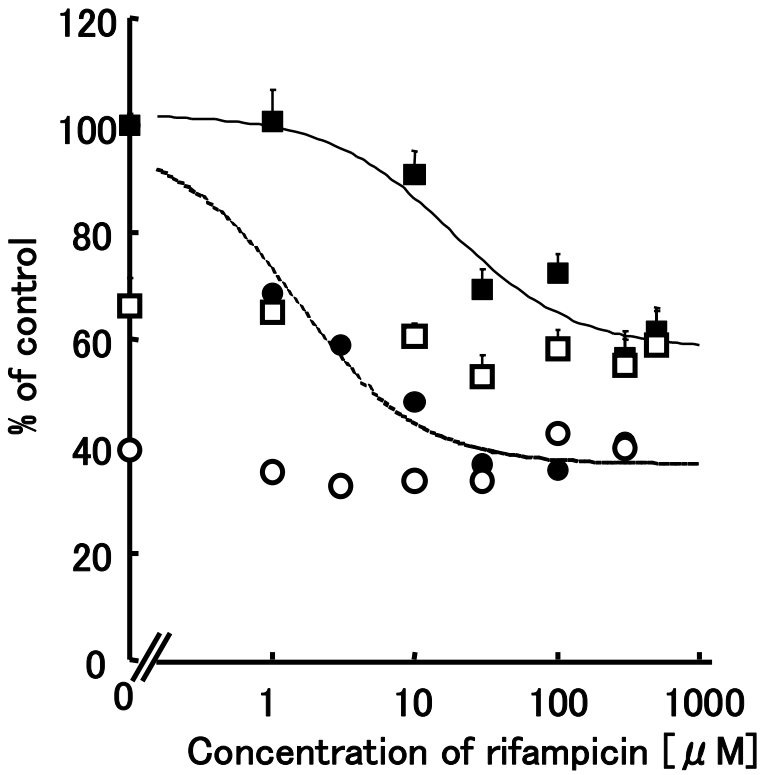

Figure 30

Concentration-dependent effect of rifampicin on the function of Oatp1 and Oatp2.

Uptake of 0.1 μM [^{3}H]-$E_2$17βG (■) or 50nM [^{3}H]-digoxin (●) by Oatp1 and Oatp2 expressing LLC-PK_1 cells, respectively, was examined in the presence or absence of rifampicin. Uptake of $E_2$17βG (□) and digoxin (○) in vector-transfected cells is also shown in this figure. Results are given as a % of the control. Each point and bar represents the mean ± S.E. (n = 9 from 3 independent cell preparations). The solid and dotted lines represent the fitted line for the Oatp1-mediated uptake of $E_2$17βG and Oatp2-mediated uptake of digoxin, respectively.

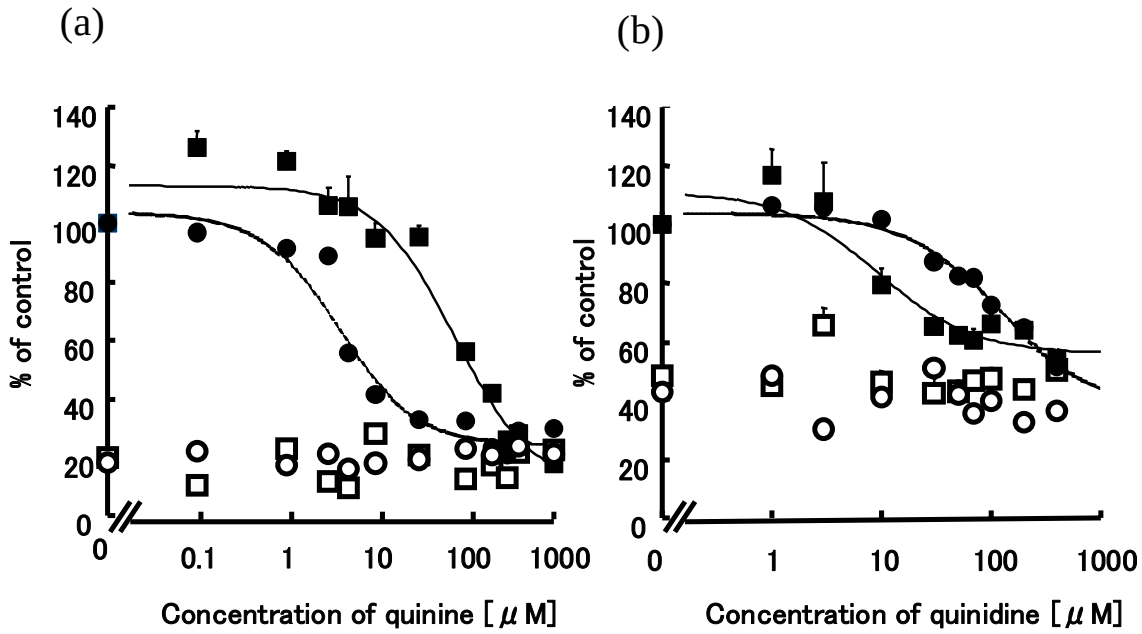

Figure 31

Concentration-dependent effect of quinine (a) and quinidine (b) on the function of Oatp1 and Oatp2.

Uptake of 0.1 μM [^{3}H]-$E_2$17βG (■) or 50nM [^{3}H]-digoxin (●) by Oatp1 and Oatp2 expressing LLC-PK_1 cells, respectively, was examined in the presence or absence of quinine (a) or quinidine (b). Uptake of $E_2$17βG (□) and digoxin (○) in vector-transfected cells is also shown in this figure. Results are given as a % of the control. Each point and bar represents the mean ± S.E. (n = 9 from 3 independent cell preparations). The solid and dotted lines represent the fitted line for the Oatp1-mediated uptake of $E_2$17βG and Oatp2-mediated uptake of digoxin, respectively.

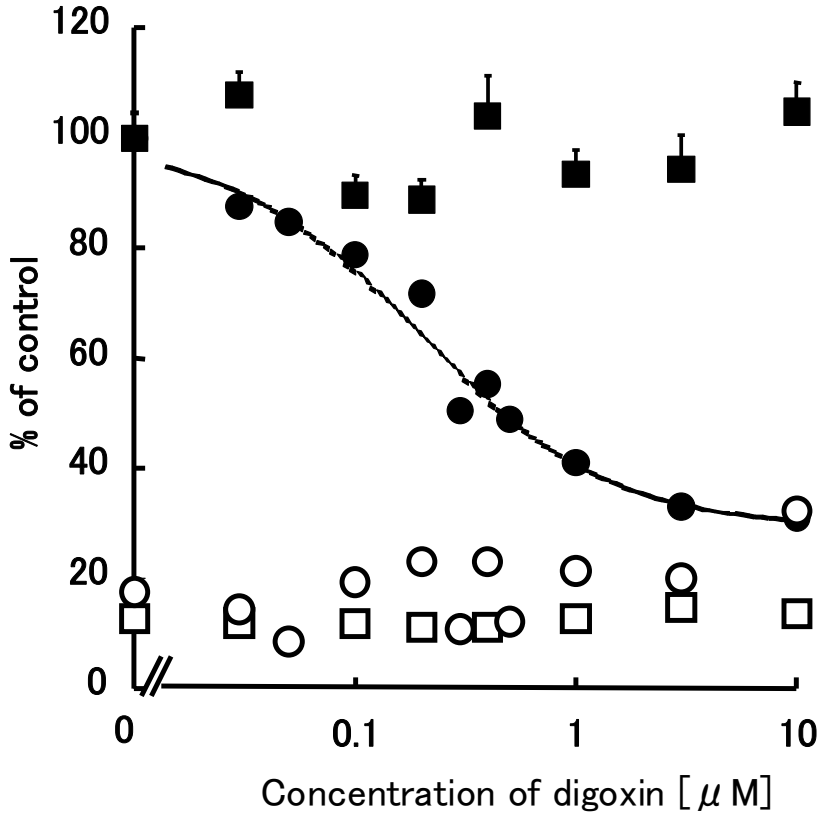

Figure 32

Concentration-dependent effect of digoxin on the function of Oatp1 and Oatp2.

Uptake of 0.1 μM [^{3}H]-$E_2$17βG (■) or 50nM [^{3}H]-digoxin (●) by Oatp1 and Oatp2 expressing LLC-PK_1 cells, respectively, was examined in the presence or absence of different concentrations of digoxin. Uptake of $E_2$17βG (□) and digoxin (○) in vector-transfected cells is also shown in this figure. Results are given as a % of the control. Each point and bar represents the mean ± S.E. (n = 9 from 3 independent cell preparations). The dotted line represents the fitted line for Oatp2-mediated uptake of digoxin.